Spring 2010

Novel pathways for the formation of iodinated disinfection by-products

John Blake McAskill
University of Iowa

NOVEL PATHWAYS FOR THE FORMATION OF IODINATED DISINFECTION BY-PRODUCTS

by

John Blake McAskill

A thesis submitted in partial fulfillment
of the requirements for the Master of Science degree
in Civil and Environmental Engineering
in the Graduate College of
The University of Iowa

May 2010

Thesis Supervisor: Professor Richard L. Valentine

Graduate College
The University of Iowa
Iowa City, Iowa

CERTIFICATE OF APPROVAL

_____

MASTER'S THESIS

_____

This is to certify that the Master's thesis of

John Blake McAskill

has been approved by the Examining Committee for the
thesis requirement for the Master of Science degree in
Civil and Environmental Engineering at the May 2010 graduation.

Thesis Committee: _____
Richard Valentine, Thesis Supervisor

_____
Michelle Scherer

_____
Gene Parkin

TABLE OF CONTENTS

LIST OF TABLES

LIST OF FIGURES

CHAPTER 1
INTRODUCTION AND OBJECTIVES

Disinfection by-products from drinking water treatment have been long recognized and have been well documented. Chlorinated disinfectants can oxidize iodide, resulting in the formation of HOI, which can in theory react with natural organic matter to produce various iodinated halomethanes and other iodinated DBPs. Iodide is naturally found in natural drinking water at average concentrations of 20 µg/l (Moran, Oktay, & Santschi, 2002), and seawater may have iodide concentrations of 30 µg/l (Yokota, Fukushi, Takeda, & Wakida, 2004). A survey of drinking water treatment plants found a plant with 104 µg/l iodide (Richardson et al., 2008). Reactions between these disinfectants, natural organic matter (NOM), and iodide can produce a variety of halogenated disinfection by-products (Richardson, 2003a).

Iodinated organic compounds have been shown to form in chlorinated drinking water systems. Hua et al (2006) showed that HOI produced by the oxidation of iodide reacts more rapidly than free chlorine, HOCl, resulting in the formation of iodoform. Richardson et al (2006) surveyed over 100 distribution systems and found iodine containing trihalomethane concentrations as high at 25 µg/l in one plant. Iodoacetic acid was identified for the first time in waters treated with chloramines (Richardson, 2003b). Richardson et al (2008) studied 23 drinking water treatment plants in the United States and Canada and measured concentrations of several iodinated disinfection by-products. Iodoform was found in waters from most plants with a maximum concentration of 1.7 µg/l. Plants with chlorine only treatment or long free chlorine contact times had the lowest occurrences of iodo-DBPs (Richardson, et al., 2008).

Disinfection treatment methods play an important role in iodide fate. Bichsel and von Gunten (2000a) researched natural waters treated by ozone, chlorine, and chloramines. Ozone oxidized greater than 90% of the naturally present iodide to iodate.

Chlorination resulted in both iodate and iodoform formation, with iodoform formation decreasing with increasing chlorine doses. When chloraminated, iodoform and other iodo-trihalomethanes were the main products.

The U.S. Environmental Protection Agency (EPA) has specified maximum contaminant levels (MCL) of 80 µg/l for total trihalomethanes and 60 µg/l for a group of five haloacetic acids (U.S. EPA, 1998). Interestingly, these MCLs only include chlorinated and brominated species. The regulated trihalomethanes are chloroform, bromodichloromethane, dibromochloromethane, and bromoform. The five regulated haloacetic acids are chloroacetic acid, dichloroacetic acid, trichloracetic acid, bromoacetic acid, and dibromoacetic acid. Iodinated analogs, while observed in drinking water distribution systems, remain unregulated. Although these iodinated species are generally produced at the low microgram per liter range, they have been identified to exhibit greatly increased toxicological effects compared to their chlorinated and brominated analogs (Cemeli, Wagner, Anderson, Richardson, & Plewa, 2006).

Plewa et al (2004) studied haloacetic acids and their cytotoxicities and genotoxicities in *Salmonella typhimurium* cells and in Chinese hamster ovary cells. Iodoacetic acid was shown to be much more toxic than the brominated and chlorinated analogs. In *S. typhimurium,* iodoacetic cytotoxicity was 2.9 times higher than bromoacetic acid and 53.5 times higher than chloroacetic acid. In Chinese hamster ovary cells, iodoacetic acid was 3.2 times more cytotoxic than bromoacetic acid and 287.5 times more than chloroacetic acid. Genotoxicity showed similar results, with iodoacetic acid being 2.6 times and 523.3 times more mutagenic in *S. typhimurium* than bromoacetic acid and chloroacetic acid, respectively. Iodoacetic acid was 2.0 times more genotoxic than bromoacetic acid and 47.2 times more genotoxic than chloroacetic acid in Chinese hamster ovary cells. Their research suggests that iodinated organic compounds are emerging contaminants of importance.

Prior work on DBP formation has dealt almost exclusively with reactions involving aqueous phase chemical disinfectants that are generally quite reactive oxidants. These are capable of oxidizing iodide and bromide, and which lead to the formation of various chlorinated, brominated and iodinated DBPs. A need exists to better characterize reactions that lead to the formation of DBPs in drinking water, especially the formation of the relatively more toxic brominated and iodinated DBPs. Studies of the formation of iodinated DBPs are particularly needed since reactions of iodide have been largely neglected even though iodinated DBPs are considered more toxic than either chlorinated or brominated species. Furthermore, theoretical considerations suggests that certain metal oxides that may exist in distribution systems might also oxidize iodide and lead to the formation of iodinated DBPs. This potential pathway has only recently been proposed but could be important in some distribution systems (e.g. those receiving desalinated water containing relatively high iodide concentrations).

The primary hypothesis of this research is that metal oxides and authentic pipe deposits represent a reservoir of oxidation potential and that iodide oxidation is possible. It is further hypothesized that reactions of HOI with NOM can lead to the formation of measureable amounts of iodoform and iodoacetic acid. This hypothesis is partially based on evidence that lead(IV) oxide (PbO_2) is capable of oxidizing iodide, leading to the formation of iodoform in the presence of NOM, as well as thermodynamic considerations (Lin, Washburn, & Valentine, 2008). The primary objective of this research project was to demonstrate proof-of-concept of this novel DBP formation pathway using lead(IV) and manganese(IV) oxides as model oxides, and several collected authentic pipe deposit samples consisting primarily of inorganic oxides. A schematic showing the proposed reaction pathway is shown in Figure 1.

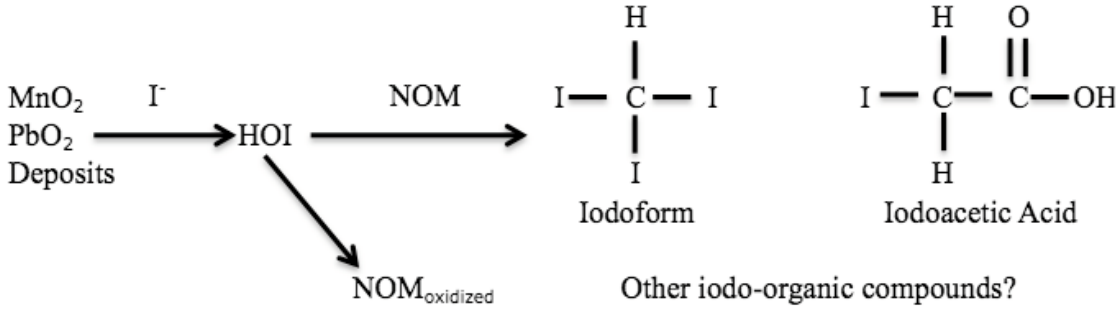

Figure 1. Schematic for proposed pathway for the oxidation of iodide to HOI by model oxides and pipe deposits, resulting in iodo-DBP formation from reactions with NOM.

CHAPTER 2
LITERATURE REVIEW

Past research has shown that disinfectants, namely free chlorine and chloramines, are capable of oxidizing halogens naturally found in drinking water. Only recently have studies focused on the formation of iodinated disinfection by-products from reactions with metal oxides. This literature review focuses on past and present research on the formation of iodo-DBPs, specifically the oxidation of iodide in drinking water systems, the role of metal oxides on iodide oxidation, and the formation of iodo-DBPs from reactive iodine species and natural organic matter.

2.1 Oxidation of Iodide in Drinking Water Distribution Systems

The occurrence of iodinated organic compounds has only recently been studied. Hua et al (2006) studied the effect of bromide and iodide in drinking water treatment with chlorination. While high levels of chlorination can oxidize iodide to iodate, a harmless, stable form of iodine found naturally in fresh water, HOI was shown to react two to three times faster with trihalomethane precursors than HOCl, suggesting iodine substitutes more efficiently the trihalomethane precursors than chlorine. At a chlorine dose of 0.5 mg/l, only a small fraction (0.09 μM) of iodate was formed. As chlorine dosage was increased to 5 mg/l, 95% of initial iodide was oxidized to iodate. (Hua, et al., 2006). Iodate, IO_3^-, is the desired sink for drinking water treatment because it is less reactive with NOM and may limit iodo-DBP formation. Important reactions are shown below:

$$HOCl + I^- = HOI + Cl^- \quad (1)$$

$$HOI + NOM = \text{Iodinated organic compounds} \quad (2)$$

Bichsel and von Gunten (1999) showed that HOI can be oxidized to iodate by ozone and chlorine species, but not by chloramines. Their research also found the proton dissociation constant of HOI to be pKa=10.4±0.1 at 25°C. Relevant dissociation equations are shown below, where Equations 3 and 4 are rate limiting.

$$HOI + HOI = IO_2^- + I^- + 2H^+ \quad (3)$$

$$HOI + OI^- = IO_2^- + I^- + H^+ \quad (4)$$

$$IO_2^- + HOI = IO_3^- + I^- + H^+ \quad (5)$$

HOI disproportionation is slow under normal drinking water treatment conditions, with half-lives on the scale of days to years (Bichsel & von Gunten, 2000b). HOI either reacts with NOM and forms iodinated organic compounds or is oxidized further to iodate.

2.2 Iodide Oxidation by Metal Oxides and Formation of Iodinated DBPs

Pipe deposits in distribution systems are usually comprised of iron oxides, manganese oxides, and other hydroxides and solids of various states (Sarin, Snoeyink, Bebee, Kriven, & Clement, 2001). Figure 2 shows a diagram of a typical profile of a water distribution pipe with deposits.

Lead, while not typically thought of as being present in drinking water systems, can actually accumulate in distribution pipes. Recent studies have shown that lead oxide (PbO_2) can form in the presence of lead bearing material found in drinking water distribution systems and household appliances (Lytle & Schock, 2005).

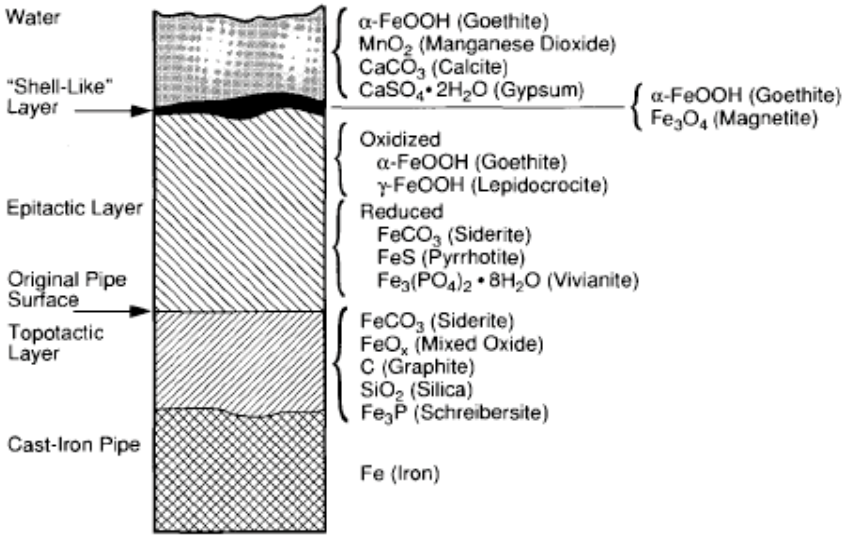

Figure 2. Schematic profile of typical pipe scale (Benjamin, Sontheimer, & Leroy, 1996).

Redox potentials show that lead(IV) oxide and manganese dioxide are perhaps the most likely oxides capable of oxidizing iodide to iodine. Table 1 shows several relevant redox half reactions and indicates that the proposed oxidation of iodide should be favorable. At neutral pH, iodide oxidation by lead oxide will produce 1.27×10^{-4} M I_2 at equilibrium, and oxidation by manganese dioxide will produce 1.69×10^{-7} M I_2 at equilibrium. Figure 3 shows iodine concentration as a function of pH. Although a small concentration of HOI/I_2 is formed, iodo-DBPs may pose a health risk at the ng/l level, warranting further study.

Table 1. Redox Potentials in Water (Stumm, 1992)

Reaction (unbalanced Ox → Red)	E^o (volts)	E_h @ pH 7 (volts)
$PbO_2(s) \rightarrow Pb^{2+}$	+1.46	+0.63
$Cl_2 \rightarrow 2\ Cl^-$	+1.39	+1.39
$MnO_2(s) \rightarrow Mn^{2+}$	+1.29	+0.46
$O_2 \rightarrow H_2O$	+1.23	+ 0.82
$Br_2 \rightarrow 2\ Br^-$	+1.07	+1.07
$Fe^{+3} \rightarrow Fe^{2+}$	+0.78	+0.78
$I_2 \rightarrow 2\ I^-$	+ 0.62	+0.62

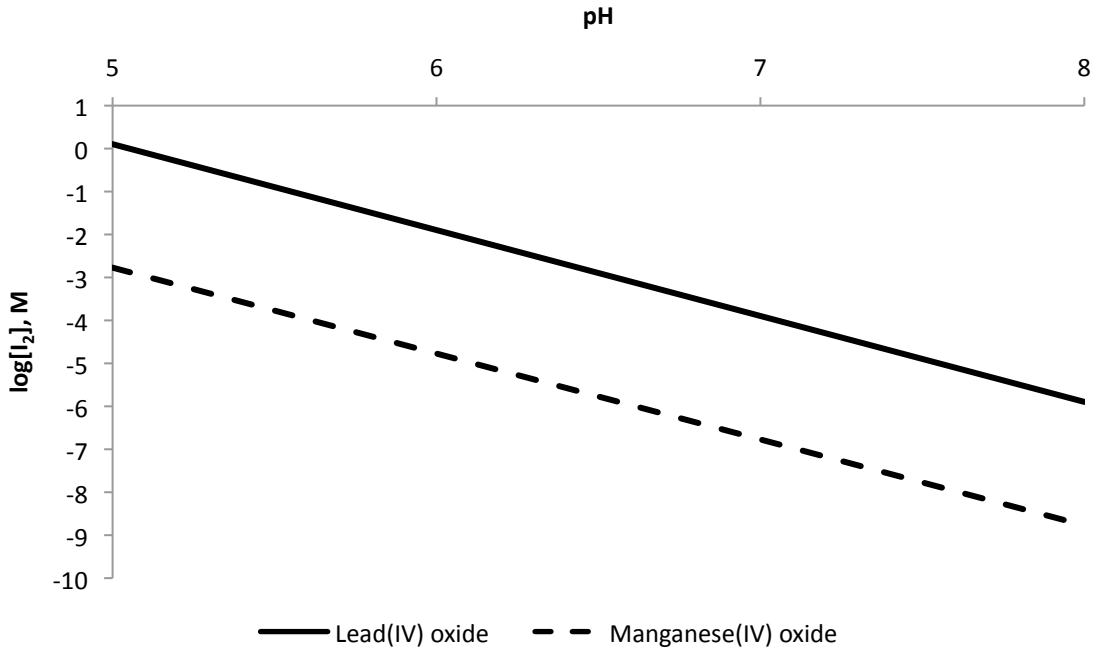

Figure 3. Iodine formation from the oxidation of iodide by PbO_2 and MnO_2.

Lin and Valentine were the first to report on the reactivity of lead oxide in water using iodide as a probe compound (Lin, et al., 2008). They found that lead oxide can oxidize iodide according to the following reactions:

PbO_2 reduction: $4H^+ + PbO_2 + 2e^- = Pb^{2+} + 2H_2O$ (6)

I^- oxidation: $I^- + H_2O = HOI + 2e^- + H^+$ (7)

At the pH values used in the experiments, HOI was the dominant species. In the presence of excess iodide, HOI was rapidly transformed according to the following reactions:

$I^- + HOI + H^+ = I_2 + H_2O$ (8)

$I^- + I_2 = I_3^-$ (9)

The experimental conditions resulted in more than 95% of the HOI being converted to I_3^-. The overall redox reaction can be expressed as:

$PbO_2 + 3I^- + 4H^+ = Pb^{2+} + I_3^- + 2H_2O$ (10)

Based upon their work on iodide oxidation of lead oxide, they proposed that oxidation of iodide by lead oxide in the presence of NOM could lead to the formation of iodinated DBPs. They then showed that this hypothesis was indeed true by demonstrating the formation of iodoform in systems containing lead oxide, iodide and NOM. This study was seminal in that it was the first to report that a DBP could be formed by a reaction involving an oxide relevant to distribution systems. As such it motivated this study as well as very recent work by others on related systems.

Allard et al (2009) recently showed that manganese dioxides can oxidize iodide, with rate constants decreasing with increasing pH, consistent with thermodynamic considerations. Iodide oxidation to HOI and subsequent formation of iodinated organic compounds was highest in the pH range 5-7.5. Below pH 5, oxidized iodide was shown to be quickly oxidized further to iodate, and above pH 7.5, iodide was not oxidized to a significant extent (Allard, et al., 2009). Important reactions are shown below.

$$MnO_2 + 2I^- + 4H^+ = Mn^{2+} + I_2 + 2H_2O \quad (11)$$

$$I^- + 3MnO_2 + 6H^+ = IO_3^- + 3Mn^{2+} + 3H_2O \quad (12)$$

Iodide oxidation was shown to increase as pH decreased and birnessite (∂-MnO_2) concentrations were increased. Oxidation of iodide proceeded to iodate through a reactive iodine species intermediate. (Gallard, Allard, Nicolau, von Gunten, & Croue, 2009) also recently showed that iodide can be oxidized by birnessite in the pH range of 5-7. In the presence of natural organic matter and model compounds, iodoform was measured, and iodoacetic acid was identified but not quantified.

It should be stated that reactions of naturally occurring deposits that contain a variety of oxides in various oxidation states is expected to be more diverse than reactions of pure metal oxides. In particular, a metal oxide may exist that does indeed oxidize iodide to iodine but the fate of this species is not clear. It could oxidize NOM and potentially form iodated DBPs. Alternatively, it may also be reduced by Fe(II) back to iodide. Therefore the exact nature of the deposit material would be an important determinant in the potential formation of iodinated DBPs. The oxidative nature would likely be determined by many factors including the redox conditions under which they were formed as well as subsequent reactions that can change their nature.

CHAPTER 3
ANALYSIS AND EXPERIMENTAL METHODS

All experiments were performed in Dr. Richard Valentine's laboratory in the Environmental Engineering and Sciences Laboratories in the Seamans Center at the University of Iowa. The chemicals used in the experiments were analytical laboratory grade. All experiments were conducted with deionized water from a Barnstead ULTRO pure water system.

3.1Analytical Methods

3.1.1 Organics and lead free glassware

All batch reactor experiments were conducted in 125 ml amber glass bottles with plastic screw caps. The bottles and other glassware used in experiments were insured to be free of organic matter and lead contamination by soaking in a 2N nitric acid bath for 24 hours. Following the acid bath, the glassware was rinsed with tap water then rinsed with DI water. The air-dried glassware was capped with aluminum foil and placed in a combustion furnace for two hours at 400°C. All plastic caps and volumetric glassware were also placed in the acid bath for 24 hours, but they were not placed in the combustion furnace.

3.1.2 Natural organic matter

The source of the natural organic matter used in the experiments came from Valentine Pond in the Upper Peninsula of Michigan. A RealSoft PROS/2S reverse osmosis (RO) unit (Stone Mountain, GA) was used to process the pond water. The volume of the RO retentate was 40 L and was stored in a plastic carboy at 4°C. Prior to experimental use, the RO retentate was stirred to suspend the particles and to homogenize

the mixture. The water was filtered with a 0.45μm Millipore filter then added to a volumetric flask, which was also stored at 4°C. Total organic carbon was determined with a Shimadzu TOC-V SCH total organic carbon analyzer and was consistently measured to be about 120 mg/l as C.

3.1.3 Pure minerals and authentic pipe deposits

Lead(IV) oxide (Aqua Solutions) and manganese dioxide (Kerr McGee) were purchased for use in experiments. The PbO_2 was identified as platternite by XRD analysis, and particle sizes were in the range of 45-150 μm. The MnO_2 was electrolytic manganese dioxide determined to be either short range ordered γ-MnO2 or long range disordered ε-MnO2 phase (Simon, Morton, & Gislason 2004). Particle sizes were similar to lead oxide, in the range of 45-150 μm.

Sections of drinking water distribution service lines were obtained from several utilities. The exposed mineral scales were removed from the pipe with a hammer and chisel and ground into powder with a mortar and pestle. The powdered pipe deposit was then sieved and stored for later use. Particle sizes of the authentic pipe deposits used in this project were in the range of 45-150 μm. The pipe deposits were characterized by ICP-MS analysis at the University of Washington, in Seattle, Washington (Friedman, Hill, Reiber, Valentine, & Korshin, 2010). Important composition information is shown in Table 2. Organic carbon content, while not available for all samples, ranged from 1-5% C by weight on average. All pipes used in this study were composed of significant amounts of iron. It is expected that this is a combination of iron(II) and iron (III). Studies show that pipe deposits typically exert a large oxidant demand suggesting the important role of reduced species in determining levels of chemical oxidants in the distribution system.

Table 2. Composition information for authentic pipe deposits.

Water System	Iron, ($\mu g/g_{ext}$)	Lead, ($\mu g/g_{ext}$)	Manganese ($\mu g/g_{ext}$)
WDB-A	54917.79	25.07	232475.93
CC-A	234727.61	59.65	46692.11
J-B	283699.42	407.09	30116.88
WA-A	465447.63	53.27	3713.79
CL-D	349761.70	8.29	1393.43

3.1.4 pH measurement and calibration

Batch reactor pH values were measured with a Fisher Accumet AB15 pH meter coupled with a calomel combination pH electrode. The pH meter was calibrated with pH 4, pH 7, and pH 10 Fisher pH solutions. The electrode was stored in Fisher pH storage solution when not in use.

3.1.5 Measurement of iodoform and iodoacetic acid

Gas chromatography with electron capture detection (GC-ECD) was used to detect iodoform and iodoacetic acid. Chromatographic separation occurred with a DB-5 capillary column using a 2 µl sample injection. The temperature program, identical for iodoform and iodoacetic acid, initiated at 65°C, ramped to 230°C at a rate of 10°C/min, and held at 230°C for two minutes for a total run time of 18.5 minutes. Elution times were 16.1 minutes for iodoform and 9.5 minutes for iodoacetic acid. Method detection limits (MDL) were calculated by using the U.S. EPA method of running seven samples near the detection limit. The MDL were determined to be 1.152 µg/l for iodoform and 0.277 µg/l for iodoacetic acid. Past analyses in the lab determined MDL to be 0.165 µg/l for iodoform and 0.392 µg/l for iodoacetic acid (Washburn, 2008).

3.1.6 Iodoform analysis

Iodoform was analyzed in accordance with US EPA Method 551.1 (U.S. EPA, 1995). The method is a liquid/liquid extraction using methyl tert-butyl ether (MTBE) as the extraction solvent. Fifty milliliters (50 ml) of sample water was added to a 60 ml extraction vial after filtration with a 0.1 μm PVDF filter (BD). The samples were quenched with a 0.5 ml aliquot of 10 g/l sodium sulfite to bring the sulfite concentration in the extraction vial to 100 mg/l and given about one minute of reaction time. Sulfite, which does not partition into the MTBE layer, quenches any reactive iodine species in the sample water. Twenty grams (20 g) sodium sulfate anhydrous was added to the extraction vial to drive iodoform from the aqueous phase into the MTBE phase. The vial was shaken by hand and laid on its side to prevent the sodium sulfate from clumping while other vials were prepared. Three milliliters (3 ml) of MTBE was added to the vial, and then the vial was placed on a mechanical wrist shaker for four minutes. The vial was set upright and given about five minutes for phase separation. Using a Pasteur pipette, 1 ml of the MTBE was transferred to a GC vial. Samples were stored in a -30°C freezer.

3.1.7 Iodoacetic acid analysis

Iodoacetic acid was analyzed in accordance with US EPA Method 552.3 (U.S. EPA, 2003). The method is a liquid/liquid extraction using MTBE as the extraction solvent. Iodoacetic acid, unlike iodoform, is a stable compound, so it must first be derivitized to analyze with the GC-ECD. Forty milliliters (40 ml) of sample water was added to a 60 ml extraction vial after filtration with a 0.1 μm filter. The sample was quenched with a 0.5 ml aliquot of 10 g/l sodium sulfite to bring the sulfite concentration in the extraction vial to 100 mg/l and given about one minute of reaction time. Sulfite, which does not partition into the MTBE layer, quenches any reactive iodine species in the sample water. The pH of the sample water was lowered to pH 2 with the addition of up to 2 ml concentrated sulfuric acid. Next, 18 g sodium sulfate was added to the extraction

vial and shaken until most of it was dissolved. Four milliliters (4 ml) of MTBE was added to the extraction vial, and then the vial was placed on a mechanical wrist shaker for three minutes. After allowing five minutes for phase separation, 3 ml of the MTBE layer was transferred to a glass 15 ml graduated conical centrifuge tube, and 3 ml of 10% sulfuric acid in methanol was added to the MTBE. The tube was capped and placed in a heating block for two hours at 50°C to convert the iodoacetic acid to its methyl esters. Care was taken to prevent the temperature reaching 55°C, the boiling point of MTBE. The tube was allowed to cool before 7 ml of 150 g/l sodium sulfate was added. A vortex mixer was used to insure the full equilibration of the phases. The phases were allowed to separate fully, and then the lower acidic aqueous methanol phase was removed with a disposable glass pipette. One milliliter (1 ml) of saturated sodium bicarbonate was added to the MTBE, and the tube was capped and vortex mixed for about 30 seconds at least four times. The cap was loosened in between mixing to allow the release of evolved CO_2. Using a Pasteur pipette, 1 ml of the MTBE layer was transferred to a GC vial. Samples were stored in a -30°C freezer.

3.2 Experimental Methods

3.2.1 Batch reactors

Batch reactions were studied using variable concentrations of metal oxides and deposits, added NOM, iodide, and pH. Experiments were conducted in 125 ml amber glass bottles with plastic screw caps. Samples were prepared by adding approximately 75 ml DI water to an amber glass bottle. Stock $NaHCO_3$ was added to bring the reactor to 2 mM HCO_3^-. NOM, if added, was added next, followed by oxides or pipe deposit. The pH was adjusted with 0.1 N HCl and 0.1 N NaOH. The iodide was added last to prevent localized pH-driven reactions during pH adjustment. The pH was measured both before and after the reaction period and generally was within 0.1 pH unit of the target pH.

3.2.2 Reactive iodine species detection

DPD-FAS titration was used to quantify formation of HOI, which titrates similarly to HOCl (Standard Methods 4500-Cl F, DPD Ferrous Titrimetric Method). The method called for 100 ml sample added to 5 ml phosphate buffer and 5 ml DPD indicator. Up to 5 ml of FAS titrant was used, and 1 ml titrant was equivalent to 1 mg/l Cl_2.

The phosphate buffer was prepared by dissolving 24 g anhydrous Na_2HPO_4 and 46 g anhydrous KH_2PO_4 in DI water and combined with 800 mg ethylenediamine tetraacetate (EDTA) in 100 ml DI water. The solution was diluted to 1 L with DI water, and 20 mg $HgCl_2$ was added to prevent mold growth. The DPD indicator was prepared by dissolving 1.1 g anhydrous DPD sulfate into DI water containing 8 ml 1+3 H_2SO_4 and 200 mg EDTA and diluting to 1 L. The DPD indicator was stored in a capped amber bottle at 4°C and checked frequently for discoloration. Ferrous ammonium sulfate (FAS) titrant was prepared with 1.106 g FAS and 1 ml of 1+3 H_2SO_4 made up in 1 L DI water.

CHAPTER 4
RESULTS AND DISCUSSION

The objectives of this project were to investigate the formation of iodinated disinfection by-products (iodo-DBPs) through the novel pathway of reactive iodine species, formed from iodide oxidized by metal oxides, reacting with natural organic matter. While limited research has shown that iodo-DBP formation is possible under laboratory conditions with several oxides, it has not been determined if this reaction is possible in the presence of authentic deposit material. Formation of IAA by lead oxide and manganese oxide has also not been studied. It should be stressed that this is an exploratory project aimed primarily at demonstration of this novel pathway.

4.1 Method Development: Artifacts in the Analysis of Iodoacetic Acid

Initial studies were performed using lead(IV) oxide and manganese dioxide as model oxides. In these initial studies, samples were not filtered but were settled. Initial experiments were conducted with low levels of solids, about 150 mg/l, and water samples from the batch reactors appeared clear. They were also not quenched with sodium sulfite. Formation of iodoform and iodoacetic acid was indicated even in the absence of added NOM. It should be pointed out that although NOM was not added to these solutions, some organic carbon was expected to be present in and on these materials so that some DBP formation might be rationalized. However, in the absence of added NOM, surprisingly large concentrations of iodoacetic acid were measured, much more than when NOM was added, as shown in Table 3 and Table 4.

Table 3. Experiment 21M (07-20-2009): iodoacetic acid formation in unfiltered and unquenched samples containing buffer, lead oxide, iodide, and in the presence and absence of NOM at pH 7 and 72 hours reaction time.

Reactor No.	PbO_2 (mg/L)	$NaHCO_3$ (mM)	NOM (mg/L)	I- (mg/L)	IAA formed (µg/L in water)
1	150	2	0	10	2420
2	150	2	10	10	677

Table 4. Experiment 37AGM (10-16-2009): iodoacetic acid formation in unfiltered and unquenched samples containing buffer, lead oxide, iodide, and in the presence and absence of NOM at pH 7 and 144 hours reaction time.

Reactor No.	MnO_2 (mg/L)	$NaHCO_3$ (mM)	NOM (mg/L)	I- (mg/L)	IAA formed (µg/L in water)
1	150	2	0	10	1062
2	150	2	10	10	103

The added NOM might have reduced the soluble HOI concentration that possibly generated iodoacetic acid in the derivitization-extraction mix. What could cause the formation of DBPs without any added soluble NOM added?

Several hypotheses were investigated to explain these findings, especially the seemingly impossibly large amounts of IAA. Artifacts might have been attributed to: 1) presence of significant amounts of reactive NOM associated with the oxides, 2) presence of oxide solids that somehow react to form IAA during the extraction and derivitization step, and 3) the presence of HOI that could also react to form IAA during the extraction and derivitization step.

One hypothesis to explain these results was that there was a trace amount of organic matter in the metal oxides. Experiment 22M (08-03-2009) consisted of a typical set of control and reactive batch reactors containing different combinations of buffer, lead oxide, NOM, and iodide. After 48 hours of reaction time, the samples were filtered with

0.1 μm filters and analyzed with the total organic carbon analyzer. Batch reactors without added NOM were shown to contain no dissolved organic carbon (results not shown). However, NOM can still be attached to the surface of the purchased lead oxide and could therefore account for the formation of any DBPs. Although samples were filtered with 0.1 μm filters, it may be possible that smaller oxide particles reacted with iodide and MTBE in the extraction vials. Another hypothesis for iodo-DBP formation in the absence of NOM was oxidized iodide species, such as HOI, reacting with the MTBE in extraction vials or during the iodoacetic acid derivitization procedure. Experiments confirmed this, and steps were taken to quench the remaining reactive iodine species in extraction vials prior to extraction.

4.1.1 Influence of filtration and iodide addition during derivitization on iodoacetic acid formation

Metal oxide particles in the extraction vials were suspected of possibly influencing the detection of iodoacetic acid. Initial experiments focusing on iodoform formation were conducted by letting the oxides or pipe deposits settle to the bottom the reactors before samples were removed from the top with pipettes. The oxide/pipe deposit particles did not seem to interfere with the extraction procedure, as the particles did not appear to partition from the water into the MTBE layer used in the analysis of iodoform. However, the iodoacetic acid procedure, which involves first adjusting the pH to low values, partitioning iodoacetic acid into MTBE followed by methylation, gave the first hint that oxides/pipe deposits in the extraction vials may cause problems with results.

Batch reactors were prepared with buffer, lead oxide, both with and without NOM, and iodide. Iodide was added to some samples only in the extraction-derivitization vials to determine if iodide added after filtration had any influence on iodoacetic acid formation. Iodoacetic acid appeared to be formed in reactors with and without NOM but to a much greater extent in the absence of NOM. Failure to filter with

0.1 μm filters also caused an increase in iodoacetic acid, suggesting that the lead oxide was oxidizing iodide in large amounts in the low pH of the extraction vials.

Table 5 summarizes results indicating that that iodoacetic acid was produced in the reactors containing buffer, lead oxide, and iodide (Reactors 5 and 8). Both filtered and unfiltered reactors produced a very large amount of iodoacetic acid. Samples from reactors not containing iodide to which iodide was added to the derivitization mix after filtration showed some comparatively small formation of iodoacetic acid, indicating that HOI may also have a role in addition to filtration since filtration greatly reduced IAA formation. Samples from reactors containing lead oxide and iodide but no added NOM and were filtered, produced 2166 μg/l iodoacetic acid (Reactor 5). The presence of 10 mg/l NOM as C (Reactor 8) reduced iodoacetic acid formation to 293 μg/l. Unfiltered samples produced 1350 and 2177 μg/l iodoacetic acid (Reactors 7 and 10). Reactors containing lead oxide but no iodide resulted in the apparent formation of 4.3 μg/l iodoacetic acid when the iodide was added to the derivitization mix. Lead oxide free controls did not produce significant iodoacetic acid except for perhaps Reactor 3. This may be the consequence of the oxidation of iodide by NOM at a low pH of the derivitization mix. It should be noted that these large concentrations are measured from truncated chromatograms. While the large peaks confirm a massive amount of iodoacetic acid is indeed produced, the exact concentration is only an estimate. Figure C-1 through Figure C-10 show the chromatograms.

Table 5. Experiment 23M (08-11-2009): comparison of iodoacetic acid formation in the presence of lead oxide and NOM, and iodide added to batch reactors or extraction-derivitization mix at pH 7 and 72 hours reaction time.

Reactor No.	pH, initial	pH, final	NOM (mg/L)	PbO_2 (mg/L)	I- added to reactor (mg/L)	I^- added to extraction-derivitization mix (mg/L)	IAA formed (µg/L)
1	6.90	6.81	10	0	0	0	ND
2	6.95	6.68	0	0	10	0	ND
3	7.03	7.10	10	0	10	0	7.3
4	6.95	6.84	0	150	0	0	ND
5	6.96	7.08	0	150	10	0	2166
6	6.98	7.01	0	150	0	10	4.3
7	6.96	7.08	0	150	10	0	1350 (unfiltered)
8	6.98	7.10	10	150	10	0	293
9	6.96	6.95	10	150		10	14.9
10	6.98	7.10	10	150	10	0	2177 (unfiltered)

NOTE: All samples contain 2 mM HCO_3^- buffer and, unless noted in "IAA formed" column, were filtered with 0.1 µm filters.

4.1.2 HOI formation from lead oxide and iodide

Experiments have shown that filtration greatly reduced the apparent formation of IAA that must occur in the iodoacetic acid extraction method. Iodoform and iodoacetic acid was also detected at much higher concentrations in the absence of NOM than in the presence of NOM. This may be attributable to some NOM associated with the oxides or water but the values appear unbelievably high. Formation of IAA in filtered samples, although much less than in unfiltered samples, also points to the possible role of HOI as an artifact and the existence of an unexpected reaction between reactive iodine species formed from the oxidation of iodide by metal oxides and MTBE and/or the iodoacetic acid extraction procedure. For this to occur, there would need to be a residual concentration of reactive iodine species that had not reacted with NOM.

Batch reactors containing lead oxide and iodide and lead oxide, NOM, and iodide were prepared and given various reaction times. The batch reactors were analyzed for reactive iodine species, HOI, according to Standard Methods 4500-Cl F, DPD Ferrous Titrimetric Method. The sample consisted of 100 ml from the batch reactor, filtered with 0.1 μm filters, added to 5 ml each of DPD indicator and phosphate buffer, and titrated with FAS. The FAS stock was prepared so that 1 ml of FAS was equivalent to 1 mg/l as Cl_2.

Table 6 and Figure 4 show that HOI was measureable during all reaction times in the absence of NOM. The reactors containing NOM did not produce any measureable HOI. This may be due to NOM converting all the HOI to iodoform and iodoacetic acid. The NOM may have covered the lead oxide reaction sites to some degree, which could prohibit its oxidation of iodide or reaction with HOI. These results indicate that HOI has been in all past experiments with lead oxide in the absence of NOM.

Table 6. HOI concentration as a function of time in batch reactors containing 2 mM buffer, 150 mg/l lead oxide, and 10 mg/l iodide, measured with DPD-FAS titration (Experiment 28M, 10-26-2009).

Time, min	HOI, mg/l as Cl_2	
	No added NOM	10 mg/l NOM as C
5	0.25	0
30	0.8	0
60	1.5	0
120	1	0
7200	1.1	0

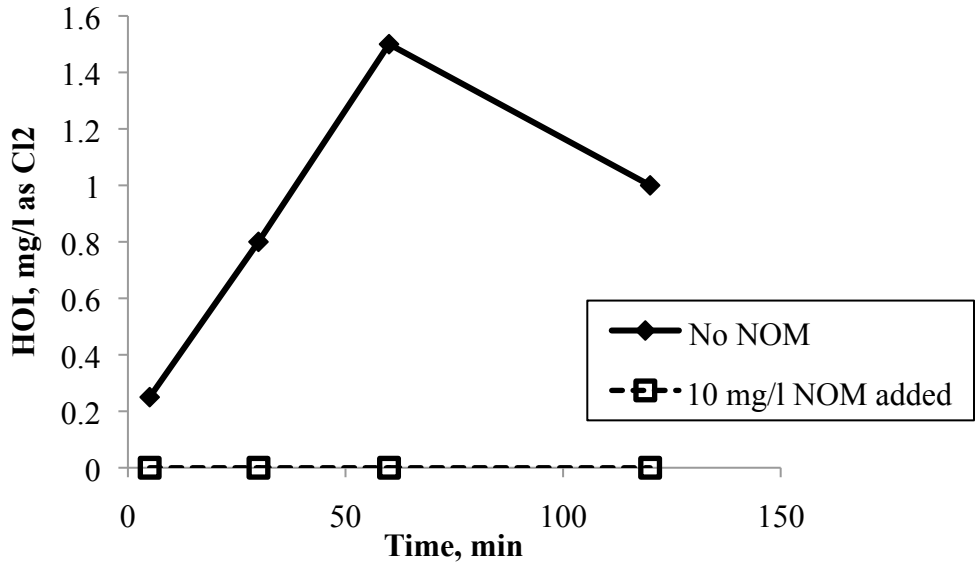

Figure 4. Formation of HOI as a function of time in batch reactors containing 2 mM buffer, either no added NOM or 10 mg/l NOM, 150 mg/l lead oxide, and 10 mg/l iodide. (Experiment 28M, 10-26-2009). The results from the 7200 minute titration was omitted to preserve the scale of the figure.

4.1.3 HOI formation from manganese dioxide and iodide

Experiments 44M (02-10-2010) and 45M (02-16-2010) investigated the formation of reactive iodine species from the reaction of manganese dioxide and iodide in the absence of NOM. Experiment 44M was conducted at varying MnO_2 concentrations, and Experiment 45M was conducted at 870 mg/l MnO_2 over a range of reaction times. The results are shown in Table 7.

When MnO_2 concentration was increased (Experiment 44M, 02-10-2010), the measured reactive iodine species concentration increased. HOI detection occurred at a minimum MnO_2 concentration of 435 mg/l, shown in Figure 5. The maximum HOI detected in the experiment was 0.6 mg/l as Cl_2. The kinetic experiment (45M, 02-16-2010) was performed over six hours, with little change in HOI formation, shown in Figure 6. No HOI was detected at five minutes reaction time. After 30 minutes, 0.2 mg/l

HOI as Cl_2 was detected, and the HOI concentration remained constant over the duration of the experiment.

Compared with a similar experiment conducted with lead oxide (28M, 10-26-2009), MnO_2 appears to have much less oxidative ability, consistent with the redox potentials in Table 1. Lead oxide experiments were conducted at 150 mg/l, where MnO_2 experiments were conducted at concentrations nearly 6 to 60 times greater. The two experiments on HOI formation from PbO_2 and MnO_2 oxidation showed that PbO_2 oxidation occurs faster and to a greater extent than MnO_2 oxidation.

Table 7. Formation of HOI from a reaction of MnO_2 and iodide in the absence of NOM as measured with DPD-FAS titration (Experiments 44M, 02-10-2010 and 45M, 02-16-2010).

Reactor No.	Time, hr	Initial pH	Final pH	MnO_2, mg/l	HOI, mg/l as Cl_2
9	48	6.85	6.72	0	0
10	48	6.98	6.40	87	0
11	48	6.95	6.65	435	0.3
12	48	6.96	6.73	870	0.4
13	48	6.95	6.51	2174	0.4
14	48	6.99	6.62	4350	0.6
15	48	6.93	6.63	8700	0.6
16	5 min	6.98	6.98	870	0
17	0.5	7.03	7.08	870	0.2
18	1	6.99	7.00	870	0.2
19	2	7.03	6.98	870	0.2
20	4	7.04	6.95	870	0.2
21	6	6.97	6.95	870	0.2

NOTE: All batch reactors contain 2 mM bicarbonate buffer and 10 mg/l iodide and were filtered with 0.1 μm filter prior to titration. No NOM was added to any reactors.

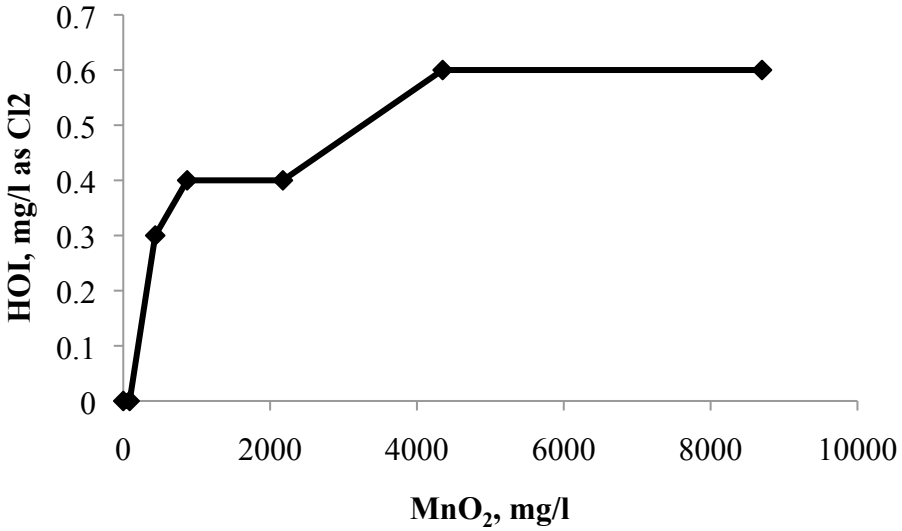

Figure 5. Formation of HOI as a function of MnO_2 concentration from a reaction of MnO_2 and iodide in the absence of NOM, Experiment 44M (02-10-2010). Initial conditions: pH 7, 48 hours reaction time, 2 mM HCO_3^-, and 10 mg/l I^-.

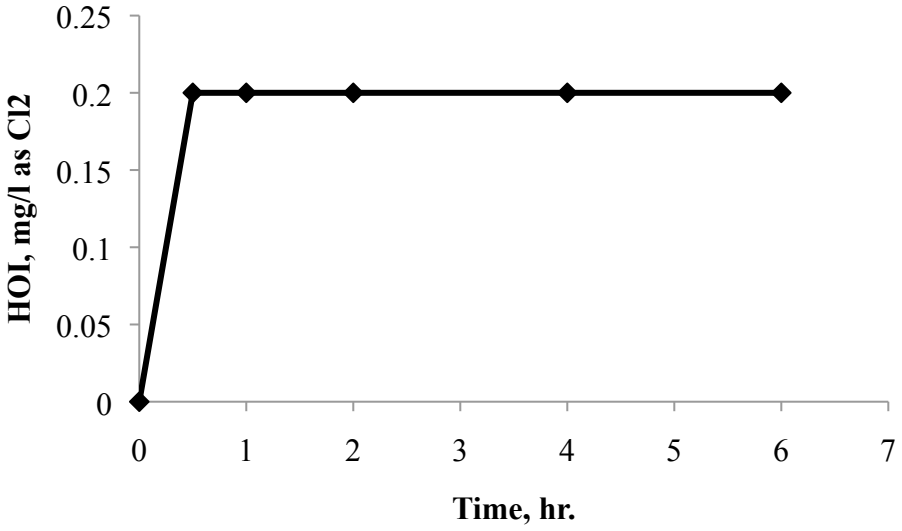

Figure 6. Formation of HOI as a function of time from a reaction of MnO_2 and iodide in the absence of NOM, Experiment 45M (02-16-2010). Initial conditions: pH 7, 2 mM HCO_3^-, 870 mg/l MnO_2, and 10 mg/l I^-.

4.1.4 Sulfite quenching of HOI

Since residual HOI was detected in batch reactors, steps were taken to quench the remaining HOI to prevent iodoform and iodoacetic acid detection resulting from the HOI artifact. Sodium sulfite was chosen as the quenching agent since it does not partition into the organic MTBE layer. Experiment 29M (10-29-2009) consisted of two batch reactors, both containing 2 mM buffer, 0.026 mM HOCl (1.84 mg/l HOCl as Cl_2) and 10 mg/l I^- with one of the reactors containing 100 mg/l sulfite as a quenching agent. Table 8 shows that 0.75 mg/l HOI as Cl_2 was formed without sulfite quenching, and no HOI was measured in the quenched sample.

Table 8. Comparison of HOI concentration in batch reactors containing buffer, HOCl, and I^- measured by DPD-FAS titration in quenched and unquenched samples (Experiment 29M, 10-29-2009).

Vial No.	$NaHCO_3$, mM	I-, mg/L	HOCl, mg/l as Cl_2	Sulfite, mg/l	HOI measured, mg/l as Cl_2
1	2	10	1.84	0	0.75
2	2	10	1.84	100	0

4.1.5 Formation of iodoform and iodoacetic acid in quenched and unquenched samples containing preformed HOI

Experiment 33M (11-16-2009) investigated the detection of iodoform and iodoacetic acid through a reaction between HOI and MTBE and/or the iodoacetic acid extraction method. The experiment was prepared in quenched and unquenched reactors containing 2 mM buffer, 0.026 mM HOCl, and 10 mg/l I^-. The experiment also studied the stability of iodoform and iodoacetic acid in 100 mg/l sulfite. Table 9 shows the results for iodoform, and Table 10 shows the results for iodoacetic acid. Iodoform did not form in either quenched or unquenched samples containing HOCl and I^- and remained stable with sulfite quenching. A large amount of iodoacetic acid, about 1300

µg/l IAA, formed in the unquenched sample containing HOCl and I^-, which reacted to produce HOI. The quenched sample containing HOCl and I^- did not show any iodoacetic acid formation. This shows that HOI is the cause of the large concentrations of IAA found in past experiments. Both iodoform and iodoacetic acid appear to be stable in the presence of excess sulfite. Chromatograms are shown in Figure C-11 through Figure C-18.

Table 9. Demonstration that HOI does not lead to the apparent formation of iodoform in the extract and stability of iodoform in the presence and absence of 100 mg/l sulfite (Experiment 33M, 11-16-2009).

Reactor No.	$NaHCO_3$, mM	HOCl, mM	I^-, mg/l	Sulfite, mg/l	CHI_3 added, µg/l in water	CHI_3 measured, µg/l in water
1	2	0.026	10	0	0	ND
2	2	0.026	10	100	0	ND
3	0	0	0	0	100	98
4	0	0	0	100	100	102

NOTE: Reactors were given about 15 minutes of reaction time, and sulfite was given about 1 minute of reaction time.

Table 10. Formation of iodoacetic acid with and without sulfite quenching and stability of iodoacetic acid in 100 mg/l sulfite (Experiment 33M, 11-16-2009.

Reactor No.	$NaHCO_3$, mM	HOCl, mM	I^-, mg/l	Sulfite, mg/l	IAA added, µg/l in water	IAA measured, µg/l in water
1	2	0.026	10	0	0	1329
2	2	0.026	10	100	0	ND
3	0	0	0	0	100	85
4	0	0	0	100	100	77

NOTE: Reactors were given about 15 minutes of reaction time, and sulfite was given about 1 minute of reaction time.

4.1.6 Comparison of iodoform and iodoacetic acid formation in lead oxide batch reactors in the presence and absence of sulfite quenching

Experiment 30M (11-02-2009) was a study of iodoform and iodoacetic acid formation for a reaction between lead oxide, NOM, and iodide with filtration and sulfite quenching of 100 mg/l. Iodoform formation, seen in Table 11, shows that the iodoform concentration in the buffer, lead oxide, and iodide reactor (Reactor 2) was reduced to 11 µg/l iodoform. Table 12 shows that iodoacetic acid formation in the buffer, lead oxide, and iodide reactor (Reactor 2) was almost completely inhibited, reducing detected iodoacetic acid from 2100 µg/l to 1 µg/l. The chromatograms are shown in Figure C-19 through Figure C-26.

Table 11. The affect of sulfite quenching on iodoform formation in batch reactors containing lead oxide and given reaction times of 72 hours (Experiment 30M, 11-02-2009).

Reactor No.	Initial pH	Final pH	HCO_3^-, mM	NOM, mg/l	PbO_2, mg/l	I-, mg/L	Sulfite, mg/l	CHI_3, µg/l in water
1	7.06	7.11	2	0	150	10	0	31
2	7.03	7.18	2	0	150	10	100	11
3	7.03	6.76	2	10	150	10	0	825
4	7.01	6.87	2	10	150	10	100	509

NOTE: All samples were filtered with 0.1 µm filters.

Table 12. The affect of sulfite quenching on iodoacetic acid formation in batch reactors containing lead oxide and given reaction times of 72 hours (Experiment 30M, 11-02-2009).

Reactor No.	Initial pH	Final pH	HCO_3^-, mM	NOM, mg/l	PbO_2, mg/l	I-, mg/L	Sulfite, mg/l	IAA measured, µg/l in water
1	7.06	7.11	2	0	150	10	0	2100
2	7.03	7.18	2	0	150	10	100	1
3	7.03	6.76	2	10	150	10	0	410
4	7.01	6.87	2	10	150	10	100	30

NOTE: All samples were filtered with 0.1 µm filters.

4.2 Formation of Iodoform and Iodoacetic Acid from Model Oxides

4.2.1 Iodoform and iodoacetic acid formation in batch reactors from varying NOM and PbO_2 concentrations

The impact of metal oxide and natural organic matter concentration were important variables studied in this project. Iodoform and iodoacetic acid formation was expected to increase with an increasing metal oxide concentration. As long as surface sites were available, the metal oxides were expected to be oxidation reservoirs for the formation of reactive iodine species. Also key to the availability of surface sites, the concentration of NOM was expected to increase the formation of iodo-DBPs up to a certain concentration. As NOM concentrations increase, the metal oxide particles are hypothesized to be covered by the NOM until finally the metal oxides can no longer provide oxidation sites for iodide, causing a decrease in the iodo-DBP formation.

Batch reactors were prepared with bicarbonate buffer and iodide, and either constant NOM and varying PbO_2 concentration or varying NOM and constant PbO_2 concentration. All samples were filtered with a 0.1 µm filter and quenched with 100 mg/l sodium sulfite.

Iodoform and iodoacetic acid formation are summarized in Table 13 and shown in Figure 7, as a function of lead oxide concentration, and Figure 8, as a concentration of added NOM. As anticipated, as lead oxide concentration was increased, DBP formation also increased, indicating that lead oxide did indeed act as an oxidant reservoir. When NOM was varied, iodoform and iodoacetic acid concentrations reached maximum concentrations at 5 mg/l NOM as C. At 5 mg/l NOM as C, 365 µg/l iodoform and 36 µg/l iodoacetic acid formed (Reactor 7). Concentrations decreased at 10 mg/l NOM as C, with 212µg/l iodoform and 26 µg/l iodoacetic acid formed (Reactor 8). As hypothesized previously, this may be due to a reduced rate of iodide oxidation caused by an increased surface coverage by NOM, or to a reduction in HOI concentration because of increased reaction with NOM as a general oxidant not leading to IAA formation, which likely requires a higher ratio of HOI to NOM. Chromatograms are shown in .Figure C-28 through Figure C-42.

Table 13. Experiments 38M and 39M (01-22-2010): Iodoform and iodoacetic acid formation by lead oxide, NOM, and iodide after 72 hours reaction time.

Reactor No.	Initial pH	Final pH	NOM, mg/l	PbO_2, mg/l	CHI_3, µg/l in water	IAA, µg/l in water
1	7.00	6.89	10	0	ND	ND
2	6.98	7.10	10	5	ND	ND
3	7.01	7.14	10	50	17	14
4	6.99	7.04	10	150	174	34
5	7.01	7.24	0	150	7	ND
6	7.02	7.14	1	150	202	21
7	7.00	7.02	5	150	365	36
8	7.00	7.02	10	150	212	26

NOTE: All batch reactors contain 2 mM bicarbonate buffer and 10 mg/l iodide and were quenched with 100 mg/l sulfite after filtration.

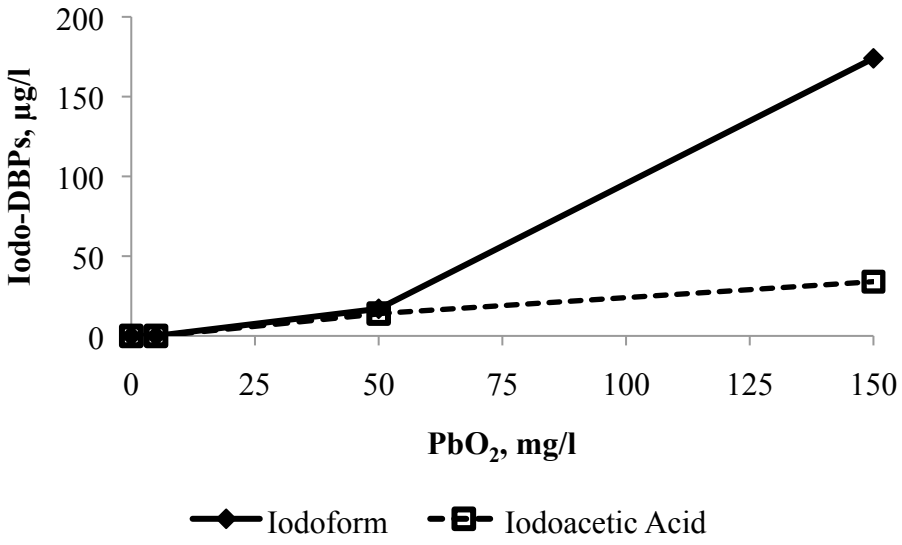

Figure 7. Formation of iodoform and iodoacetic acid as a function of lead oxide concentration, Experiments 38M and 39M (01-22-2010). Initial conditions: pH 7, 72 hours reaction time, 2 mM HCO_3^-, 10 mg/l I^-. Samples were quenched with 100 mg/l sulfite after 0.1µm filtration.

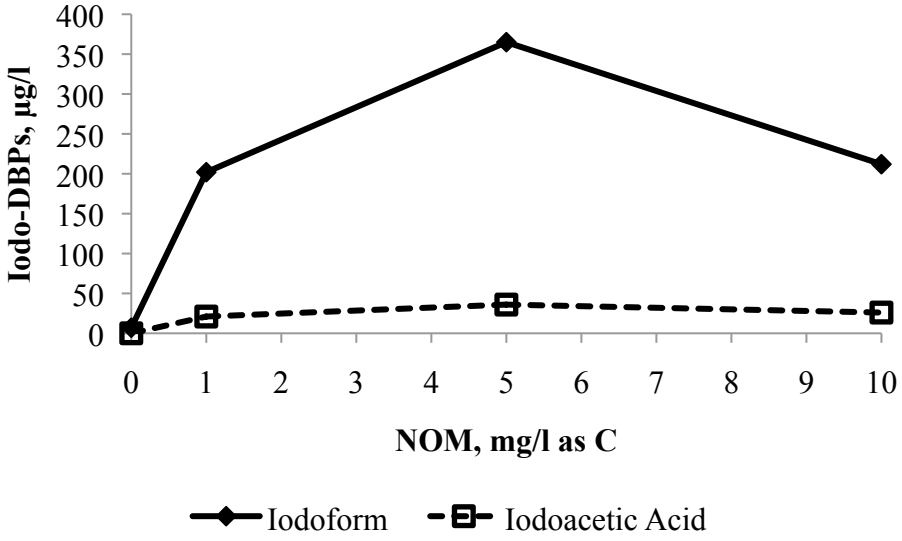

Figure 8. Formation of iodoform and iodoacetic acid as a function of NOM concentration, Experiments 38M and 39M (01-22-2010). Initial conditions: pH 7, 72 hours reaction time, 2 mM HCO_3^-, 150 mg/l PbO_2, 10 mg/l I^-. Samples were quenched with 100 mg/l sulfite after 0.1µm filtration.

4.2.2 Iodoform and iodoacetic acid formation in batch reactors from varying MnO_2 and NOM concentration

Experiments studying the formation of iodoform and iodoacetic acid from the oxidation of iodide by lead oxide have shown that high concentrations of these iodo-DBPs were detected at relatively low concentrations of lead oxide. Manganese dioxide was shown to also oxidize iodide, but to a lesser extent than lead oxide. To study the formation of iodoform and iodoacetic acid in the presence of manganese dioxide, MnO_2 concentrations were increased.

Batch reactors were prepared with bicarbonate buffer, NOM, 500 mg/l or 1000 mg/l MnO_2, and iodide at pH 7. Results are summarized in Table 14. Figure 9 shows iodoacetic acid concentrations increasing with increasing reaction times. MnO_2 was expected to act as an oxidant reservoir, and it was expected that iodoacetic acid concentrations would increase with increasing MnO_2, as shown in Figure 10. The formation of iodoform in the batch reactors was also studied, but iodoform was not detected. Gallard et al performed a similar experiment at pH 5 in which only 2 µg/l iodoform was detected (Gallard, et al., 2009). At the higher pH used in this experiment it is reasonable that no iodoform would form. Chromatograms are shown in Figure C-43 through Figure C-48.

Table 14. Iodoacetic acid formation in reactors containing NOM, MnO_2, and iodide after 48 or 72 hours reaction time (Experiments 43M, 02-05-2010 and 48M, 02-24-2010).

Reactor No.	Reaction time, hr.	Initial pH	Final pH	NOM, mg/l	MnO_2, mg/l	CHI_3, µg/l in water	IAA, µg/l in water
1	48	6.96	7.05	0	1000	ND	ND
2	48	6.99	6.78	10	500	ND	6
3	48	6.99	6.69	10	1000	ND	30
4	72	6.85	6.56	0	1000	ND	4
5	72	6.87	6.68	10	500	ND	28
6	72	6.83	6.70	10	1000	ND	63

NOTE: All batch reactors contain 2 mM bicarbonate buffer, 10 mg/l NOM as C, and 10 mg/l iodide and were quenched with 100 mg/l sulfite after 0.1 µm filtration.

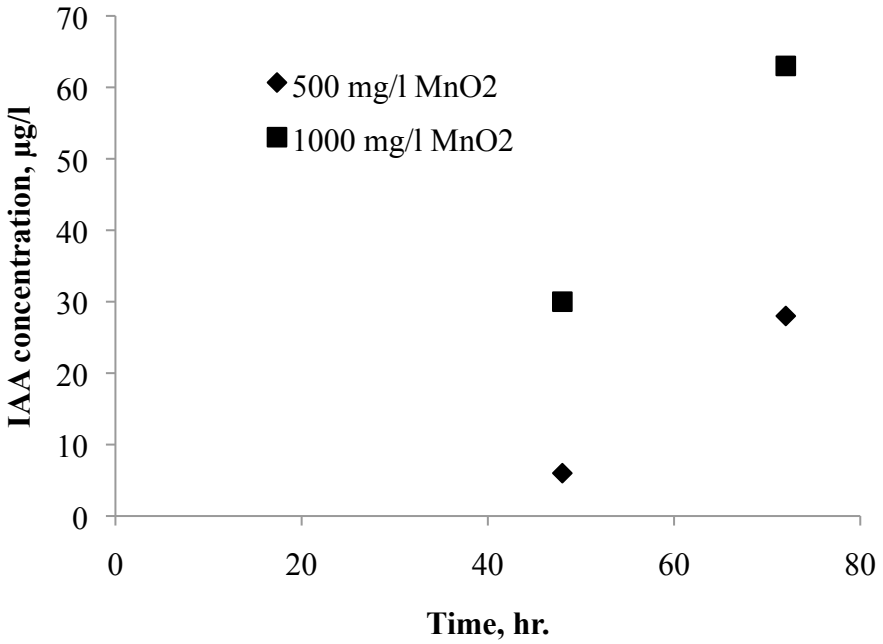

Figure 9. Formation of iodoacetic acid as a function of time, Experiments 43M (02-05-2010) and 48M (02-24-2010). All samples were quenched with 100 mg/l sulfite after 0.1 µm filtration. Initial conditions: pH 7, 2 mM HCO_3^-, 10 mg/l NOM as C, and 10 mg/l I^-.

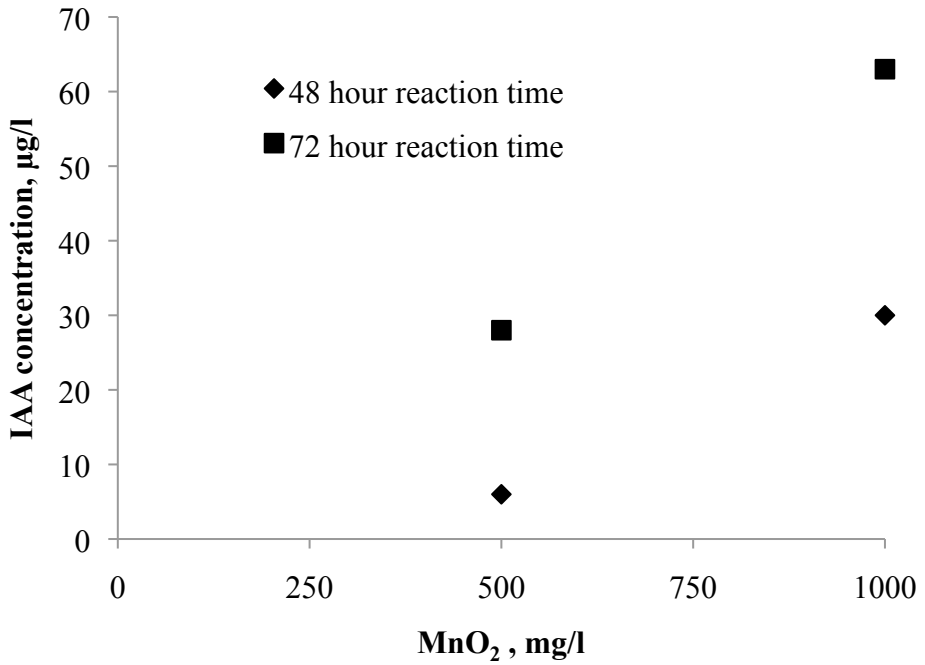

Figure 10. Formation of iodoacetic acid as a function of MnO_2 concentration, Experiments 43M (02-05-2010) and 48M (02-24-2010). All samples were quenched with 100 mg/l sulfite after 0.1 µm filtration. Initial conditions: pH 7, 2 mM HCO_3^-, 10 mg/l NOM as C, and 10 mg/l I^-.

Further studies were conducted to see if iodoform could be formed from manganese dioxide. Batch reactors were prepared at pH 7 and given 48 hours of reaction time. Similar conditions with lower NOM concentrations, 2 mM HCO_3^-, 5 mg/l C added NOM, 1000 mg/l MnO_2, and 10 mg/l I^-, were used unless the NOM or MnO_2 was varied. The results are summarized in Table 15. Like the lead oxide experiments, iodoform and iodoacetic acid concentrations increased with increasing MnO_2, shown in Figure 11, demonstrating the reservoir of oxidation potential of metal oxides. When NOM was varied, iodoform formation decreased after 1 mg/l C from added NOM, but iodoacetic acid increased throughout the experiment, shown in Figure 12. Chromatograms are shown in Figure C-49 through Figure C-64. A possible theory for this trend is that higher HOI concentrations result in the formation of iodoform, whereas lower HOI

concentrations result in iodoacetic acid formation. This is consistent with the oxidation potential of lead oxide and manganese dioxide. Proposed reactions are shown below.

$$NOM + xHOI = CHI_3 \quad (13)$$

$$NOM + yHOI = CH_2ICOOH \quad (14)$$

where x>y

Table 15. Iodoform and iodoacetic acid formation from varying NOM and MnO_2 concentrations after 48 hours reaction time (Experiment 57M, 04-10-2010).

Reactor No.	Initial pH	Final pH	NOM, mg/l	MnO_2, mg/l	CHI_3, µg/l in water	IAA, µg/l in water
1	7.04	6.92	0	1000	5	5
2	7.05	6.92	1	1000	27	7
3	7.02	6.71	5	1000	7	25
4	7.03	6.6	10	1000	ND	38
5	7.08	6.85	5	0	ND	ND
6	7.03	6.76	5	250	ND	7
7	7	6.75	5	500	ND	18
8	7	6.7	5	1000	10	27

NOTE: All batch reactors contain 2 mM HCO_3^-, and 10 mg/l I^- and were filtered with 0.1 µm filters and quenched with 100 mg/l sulfite.

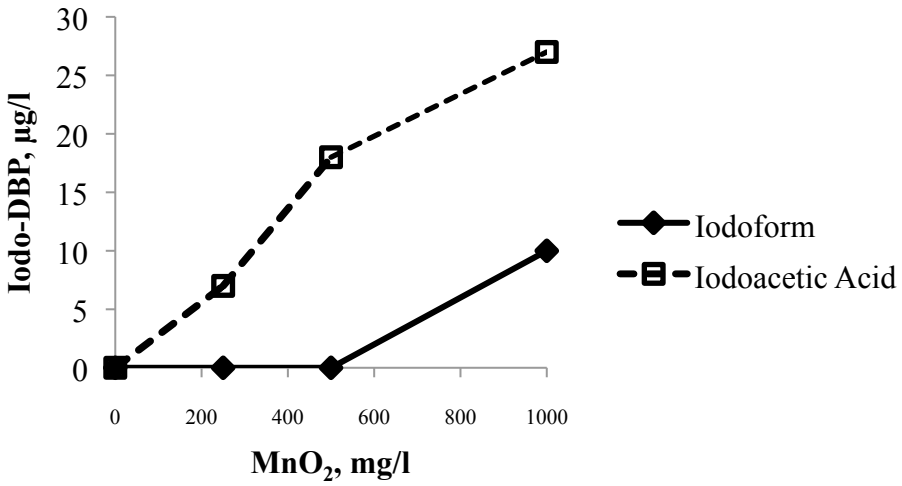

Figure 11. Formation of iodoform and iodoacetic acid as a function of MnO_2 concentration, Experiment 57M (04-10-2010). All samples were quenched with 100 mg/l sulfite after 0.1 µm filtration. Initial conditions: pH 7, 2 mM HCO_3^-, 5 mg/l NOM as C, and 10 mg/l I^-.

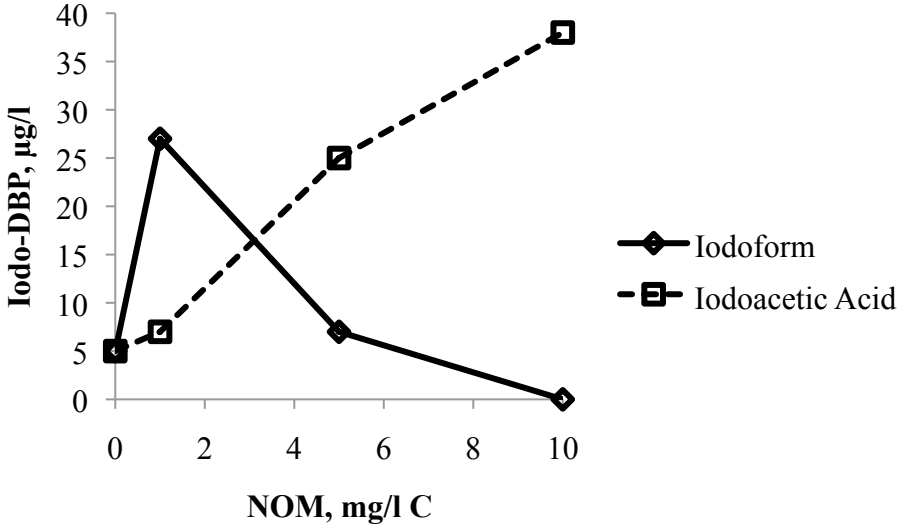

Figure 12. Formation of iodoform and iodoacetic acid as a function of added NOM concentration, Experiment 57M (04-10-2010). All samples were quenched with 100 mg/l sulfite after 0.1 µm filtration. Initial conditions: pH 7, 2 mM HCO_3^-, 1000 mg/l MnO_2, and 10 mg/l I^-.

4.2.3 Iodoform and iodoacetic acid formation in batch reactors containing NOM, goethite (FeO(OH)), and iodide

Previous experiments have shown that iodoform and iodoacetic acid can form from reactions of NOM and oxidized iodine species that were oxidized by lead oxide and manganese dioxide. Iron, a major component of pipe deposits, was also investigated for potential iodoform and iodoacetic acid formation. Goethite (FeO(OH)) was prepared in the Scherer Lab in the environmental engineering laboratories at the University of Iowa as described by Cwiertny et al (2008). KOH was rapidly added to $Fe(NO_3)_3$ and held in a closed flask at 70°C for 60 hours. The goethite particles that formed were microrods, similar to those shown in Figure 13. The goethite used in this experiment had a specific surface area of 33 m^2/g, and the particles were sieved so that they ranged between 45-150 µm.

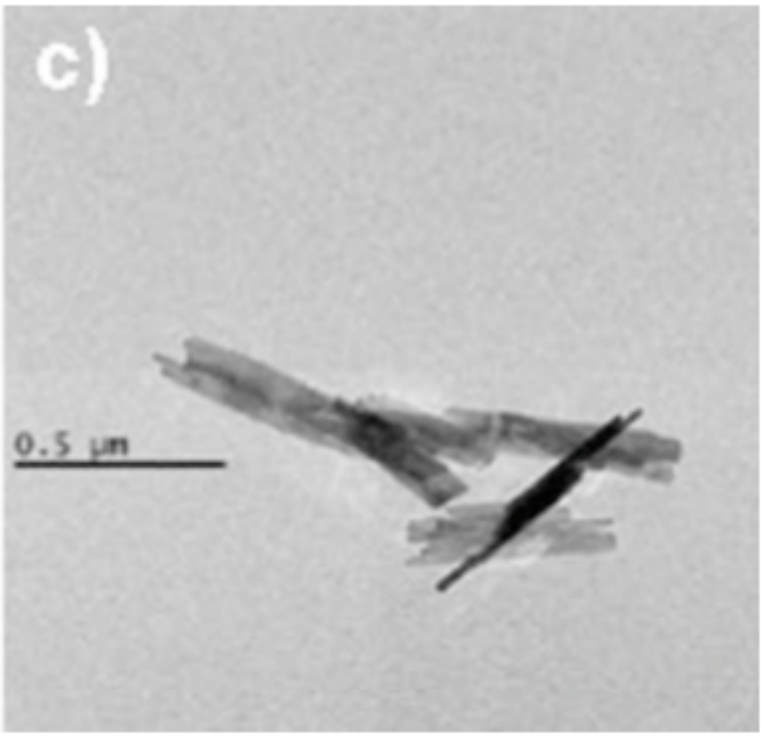

Figure 13. TEM image of synthesized microrod goethite (Cwiertny, et al., 2008).

Formation of HOI in batch reactors containing buffer, goethite, and iodide was measured over four hours by DPD-FAS titration. The results are summarized in Table 16 and Figure 14. HOI formation increased over the duration of the experiment from no formation initially to 0.2 mg/l HOI at four hours. One sample with added NOM was analyzed after two hours, and no HOI was measured, as expected.

Table 16. Formation of HOI from a reaction of FeO(OH) and iodide in the absence of NOM as measured with DPD-FAS titration (Experiment 60M, 04-22-2010).

Reactor No.	Time, hr	Initial pH	Final pH	FeO(OH), mg/l	HOI, mg/l as Cl_2
1	0	6.98	6.98	1000	0
2	1	6.96	6.97	1000	0.1
3	2	7.02	6.95	1000	0.2
4	4	6.95	6.95	1000	0.2

NOTE: All samples contain 2 mM HCO_3^- and 10 mg/l I^- and were filtered with 0.1 µm filters prior to quenching with 100 mg/l sulfite.

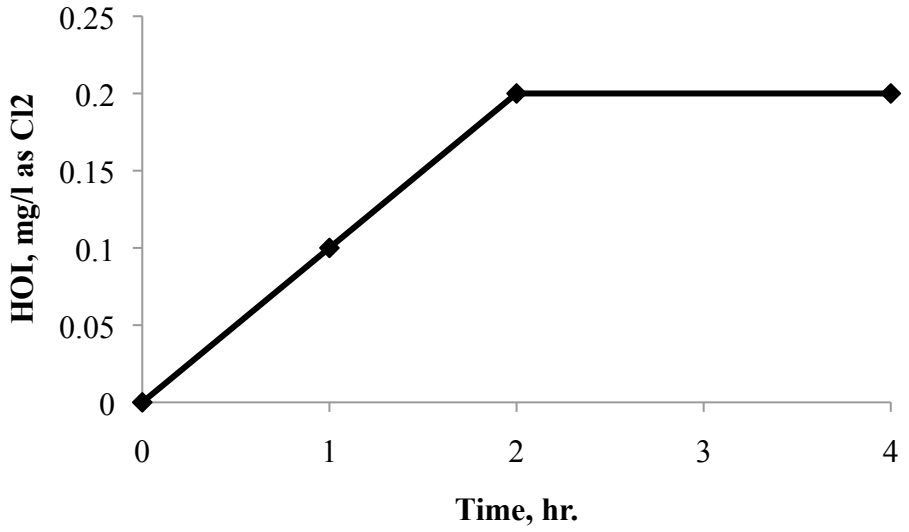

Figure 14. Formation of HOI as a function of time from a reaction of FeO(OH) and iodide in the absence of NOM, Experiment 60M (04-22-2010). Initial conditions: pH 7, 2 mM HCO_3^-, 1000 mg/l FeO(OH), and 10 mg/l I^-.

Batch reactors were prepared with 2 mM HCO_3^- buffer, 5 mg/l added NOM as C (if added), 1000 mg/l FeO(OH), and 10 mg/l I^-. Batch reactors were adjusted to either pH 6 or 7 and given 48 hours reaction time. Samples were filtered with 0.1 µm filters and quenched with 100 mg/l sulfite. Table 17 summarizes the results. Some iodoform formed without added NOM, likely due to organic carbon. The formation was much higher with added NOM, with 165 to 252 µg/l CHI_3 forming at pH 6 and 135 to 237 µg/l CHI_3 forming at pH 7. Iodoacetic acid formation occurred with added NOM only, with 26 to 33 µg/l IAA forming at pH 6 and 22 to 26 µg/l IAA forming at pH 7. Small peaks equivalent to 9 µg/l and 7 µg/l IAA at pH 6 and 7, respectively, were detected at 9.48 minutes in batch reactors without added NOM. While these peaks are probably not positive detection of iodoacetic acid, they should be noted. These results may suggest that the large amounts of iron found in the pipe deposits used in this project are composed mainly of iron(II), since iron(III) has been shown to form iodoform and iodoacetic acid. The iron(II) may act as a sink, with HOI oxidizing Fe(II) to Fe(III) instead of oxidizing NOM. Chromatograms are shown in Figure C-65 through Figure C-78.

Table 17. Formation of iodoform and iodoacetic acid from batch reactors containing NOM, goethite, and iodide (Experiment 59M, 04-21-2010) at pH 7 and 48 hours reaction time.

Reactor No.	Initial pH	Final pH	NOM, mg/l C	FeO(OH) mg/l	CHI_3, µg/l in water	IAA, µg/l in water
1	7.08	6.74	5	0	ND	ND
2	6.06	5.75	0	1000	30	9?
3	7.02	6.56	0	1000	29	7?
4	6.05	5.57	5	1000	252	33
5	6.01	5.62	5	1000	165	26
6	7.02	7.02	5	1000	237	26
7	7.05	6.75	5	1000	135	22

NOTE: All batch reactors contain 2 mM HCO_3^- and 10 mg/l I^- and were filtered with 0.1 µm filters prior to quenching with 100 mg/l sulfite.

4.3 Formation of Iodinated Disinfection By-Products from Authentic Pipe Deposits

Iodoform and iodoacetic acid have been shown to form under laboratory conditions containing model metal oxides, natural organic matter, and iodide. The extraction methods for both iodinated compounds have been developed so that a residual reactive iodine species will not affect their detection. The most important question of this project remains: Can iodoform and iodoacetic acid form in municipal drinking water systems? It must be stressed that this study was a high-risk exploratory project. The pathway for the formation of these iodo-DBPs has been hypothesized but has not been studied before.

Sections of drinking water distribution pipe were acquired from municipal drinking water authorities from various locations across the United States. The mineral deposits that had built up over time inside these pipes were removed with a hammer and chisel, ground to a powder, sieved, and stored by sieve size. Particle sizes of the authentic pipe deposits used in this project were in the range of 45-150 μm. Since the iodo-DBP formation is a surface reaction, small particles were necessary to have the greatest possible surface area for reactions.

Although lead oxide was shown to have the greatest oxidation potential, authentic pipe deposit studies focused on manganese dioxide. Manganese is used in drinking water treatment and is relatively common in pipe deposits, making it a good oxidant to study. This project looked at the formation of iodoform and iodoacetic acid from the authentic pipe deposits that contained high masses of manganese per mass of extracted deposit. Batch reactors were prepared with 2 mM bicarbonate buffer, 1000 mg/l authentic pipe deposit and 10 mg/l iodide and given 48 hours reaction time. Samples were filtered with 0.1 μm filters and quenched with 100 mg/l sulfite. Batch reactors with added NOM contained 5 mg/l NOM as C. The concentration was decreased from 10 mg/l added

NOM as C as used in previous experiments since it was shown that reactors containing 5 mg/l added NOM as C produced more iodoform and iodoacetic acid, possibly due to less oxide coverage by the NOM. The authentic pipe deposit particles were composed of many different compounds, so surface reaction sites were possibly less available than the sites available on the model metal oxides. A decrease in NOM concentration may also decrease the potential for site coverage by NOM.

Of the five authentic pipe deposits that were studied, only one showed the formation of iodoform. The deposit, WDB-A, was a very unique sample with a high percentage of manganese in its composition. At 230,000 µg Mn per gram of deposit, it had a manganese mass nearly five times greater than any other deposit. While there are likely many other factors involved, the high levels of manganese in WDB-A could indicate an important factor when determining the potential for iodo-DBP formation in drinking water distribution systems.

Table 18 shows that the formation of iodoform occurred at pH 6 and 7, with higher concentrations at pH 6. Iodoform formation without NOM, 42 µg/l at pH 6 and 38 µg/l at pH 7, was not considered erroneous since there was most likely organic carbon associated with the authentic pipe deposit. A very large amount of iodoform, 469 µg/l, was formed in the presence of NOM at pH 6 and decreased to 40 µg/l at pH 7. Chromatograms for this experiment are shown in Figure C-79 through Figure C-84.

The pipe deposit "WDB-A" also formed a high concentration of iodoacetic acid, shown in Table 18. Without the addition of NOM, iodoacetic acid formation was greatest at pH 6, 15 µg/l, and then decreased to 5 µg/l at pH 7. With authentic pipe deposits, iodoacetic acid formation may be possible without the addition of NOM since there is likely organic carbon associated with the deposits. Iodoacetic acid formation occurred in the presence of added NOM, but the concentration unexpectedly increased from 36 µg/l at pH 6 to 41 µg/l at pH 7. Chromatograms for this experiment are shown in Figure C-85 through Figure C-90.

Table 18. Formation of iodoform and iodoacetic acid from authentic pipe deposit "WDB-A" (Experiment 50M, 03-09-2010).

Reactor No.	Initial pH	Final pH	NOM, mg/l	WDB-A, mg/l	CHI_3, µg/l in water	IAA, µg/l in water
1	6.01	6.04	0	0	ND	2
2	5.99	6.02	5	0	ND	ND
3	6.00	6.31	0	1000	42	15
4	7.00	7.13	0	1000	38	5
5	5.98	6.29	5	1000	469	36
6	6.95	7.01	5	1000	40	41

NOTE: All reactors contain 2 mM bicarbonate buffer and 10 mg/l iodide and were given 48 hours to react. Samples were quenched with 100 mg/l sulfite after 0.1 µm filtration.

Other authentic pipe deposits used in the study were shown to form small amounts of iodoacetic acid, but no iodoform was detected. The deposit, "J-B," (Experiment 52M, 03-15-2010) was composed of 30,000 micrograms manganese per gram of deposit, nearly eight times less than WDB-A. The results showed that 2 µg/l iodoacetic acid formed at pH 6 and pH 7. Similar results occurred with WA-A pipe deposits, with 2 µg/l IAA forming in batch reactors at pH 7 with added NOM. In CL-D, 1 µg/l IAA formed at pH 7 with added NOM. No iodoacetic acid formed in CC-A. With the low levels of lead and manganese in the composition of these four pipe deposits, little iodide oxidation is expected. This is consistent with the hypothesis that low levels of HOI concentrations could lead to preferential formation of iodoacetic acid.

Table 19. Summary of iodoform formation in batch reactors containing 2 mM bicarbonate, 5 mg/l NOM as C (if added), 1000 mg/l authentic pipe deposit, and 10 mg/l I^- after 48 hours reaction time.

Water System	Lead, ($\mu g/g_{ext}$)	Manganese ($\mu g/g_{ext}$)	CHI_3, µg/l			
			pH 6, no NOM	pH 7, no NOM	pH 6, w/ NOM	pH 7, w/ NOM
WDB-A	25.07	232475.93	42	38	469	40
CC-A	59.65	46692.11	ND	ND	ND	ND
J-B	407.09	30116.88	ND	ND	ND	ND
WA-A	53.27	3713.79	ND	ND	ND	ND
CL-D	8.29	1393.43	ND	ND	ND	ND

Table 20. Summary of iodoacetic acid formation in batch reactors containing 2 mM bicarbonate, 5 mg/l NOM as C (if added), 1000 mg/l authentic pipe deposit, and 10 mg/l I^- after 48 hours reaction time.

Water System	Lead, ($\mu g/g_{ext}$)	Manganese ($\mu g/g_{ext}$)	IAA, µg/l			
			pH 6, no NOM	pH 7, no NOM	pH 6, w/ NOM	pH 7, w/ NOM
WDB-A	25.07	232475.93	15	5	36	41
CC-A	59.65	46692.11	ND	ND	ND	ND
J-B	407.09	30116.88	ND	ND	2	2
WA-A	53.27	3713.79	ND	ND	ND	2
CL-D	8.29	1393.43	ND	ND	ND	1

4.3.1 Formation of iodoform and iodoacetic acid from batch reactors containing NOM, pre-oxidized pipe deposit, and iodide

Previous experiments have shown that goethite, and iron(III) oxide, is capable of oxidizing iodide, resulting in the formation of iodoform and iodoacetic acid. Since the four pipe deposits that are low in manganese did not show much iodoform or iodoacetic acid formation, they may be composed mainly of iron(II) oxides. To investigate this, pipe deposit CC-A was added to DI water along with a molar concentration of hydrogen peroxide (H_2O_2) equivalent to the molar concentration of the iron in pipe deposit. A 500 ml beaker was filled with DI water, and 2 g CC-A pipe deposit were added. For 4000

mg/l of CC-A and assuming an iron content of 23.5%, 15 mM H_2O_2 was added. After 24 hours reaction time, the particles were allowed to settle and the supernatant was removed. The particles were rinsed with 500 ml fresh DI water, centrifuged, and added to a volume of 500 ml fresh DI water. Aliquots of this 4000 mg/l CC-A suspension were used in the following experiment (Experiment 62M, 04-23-2010).

Batch reactors were prepared with 2 mM HCO_3^-, 5 mg/l added NOM as C, 1000 mg/l CC-A pipe deposit, and 10 mg/l I^- (Experiment 62M, 04-23-2010). The reactors were adjusted to pH 7 and given 48 hours reaction time. About 5 µg/l IAA formed in the two batch reactors containing added NOM only, and no iodoform was detected in any batches. Note that previous experiments with batch reactors containing CC-A did not result in the formation of iodoform or iodoacetic acid. This may suggest that the content of oxidized pipe deposits in natural systems could change to favor the oxidation of iodide or other halogens. Chromatograms are found in Figure C-91 through Figure C-95.

Table 21. Formation of iodoform and iodoacetic acid in batch reactors containing pre-oxidized CC-A pipe deposit (Experiment 62M, 04-23-2010).

Reactor No.	Initial pH	Final pH	NOM, mg/l C	CC-A, mg/l	CHI_3, µg/l in water	IAA, µg/l in water
1	7.05	6.83	5	0	ND	ND
2	7.04	6.85	0	1000	ND	ND
3	7.03	6.95	0	1000	ND	ND
4	7.05	6.88	5	1000	ND	4
5	7.01	6.83	5	1000	ND	5

NOTE: All reactors contain 2 mM HCO_3^- buffer and 10 mg/l I^-. All samples were filtered with 0.1 µm filters prior to quenching with 100 mg/l sulfite.

CHAPTER 5
CONCLUSIONS

The objective of this project was to investigate a novel pathway for the formation of the iodinated disinfection by-products iodoform and iodoacetic acid. Initial research showed surprisingly high levels of iodoacetic acid formation in batch reactors with no added NOM. This was ultimately attributed to reactions involving unfiltered solids reacting during the extraction-derivitization process and to reactions of excessive HOI. These artifacts were adequately addressed by filtering samples with a 0.1 μm filter and quenching with sodium sulfite. Filtration is only operational, so some artifact may occur if this analytical approach is used. Future studies need to better characterize this artifact potential at low iodoacetic acid formation potentials. Possibly investigate their formation as a function of known additions of particulate metal oxides to provide a constraint on the significance of the artifact.

Lead(IV) oxide, manganese(IV) oxide, and iron(III) oxide as goethite formed both iodinated disinfection by-products in the presence of high iodide concentrations at environmentally relevant, near neutral pH conditions. The two iodo-DBPs were formed in the presence of several authentic pipe deposits. Formation of these DBPs in the absence of added NOM suggests that the naturally occurring NOM associated with the deposits reacted with the reactive iodine species.

The highest concentration of NOM in batch reactors with lead oxide resulted in a reduction in DBP formation. It is hypothesized due either to a reduction in iodide oxidation rate as a consequence of increased surface coverage of the solids or to a reduction in HOI available to extensively react with NOM to produce the measured DBPs. In other words, the HOI could have simply oxidized the NOM without the formation of measureable DBPs, which would require additional HOI. Another hypothesis is that iodo-DBP speciation depends on HOI concentrations in solution.

Iodoform concentrations were greater in batch reactors with lead oxide. Conversely, iodoacetic acid concentrations were greater in manganese dioxide batch reactors. Lead oxide is a stronger oxidant than manganese dioxide, resulting in higher HOI concentrations in batch reactors with lead oxide.

Increased formation of DBPs with increasing manganese dioxide concentration was demonstrated. The formation of iodoform from authentic pipe deposits focused on the manganese composition. Although lead oxide was shown to be a stronger oxidant, manganese dioxide is more relevant to water treatment distribution systems. Iodoform was shown to form in only one of the studied authentic pipe deposits, "WDB-A." This pipe deposit was composed of about 23% manganese and contained over five times more manganese than any other authentic pipe deposit. With no NOM, 42 µg/l CHI_3 and 38 µg/l CHI_3 were measured at pH 6 and pH 7, respectively, resulting from organic carbon that is most likely associated with the pipe deposit. When NOM was added, 469 µg/l CHI_3 and 40 µg/l CHI_3 formed at pH 6 and pH 7, respectively.

Iodoacetic acid formation from authentic pipe deposits occurred in batch reactors containing "WDB-A" pipe deposit, and to a less extent in reactors with "J-B" and "WA-A" pipe deposits. With no added NOM, 15 µg/l IAA and 5 µg/l IAA formed at pH 6 and pH 7, respectively in the "WDB-A" system. When NOM was added, 36 µg/l IAA and 41 µg/l IAA formed at pH 6 and pH 7, respectively. In the "J-B" and "WA-A" pipe deposit systems, no iodoacetic acid formed in the absence of added NOM. In "J-B," 2 µg/l IAA formed at pH 6 and pH 7 with added NOM, and 2 µg/l IAA formed at pH 7 only in "WA-A." In "Cl-D," 1 µg/l IAA formed at pH 7 with added NOM. No iodoacetic acid formation occurred in "CC-A" batch reactors, but after oxidizing the particles with hydrogen peroxide, about 5 µg/l IAA was detected in batch reactors containing NOM. This suggests that oxidation of pipe deposits may change the nature of the deposits to consist of more reactive substances, such as iron(III), and to reduce or eliminate species, such as iron(II), that may have acted to reduce HOI back to iodide.

CHAPTER 6
ENGINEERING SIGNIFICANCE AND FUTURE RESEARCH

This research has shown conclusive evidence that the iodinated disinfection by-products iodoform and iodoacetic acid can be formed in systems containing natural organic matter, model metal oxides or authentic deposit material, and iodide. In these studies concentrations of iodide were several orders of magnitude higher than expected in most drinking waters, a requirement necessitated by a DBP detection limit of approximately 1 μg/l. However, iodinated disinfection by-products are more toxic than their brominated and chlorinated analogs. Health studies indicate a concern at ng/l levels (Plewa, et al., 2004). This suggests that if formation of these DBPs is linear with iodide concentration, then this formation pathway may be significant. Assuming a hypothetical iodide concentration in natural water of 100 μg/l, iodo-DBP formation of about 0.40 μg/l is possible based on the authentic pipe deposit research. Even at very low concentrations, iodo-DBPs could present a health risk. Drinking water distribution systems may also provide the surface area and contact time required for iodide oxidation.

The relatively fast rates of formation for iodoform and iodoacetic acid along with their stability in water suggests that iodide might be oxidized in a drinking water distribution system and remain stable long enough to form these DBPs at the ng/L levels.

Changing source water or treatment methods could also result in the formation of iodinated disinfection by-products. Depending on the source of the water, such as desalinated seawater, iodide concentrations could increase. With enough pipe deposit buildup in the distribution system, a high concentration of HOI could form. Seawater has relatively high iodide concentrations, so as desalinization becomes a more widespread drinking water technique, greater populations could be at risk of iodo-DBPs. Free chlorine was used in experiments to produce HOI. Likewise, changing treatment methods to free chlorine could cause unexpected oxidation of iodide.

Further research on the formation of iodinated disinfection by-products from authentic pipe deposits should continue. Only a few authentic pipe deposits were analyzed in this research. Studying the correlation between iodo-DBP formation and authentic pipe deposit composition should be an important focus going forward, this should include the role of reduced species that might act to quench HOI as fast as it is formed. Efforts should be taken to continue the acquisition of more pipe deposits from municipal drinking water authorities. Critical to further work is the use of analytical methods that can measure these iodo-DBPs at the ng/l level. The prevention of artifacts should be continued, as particles in suspension not removed by filtration could be very problematic when measuring at the ng/l level. There needs to be a better artifact characterization at low iodoacetic acid formation potentials. As research progresses further, performing experiments in conditions more like drinking water, such as lower concentrations of natural organic matter and iodide, could provide important results.

APPENDIX A
METHOD DETECTION LIMIT CALCULATIONS

Table A-1. Iodoform MDL calculations using GC-ECD.

Sample #	Peak Area (Hz-s)	Iodoform Concentration (µg/L)
1	4317.03	1.7838
2	3299.45	1.2483
3	3793.06	1.2830
4	1787.65	0.7036
5	2464.11	0.8086
6	2879.66	1.0273
7	2663.11	0.9113
Sample STDEV		0.3664
Average (µg/L) =		1.109
MDL at 99% Conf (µg/L) =		**1.152**

Table A-2. Iodoacetic acid MDL calculations using GC-ECD.

Sample #	Peak Area (Hz-s)	IAA Concentration (µg/L)
1	2688.48	3.129
2	2802.24	3.186
3	2459.98	3.013
4	2786.41	3.178
5	2396.28	2.981
6	2817.44	3.194
7	277155	3.171
Sample STDEV =		0.088
Average (µg/L) =		3.122
MDL at 99% Conf (µg/L) =		**0.277**

APPENDIX B

TOTAL ORGANIC CARBON MEASUREMENTS

Table B-1. Total organic carbon measurements of Valentine Pond RO concentrate

Date	TOC, mg/l
04-09-2009	117.1
06-05-2009	131.0
08-11-2009	124.6
11-19-2009	114.3
03-22-2010	116.9

APPENDIX C

CHROMATOGRAMS

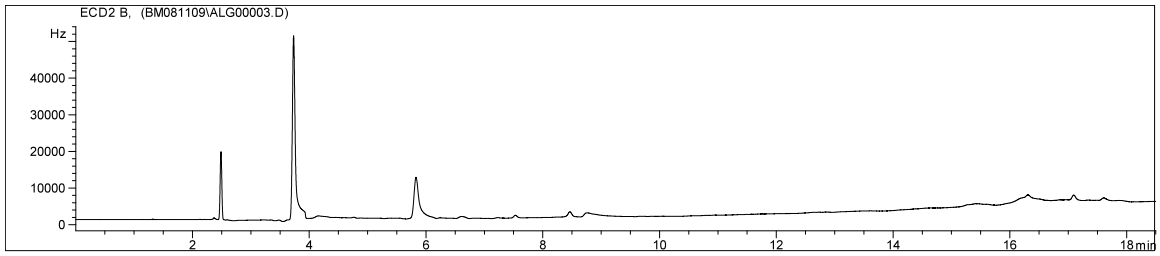

Figure C-1. Batch reactors containing 2 mM buffer and 10 mg/l NOM as C, pH 7, 72 hours reaction time, Experiment 23M (08-11-2009). No peak at iodoacetic acid retention time of 9.76 minutes was present.

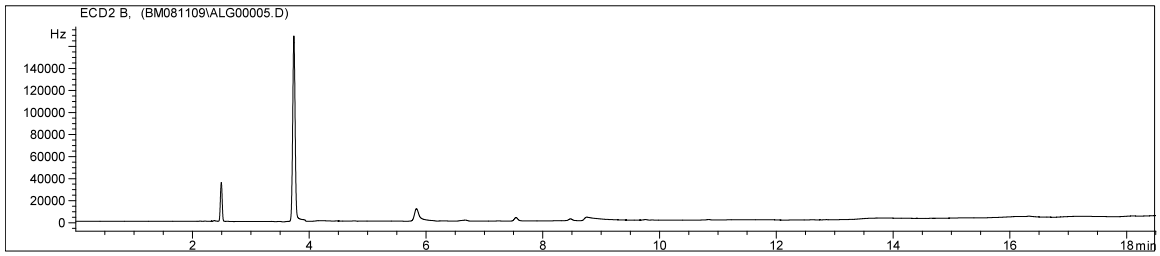

Figure C-2. Batch reactors containing 2 mM buffer and 10 mg/l I^-, pH 7, 72 hours reaction time, Experiment 23M (08-11-2009). No peak at iodoacetic acid retention time of 9.76 minutes was present.

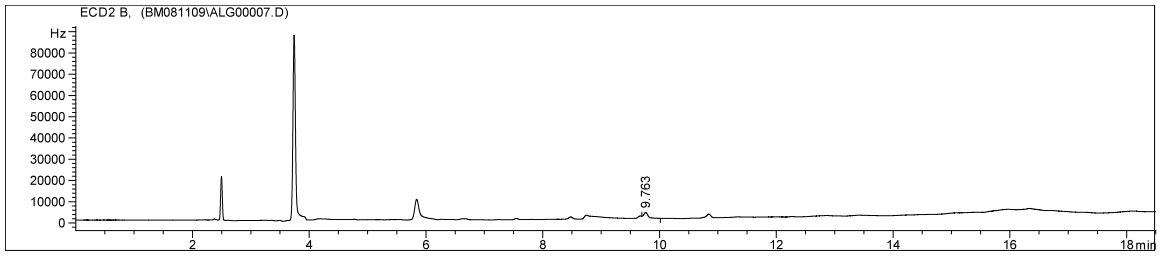

Figure C-3. Batch reactors containing 2 mM buffer, 10 mg/l NOM as C, and 10 mg/l I^-, pH 7, 72 hours reaction time, Experiment 23M (08-11-2009). A peak equivalent to 7.29 µg/l IAA was present at the iodoacetic acid retention time of 9.76 minutes.

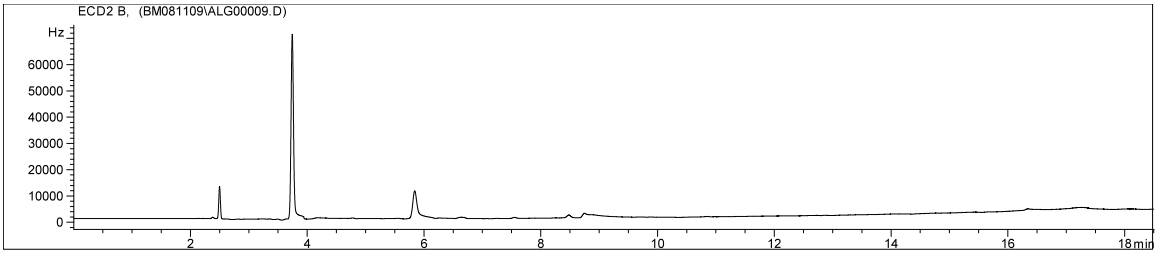

Figure C-4. Batch reactors containing 2 mM buffer and 150 mg/l lead oxide, pH 7, 72 hours reaction time, Experiment 23M (08-11-2009). No peak at iodoacetic acid retention time of 9.76 was present.

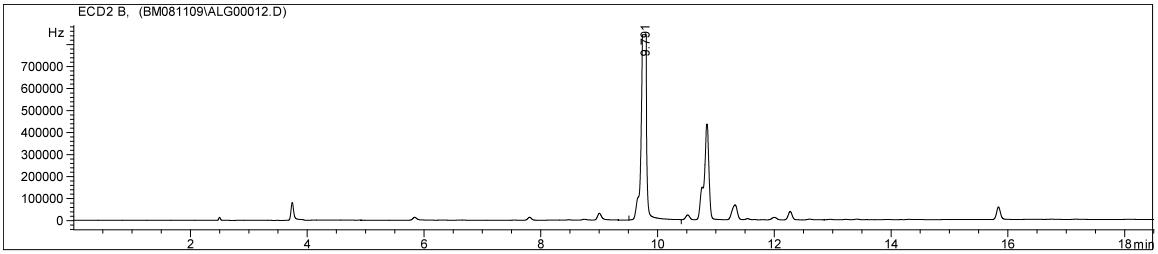

Figure C-5. Batch reactors containing 2 mM buffer, 150 mg/l lead oxide, and 10 mg/l I^-, filtered sample, pH 7, 72 hours reaction time, Experiment 23M (08-11-2009). A peak equivalent to 2166 µg/l IAA was present at the iodoacetic acid retention time of 9.76 minutes.

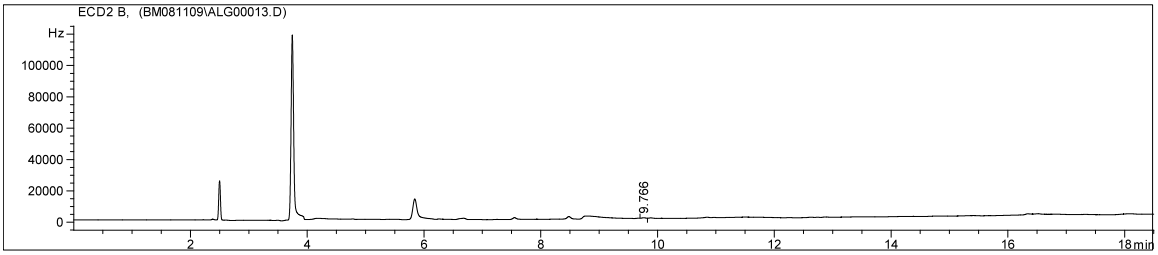

Figure C-6. Batch reactors containing 2 mM buffer, 150 mg/l lead oxide, and 10 mg/l I^- (I^- added after filtration), pH 7, 72 hours reaction time, Experiment 23M (08-11-2009). A peak equivalent to 4.33 µg/l IAA was present at the iodoacetic acid retention time of 9.76 minutes.

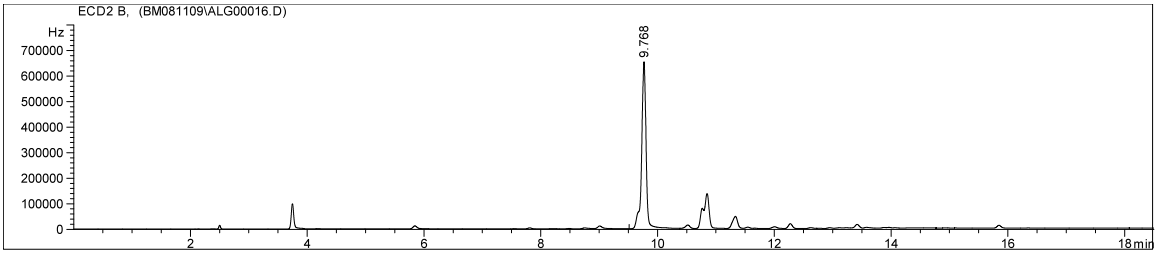

Figure C-7. Batch reactors containing 2 mM buffer, 150 mg/l lead oxide, and 10 mg/l I^-, unfiltered sample, pH 7, 72 hours reaction time, Experiment 23M (08-11-2009). A peak equivalent to 1350 µg/l IAA was present at the iodoacetic acid retention time of 9.76 minutes.

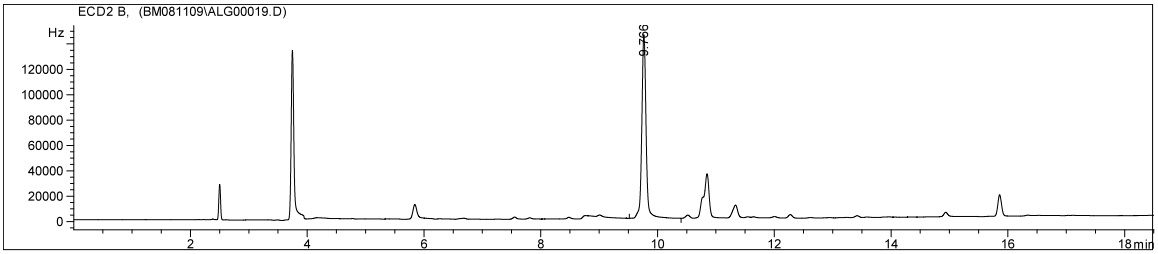

Figure C-8. Batch reactors containing 2 mM buffer, 10 mg/l NOM as C, 150 mg/l lead oxide, and 10 mg/l I^-, filtered sample, pH 7, 72 hours reaction time, Experiment 23M (08-11-2009). A peak equivalent to 293 µg/l IAA was present at the iodoacetic acid retention time of 9.76 minutes.

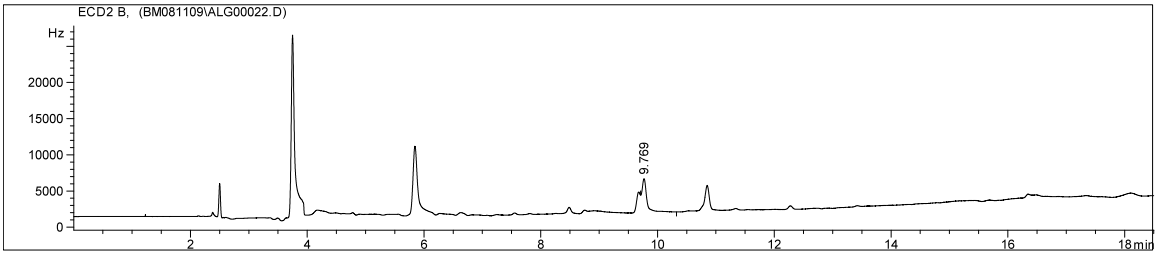

Figure C-9. Batch reactors containing 2 mM buffer, 10 mg/l NOM as C, 150 mg/l lead oxide, and 10 mg/l I^- (I^- added after filtration), pH 7, 72 hours, Experiment 23M (08-11-2009). A peak equivalent to 14.93 µg/l IAA was present at the iodoacetic acid retention time of 9.76 minutes.

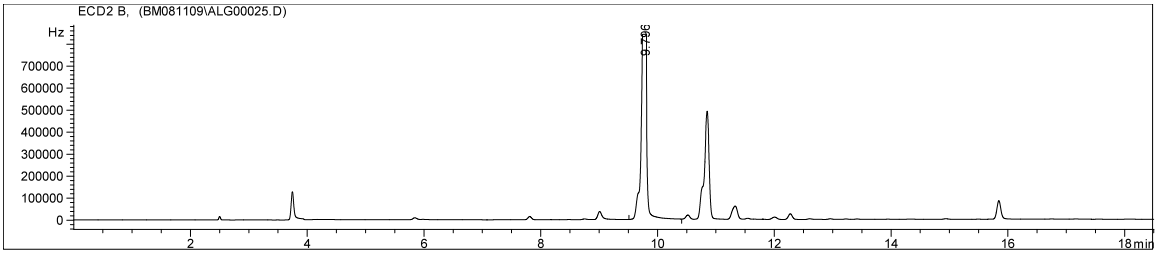

Figure C-10. Batch reactors containing 2 mM buffer, 10 mg/l NOM as C, 150 mg/l lead oxide, and 10 mg/l I^-, unfiltered sample, pH 7, 72 hours reaction time, Experiment 23M (08-11-2009). A peak equivalent to 2177 µg/l IAA was present at the iodoacetic acid retention time of 9.76 minutes.

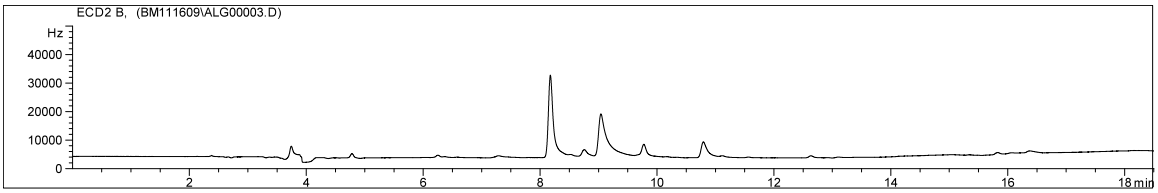

Figure C-11. Batch reactor containing 2 mM HCO_3^-, 0.078 mM HOCl, 10 mg/l I^-, and no sulfite (Experiment 33M, 11-16-2009). Initial conditions: pH 7 and 15 minutes reaction time. No iodoform was detected in this chromatogram.

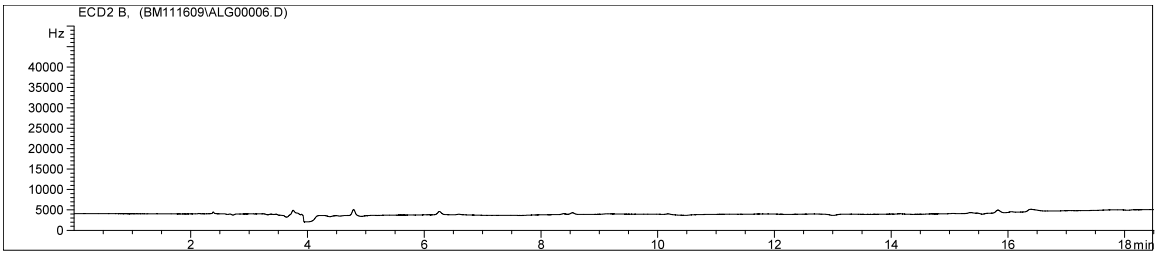

Figure C-12. Batch reactor containing 2 mM HCO_3^-, 0.078 mM HOCl, 10 mg/l I^-, and 100 mg/l sulfite as a quenching agent (Experiment 33M, 11-16-2009). Initial conditions: pH 7 and 15 minutes reaction time. No iodoform was detected in this chromatogram.

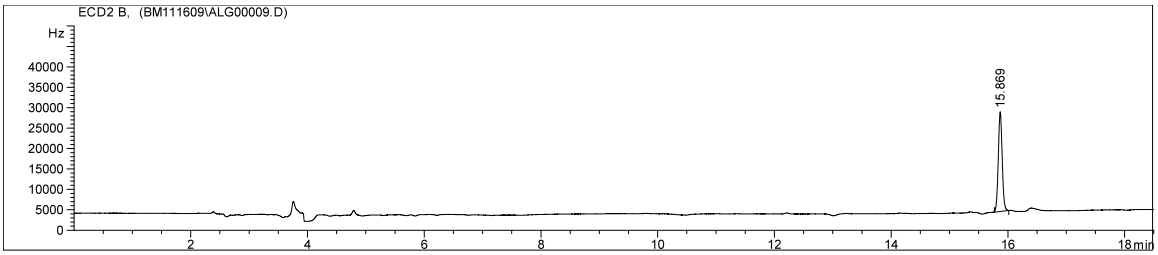

Figure C-13. Batch reactor containing 100 µg/l CHI_3 spike in DI water only (Experiment 33M, 11-16-2009). Initial conditions: pH 7 and 15 minutes reaction time. The peak at 15.9 minutes corresponds to 98 µg/l CHI_3.

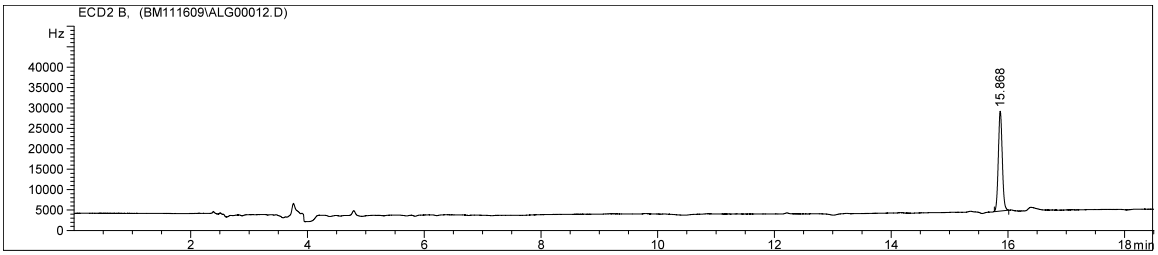

Figure C-14. Batch reactor containing 100 µg/l CHI_3 spike in DI water with 100 mg/l sulfite as a quenching agent. Initial conditions: pH 7 and 15 minutes reaction time. The peak at 15.9 minutes corresponds to 102 µg/l CHI_3.

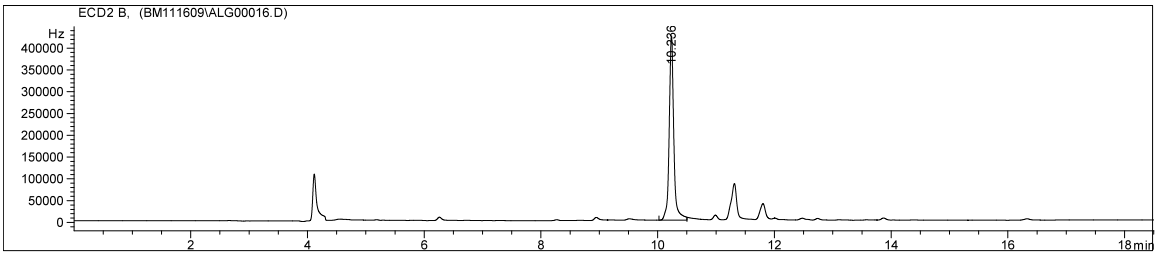

Figure C-15. Batch reactor containing 2 mM HCO_3^-, 0.078 mM HOCl, 10 mg/l I^-, and no sulfite (Experiment 33M, 11-16-2009). Initial conditions: pH 7 and 15 minutes reaction time. The peak at 10.2 minutes corresponds to 1329 µg/l IAA.

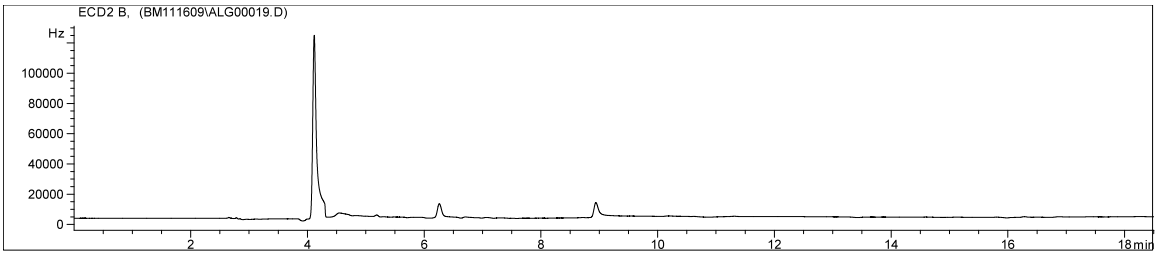

Figure C-16. Batch reactor containing 2 mM HCO_3^-, 0.078 mM HOCl, 10 mg/l I^-, and 100 mg/l sulfite as a quenching agent (Experiment 33M, 11-16-2009). Initial conditions: pH 7 and 15 minutes reaction time. No iodoacetic acid was detected in this chromatogram.

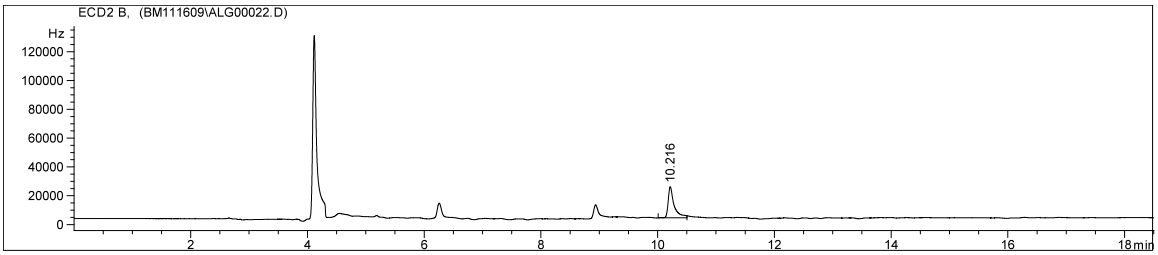

Figure C-17. Batch reactor containing 100 µg/l IAA spike in DI water only (Experiment 33M, 11-16-2009). Initial conditions: pH 7 and 15 minutes reaction time. The peak at 10.2 minutes corresponds to 85 µg/l IAA.

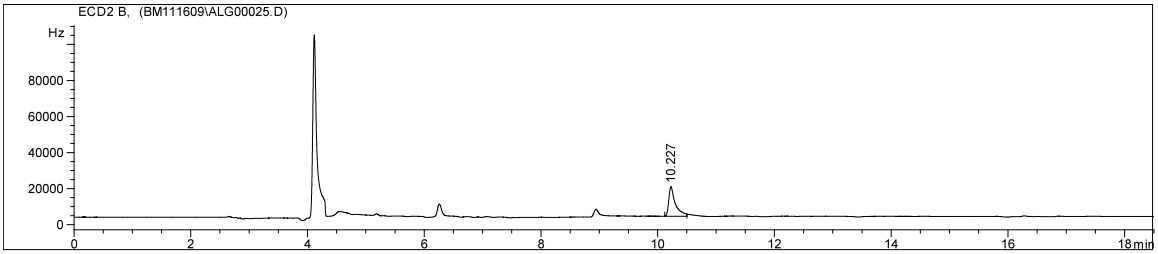

Figure C-18. Batch reactor containing 100 µg/l CHI_3 spike in DI water with 100 mg/l sulfite as a quenching agent. Initial conditions: pH 7 and 15 minutes reaction time. The peak at 10.2 minutes corresponds to 77 µg/l CHI_3.

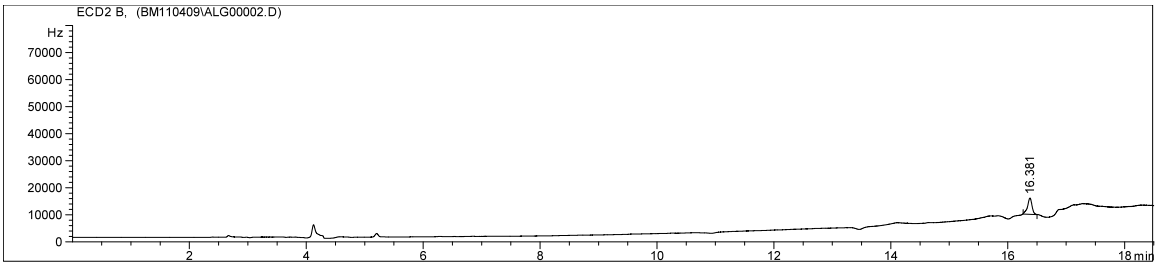

Figure C-19. Batch reactor containing 2 mM HCO_3^-, 150 mg/l PbO_2, and 10 mg/l I^- without sulfite quenching (Experiment 30M, 11-02-2010). The peak at 16.4 minutes corresponds to approximately 31 µg/l IAA detected. Initial conditions: pH 7 and 72 hours reaction time.

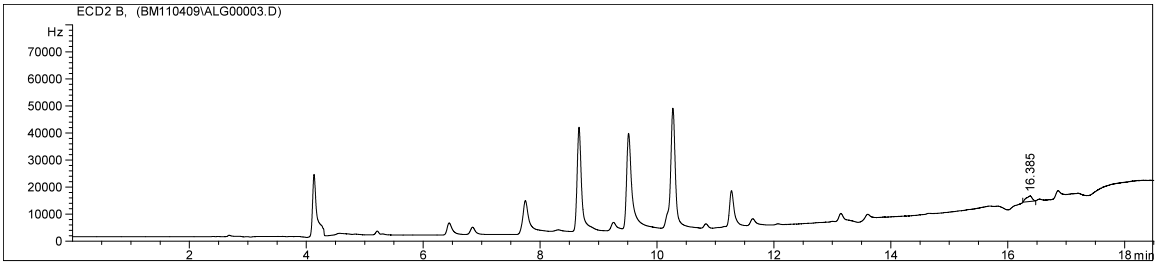

Figure C-20. Batch reactor containing 2 mM HCO_3^-, 150 mg/l PbO_2, 10 mg/l I^-, and 100 mg/l sulfite as a quenching agent (Experiment 30M, 11-02-2010). The peak at 16.4 minutes corresponds to 11 µg/l IAA detected. Initial conditions: pH 7 and 72 hours reaction time.

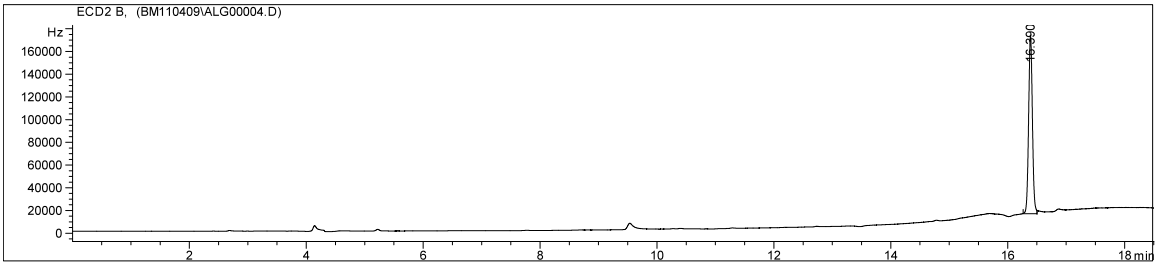

Figure C-21. Batch reactor containing 2 mM HCO_3^-, 10 mg/l NOM as C, 150 mg/l PbO_2, and 10 mg/l I^- without sulfite quenching (Experiment 30M, 11-02-2010). The peak at 16.4 minutes corresponds to approximately 825 µg/l IAA detected. Initial conditions: pH 7 and 72 hours reaction time.

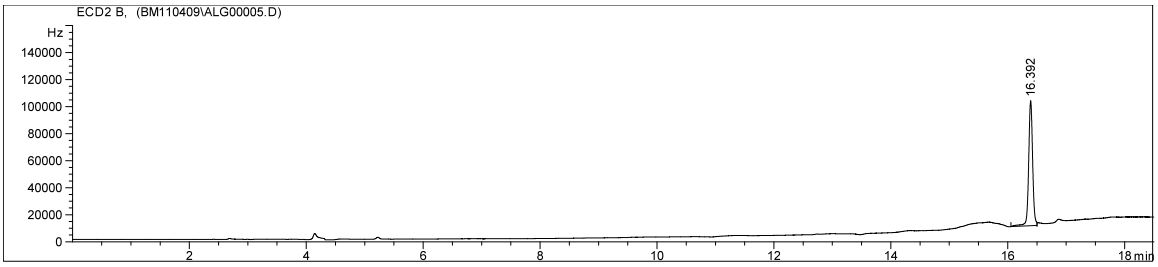

Figure C-22. Batch reactor containing 2 mM HCO_3^-, 150 mg/l PbO_2, 10 mg/l I^-, and 100 mg/l sulfite as a quenching agent (Experiment 30M, 11-02-2010). The peak at 16.4 minutes corresponds to 509 µg/l IAA detected. Initial conditions: pH 7 and 72 hours reaction time.

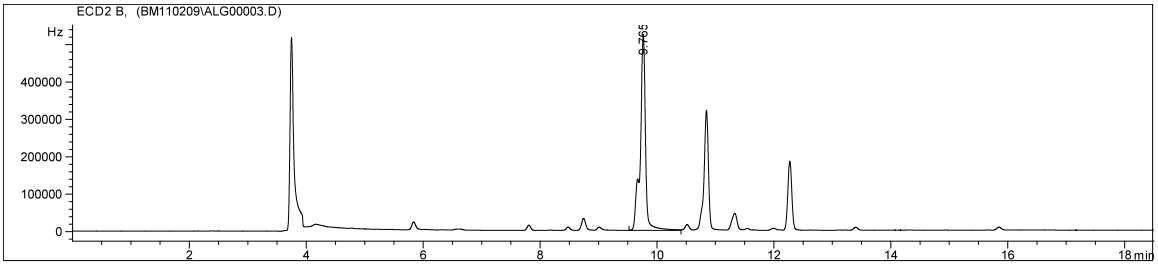

Figure C-23. Batch reactor containing 2 mM HCO_3^-, 150 mg/l PbO_2, and 10 mg/l I^- without sulfite quenching (Experiment 30M, 11-02-2010). The peak at 9.7 minutes corresponds to approximately 2100 µg/l IAA detected. Initial conditions: pH 7 and 72 hours reaction time.

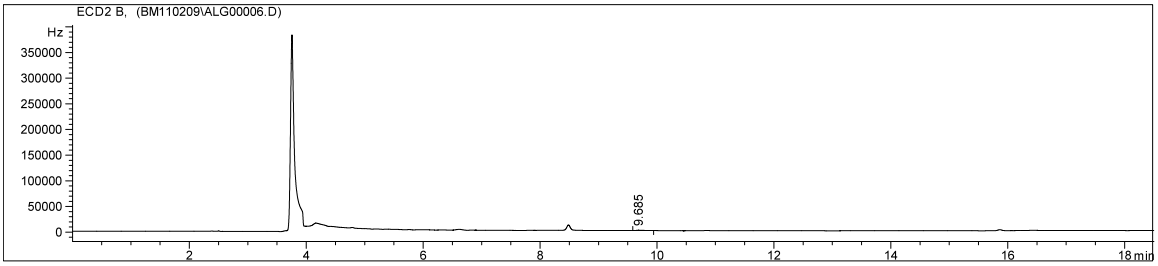

Figure C-24. Batch reactor containing 2 mM HCO_3^-, 150 mg/l PbO_2, 10 mg/l I^-, and 100 mg/l sulfite as a quenching agent (Experiment 30M, 11-02-2010). The peak at 9.7 minutes corresponds to 1 µg/l IAA detected. Initial conditions: pH 7 and 72 hours reaction time.

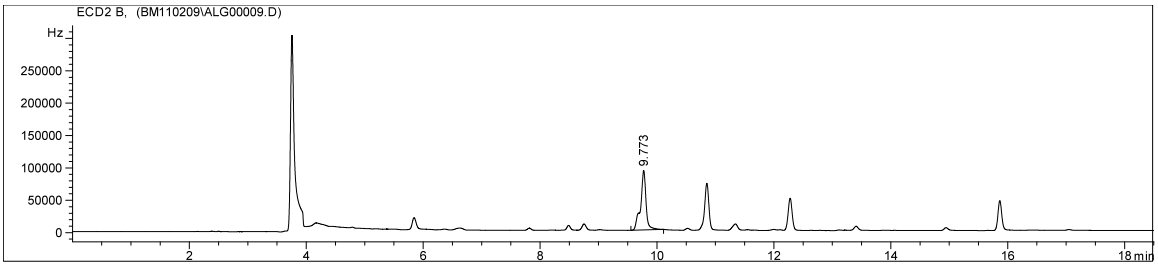

Figure C-25. Batch reactor containing 2 mM HCO_3^-, 10 mg/l NOM as C, 150 mg/l PbO_2, and 10 mg/l I^- without sulfite quenching (Experiment 30M, 11-02-2010). The peak at 9.7 minutes corresponds to approximately 410 µg/l IAA detected. Initial conditions: pH 7 and 72 hours reaction time.

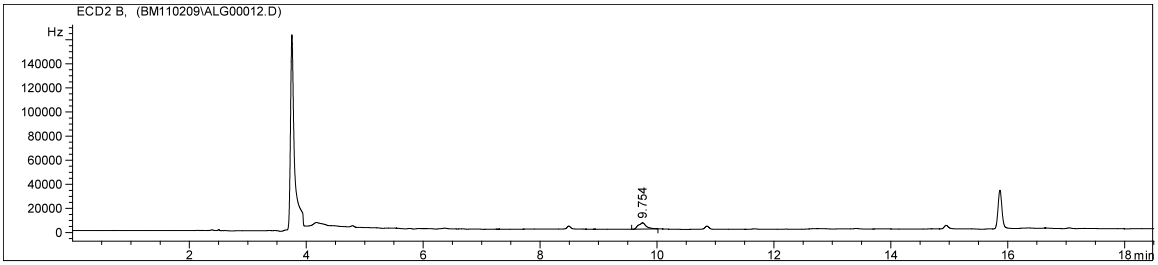

Figure C-26. Batch reactor containing 2 mM HCO_3^-, 150 mg/l PbO_2, 10 mg/l I^-, and 100 mg/l sulfite as a quenching agent (Experiment 30M, 11-02-2010). The peak at 9.7 minutes corresponds to 30 µg/l IAA detected. Initial conditions: pH 7 and 72 hours reaction time.

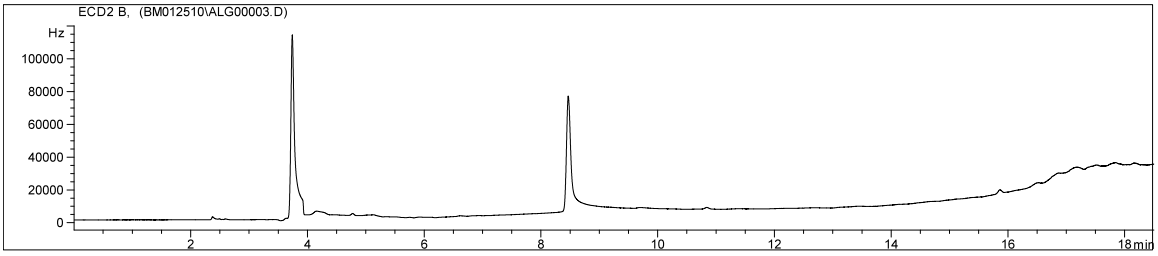

Figure C-27. Batch reactor containing 2 mM HCO_3^-, no NOM, 150 mg/l PbO_2, and 10 mg/l I^- (Experiment 39M, 01-22-2010). Initial conditions: pH 7 and 72 hours reaction time. Samples were quenched with 100 mg/l sulfite after 0.1µm filtration. No iodoacetic acid was detected in this chromatogram.

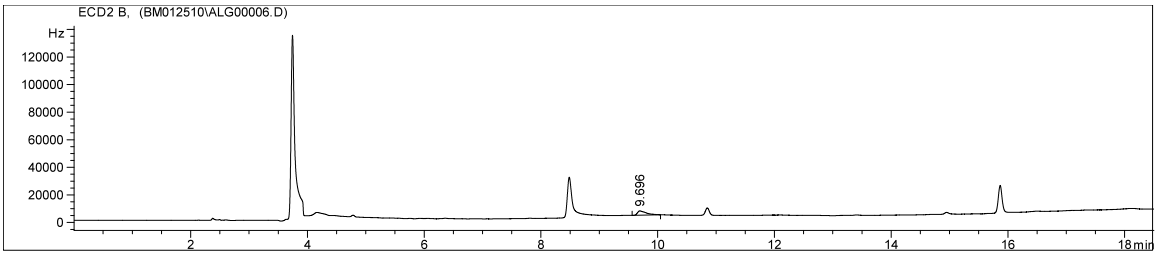

Figure C-28. Batch reactor containing 2 mM HCO_3^-, 1 mg/l NOM as C, 150 mg/l PbO_2, and 10 mg/l I^- (Experiment 39M, 01-22-2010). Initial conditions: pH 7 and 72 hours reaction time. Samples were quenched with 100 mg/l sulfite after 0.1µm filtration. The peak at 9.7 minutes corresponds to 21 µg/l IAA.

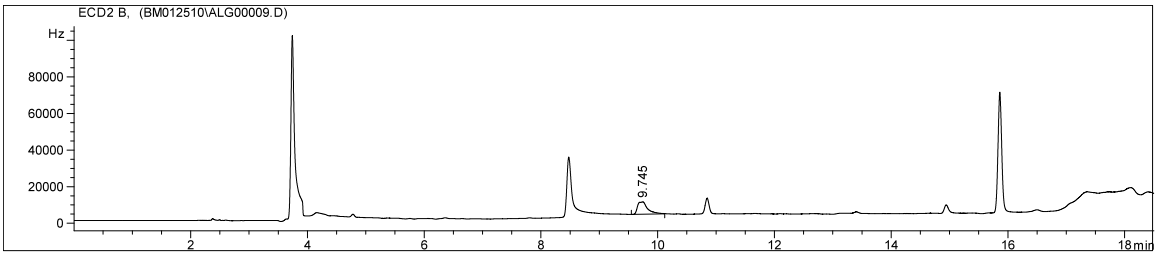

Figure C-29. Batch reactor containing 2 mM HCO_3^-, 5 mg/l NOM as C, 150 mg/l PbO_2, and 10 mg/l I^- (Experiment 39M, 01-22-2010). Initial conditions: pH 7 and 72 hours reaction time. Samples were quenched with 100 mg/l sulfite after 0.1µm filtration. The peak at 9.7 minutes corresponds to 36 µg/l IAA.

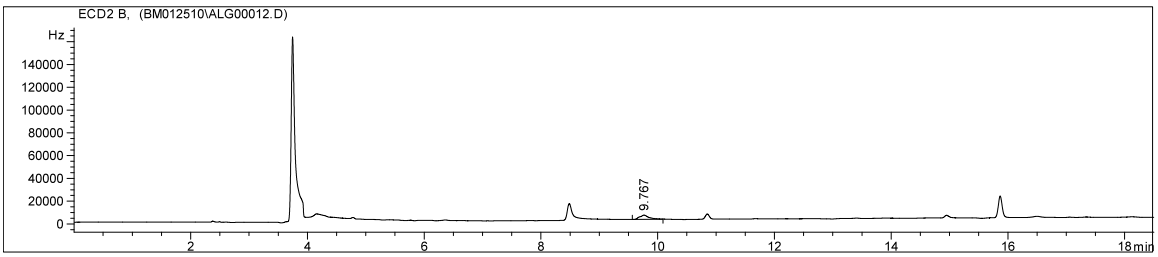

Figure C-30. Batch reactor containing 2 mM HCO_3^-, 10 mg/l NOM as C, 150 mg/l PbO_2, and 10 mg/l I^- (Experiment 39M, 01-22-2010). Initial conditions: pH 7 and 72 hours reaction time. Samples were quenched with 100 mg/l sulfite after 0.1µm filtration. The peak at 9.7 minutes corresponds to 26 µg/l IAA.

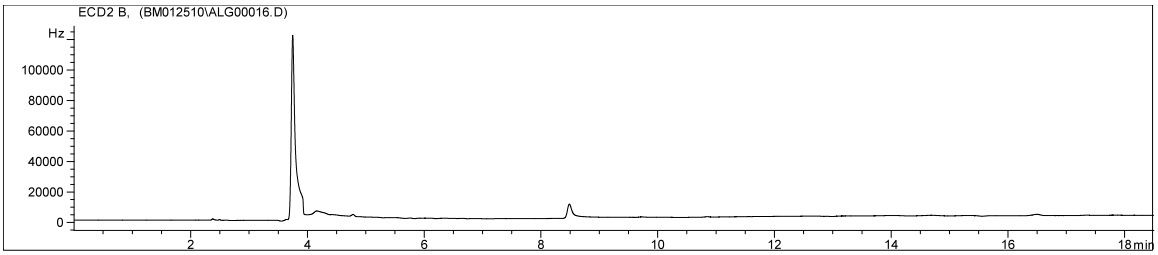

Figure C-31. Batch reactor containing 2 mM HCO_3^-, 10 mg/l NOM, no PbO_2, and 10 mg/l I^- (Experiment 38M, 01-22-2010). Initial conditions: pH 7 and 72 hours reaction time. Samples were quenched with 100 mg/l sulfite after 0.1µm filtration. No iodoacetic acid was detected in this chromatogram.

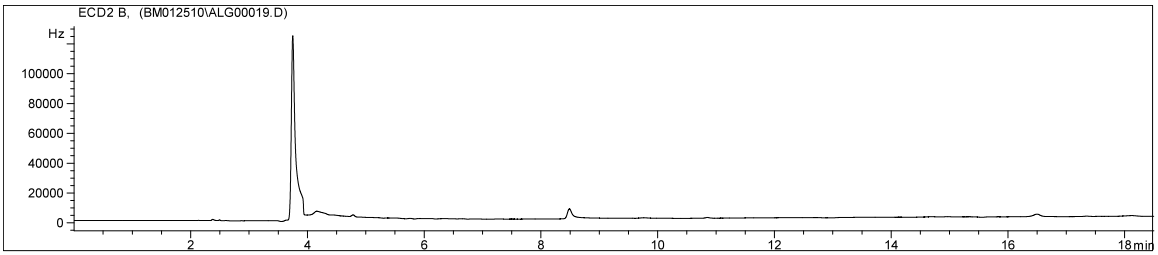

Figure C-32. Batch reactor containing 2 mM HCO_3^-, 10 mg/l NOM, 5 mg/l PbO_2, and 10 mg/l I^- (Experiment 38M, 01-22-2010). Initial conditions: pH 7 and 72 hours reaction time. Samples were quenched with 100 mg/l sulfite after 0.1µm filtration. No iodoacetic acid was detected in this chromatogram.

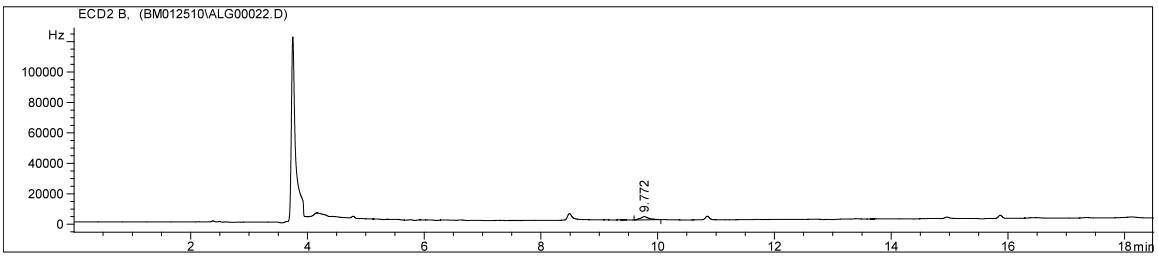

Figure C-33. Batch reactor containing 2 mM HCO_3^-, 10 mg/l NOM, 50 mg/l PbO_2, and 10 mg/l I^- (Experiment 38M, 01-22-2010). Initial conditions: pH 7 and 72 hours reaction time. Samples were quenched with 100 mg/l sulfite after 0.1µm filtration. The peak at 9.7 minutes corresponds to 14 µg/l IAA.

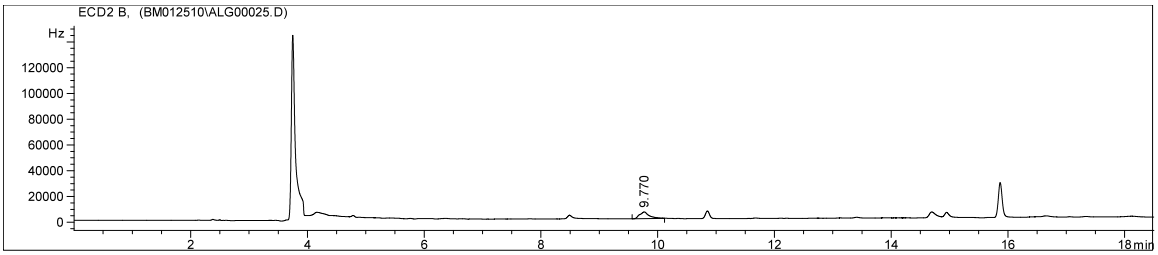

Figure C-34. Batch reactor containing 2 mM HCO_3^-, 10 mg/l NOM, 150 mg/l PbO_2, and 10 mg/l I^- (Experiment 38M, 01-22-2010). Initial conditions: pH 7 and 72 hours reaction time. Samples were quenched with 100 mg/l sulfite after 0.1µm filtration. The peak at 9.7 minutes corresponds to 34 µg/l IAA.

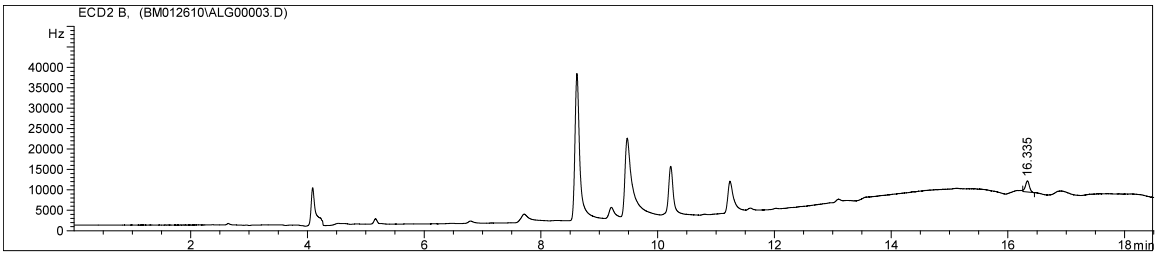

Figure C-35. Batch reactor containing 2 mM HCO_3^-, no NOM, 150 mg/l PbO_2, and 10 mg/l I^- (Experiment 39M, 01-22-2010). Initial conditions: pH 7 and 72 hours reaction time. Samples were quenched with 100 mg/l sulfite after 0.1µm filtration. The peak at 16.3 minutes corresponds to 7 µg/l CHI_3.

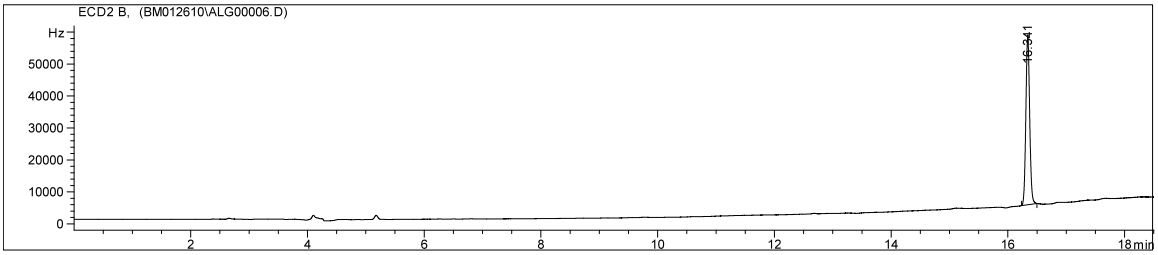

Figure C-36. Batch reactor containing 2 mM HCO_3^-, 1 mg/l NOM as C, 150 mg/l PbO_2, and 10 mg/l I^- (Experiment 39M, 01-22-2010). Initial conditions: pH 7 and 72 hours reaction time. Samples were quenched with 100 mg/l sulfite after 0.1µm filtration. The peak at 16.3 minutes corresponds to 202 µg/l CHI_3.

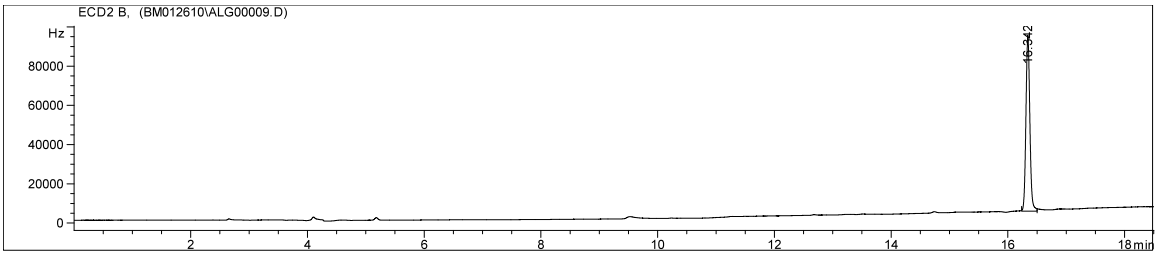

Figure C-37. Batch reactor containing 2 mM HCO_3^-, 5 mg/l NOM as C, 150 mg/l PbO_2, and 10 mg/l I^- (Experiment 39M, 01-22-2010). Initial conditions: pH 7 and 72 hours reaction time. Samples were quenched with 100 mg/l sulfite after 0.1µm filtration. The peak at 16.3 minutes corresponds to 365 µg/l CHI_3.

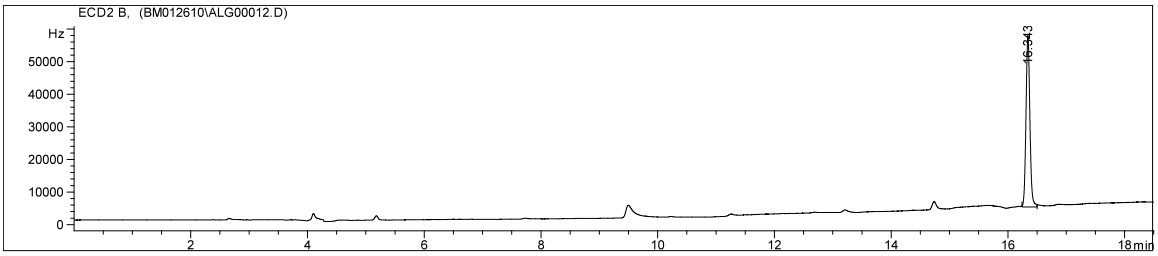

Figure C-38. Batch reactor containing 2 mM HCO_3^-, 10 mg/l NOM as C, 150 mg/l PbO_2, and 10 mg/l I^- (Experiment 39M, 01-22-2010). Initial conditions: pH 7 and 72 hours reaction time. Samples were quenched with 100 mg/l sulfite after 0.1µm filtration. The peak at 16.3 minutes corresponds to 212 µg/l CHI_3.

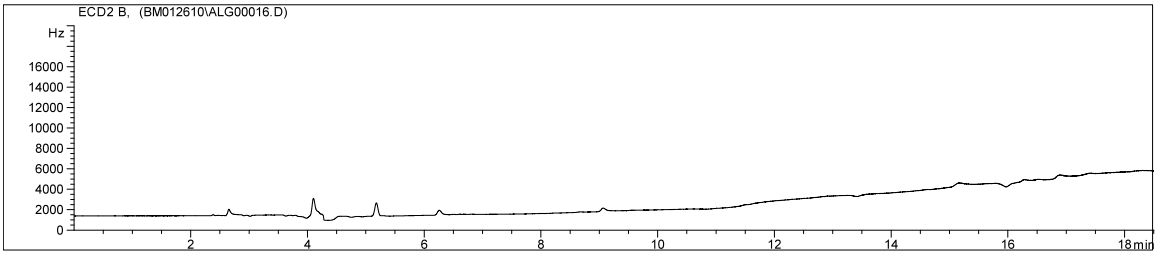

Figure C-39. Batch reactor containing 2 mM HCO_3^-, 10 mg/l NOM as C, no PbO_2, and 10 mg/l I^- (Experiment 38M, 01-22-2010). Initial conditions: pH 7 and 72 hours reaction time. Samples were quenched with 100 mg/l sulfite after 0.1µm filtration. No iodoform was detected in this chromatogram.

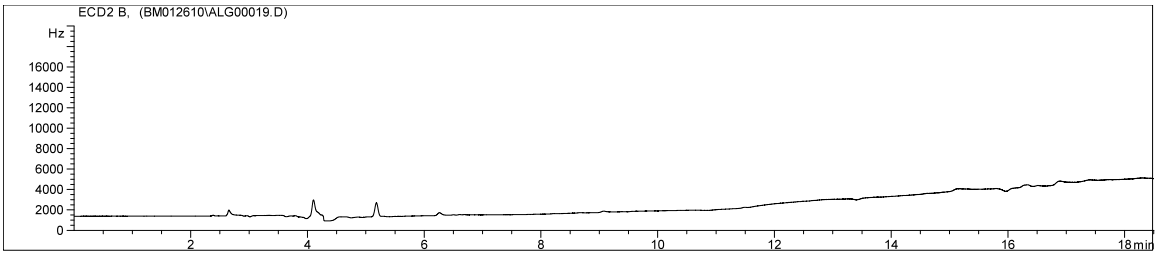

Figure C-40. Batch reactor containing 2 mM HCO_3^-, 10 mg/l NOM as C, 5 mg/l PbO_2, and 10 mg/l I^- (Experiment 38M, 01-22-2010). Initial conditions: pH 7 and 72 hours reaction time. Samples were quenched with 100 mg/l sulfite after 0.1µm filtration. No iodoform was detected in this chromatogram.

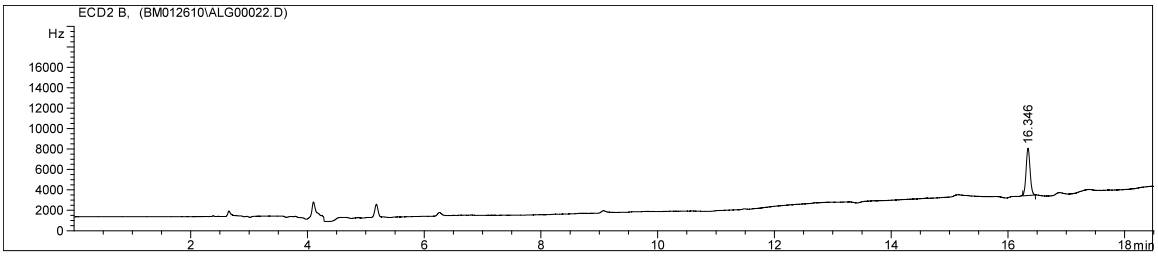

Figure C-41. Batch reactor containing 2 mM HCO_3^-, 10 mg/l NOM as C, 50 mg/l PbO_2, and 10 mg/l I^- (Experiment 38M, 01-22-2010). Initial conditions: pH 7 and 72 hours reaction time. Samples were quenched with 100 mg/l sulfite after 0.1µm filtration. The peak at 16.3 minutes corresponds to 17 µg/l CHI_3.

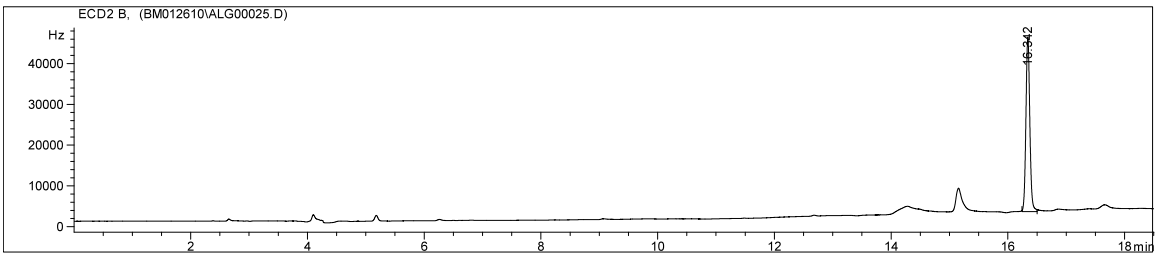

Figure C-42. Batch reactor containing 2 mM HCO_3^-, 10 mg/l NOM as C, 150 mg/l PbO_2, and 10 mg/l I^- (Experiment 38M, 01-22-2010). Initial conditions: pH 7 and 72 hours reaction time. Samples were quenched with 100 mg/l sulfite after 0.1µm filtration. The peak at 16.3 minutes corresponds to 174 µg/l CHI_3.

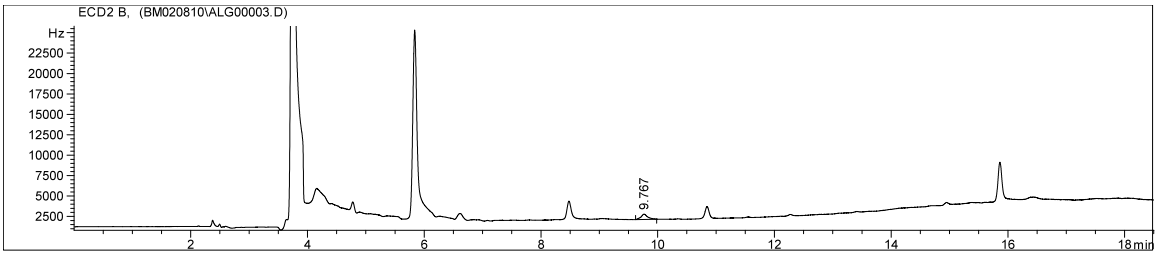

Figure C-43. Batch reactor containing 2 mM HCO_3^-, no NOM, 1000 mg/l MnO_2, and 10 mg/l I^- (Experiment 43M, 02-05-2010). Initial conditions: pH 7 and 72 hours reaction time. Samples were quenched with 100 mg/l sulfite after 0.1 µm filtration. The peak at 9.7 minutes corresponds to 4 µg/l IAA.

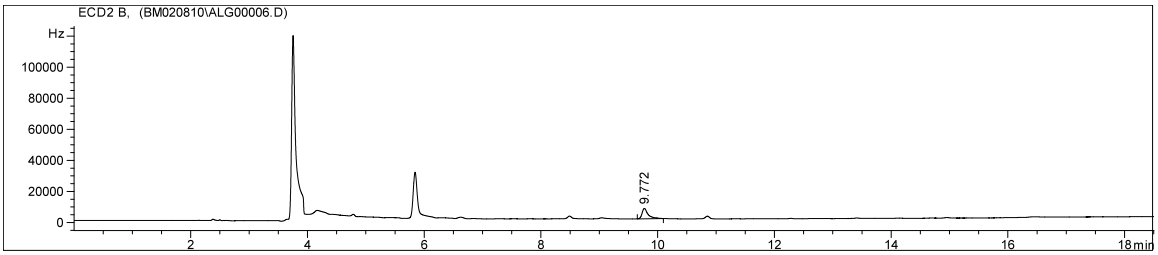

Figure C-44. Batch reactor containing 2 mM HCO_3^-, 10 mg/l NOM, 500 mg/l MnO_2, and 10 mg/l I^- (Experiment 43M, 02-05-2010). Initial conditions: pH 7 and 72 hours reaction time. Samples were quenched with 100 mg/l sulfite after 0.1 µm filtration. The peak at 9.7 minutes corresponds to 28 µg/l IAA.

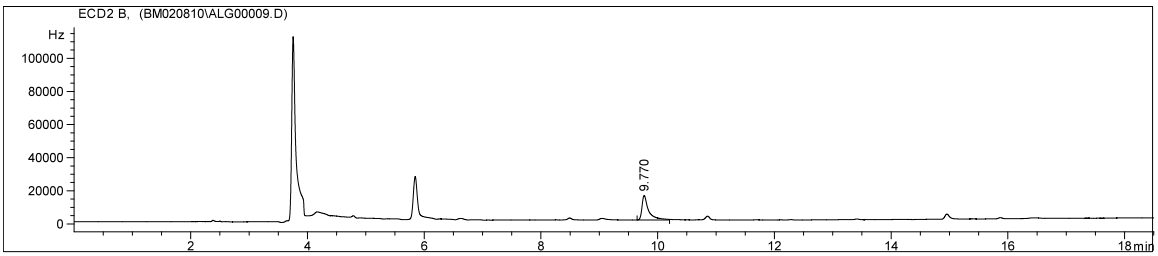

Figure C-45. Batch reactor containing 2 mM HCO_3^-, 10 mg/l NOM, 1000 mg/l MnO_2, and 10 mg/l I^- (Experiment 43M, 02-05-2010). Initial conditions: pH 7 and 72 hours reaction time. Samples were quenched with 100 mg/l sulfite after 0.1 µm filtration. The peak at 9.7 minutes corresponds to 63 µg/l IAA.

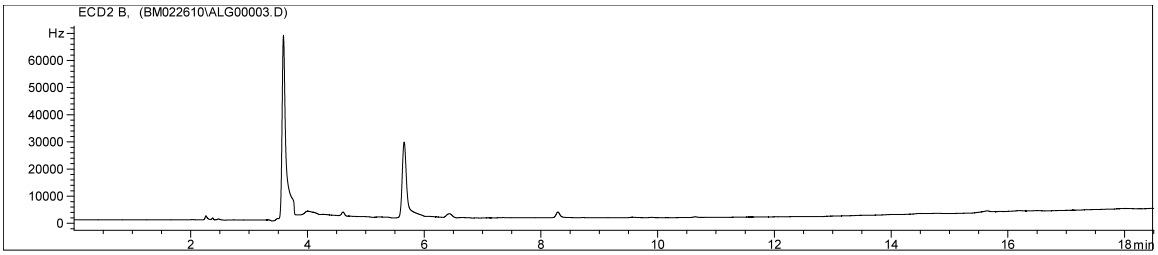

Figure C-46. Batch reactor containing 2 mM HCO_3^-, no NOM, 1000 mg/l MnO_2, and 10 mg/l I^- (Experiment 48M, 02-24-2010). Initial conditions: pH 7 and 48 hours reaction time. Samples were quenched with 100 mg/l sulfite after 0.1 µm filtration. No iodoacetic acid was detected in this chromatogram.

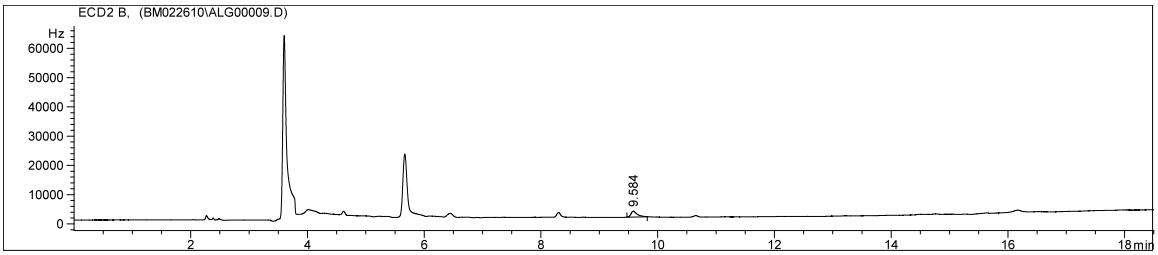

Figure C-47. Batch reactor containing 2 mM HCO_3^-, 10 mg/l NOM, 500 mg/l MnO_2, and 10 mg/l I^- (Experiment 48M, 02-24-2010). Initial conditions: pH 7 and 48 hours reaction time. Samples were quenched with 100 mg/l sulfite after 0.1 µm filtration. The peak at 9.6 minutes corresponds to 6 µg/l IAA.

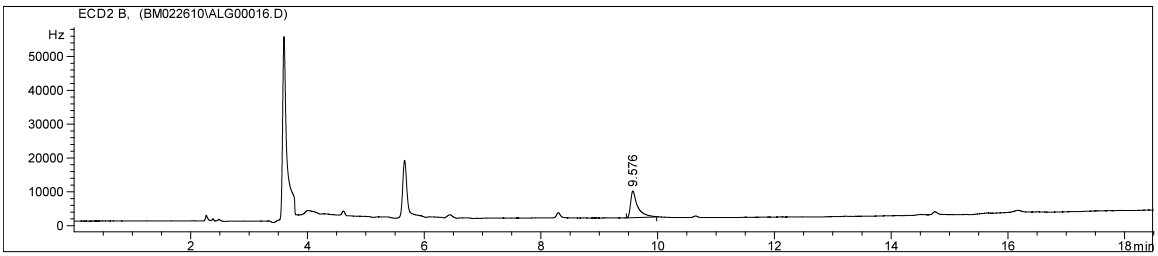

Figure C-48. Batch reactor containing 2 mM HCO_3^-, 10 mg/l NOM, 1000 mg/l MnO_2, and 10 mg/l I^- (Experiment 48M, 02-24-2010). Initial conditions: pH 7 and 48 hours reaction time. Samples were quenched with 100 mg/l sulfite after 0.1 µm filtration. The peak at 9.6 minutes corresponds to 30 µg/l IAA.

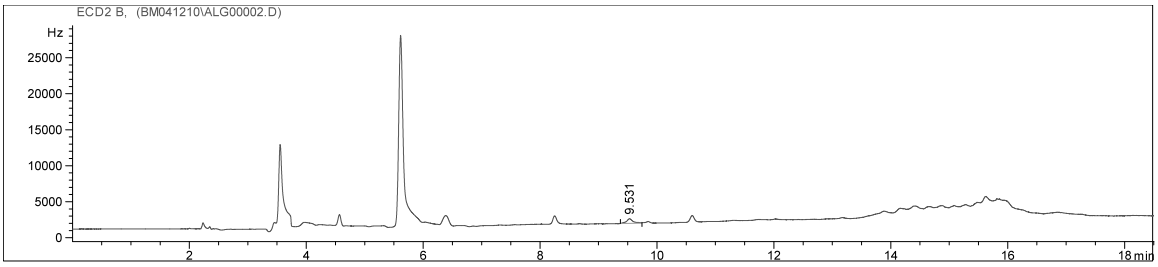

Figure C-49. Batch reactor containing 2 mM HCO_3^-, no added NOM, 1000 mg/l MnO_2, and 10 mg/l I^- at pH 7 and 48 hours reaction time (Experiment 57M, 04-10-2010). The peak at 9.55 minutes corresponds to 4 µg/l IAA.

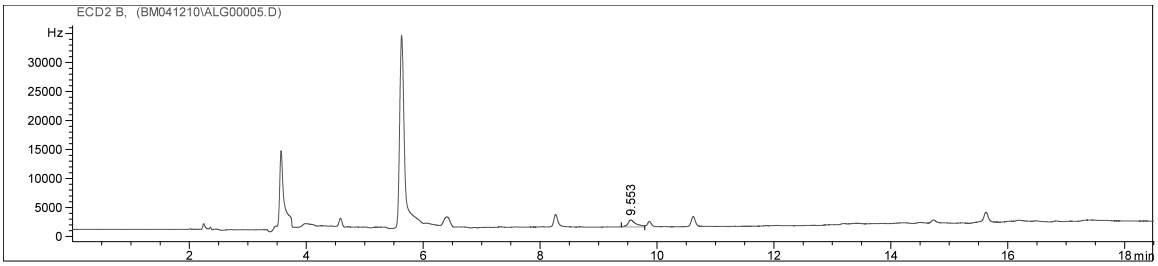

Figure C-50. Batch reactor containing 2 mM HCO_3^-, 1 mg/l C added NOM, 1000 mg/l MnO_2, and 10 mg/l I^- at pH 7 and 48 hours reaction time (Experiment 57M, 04-10-2010). The peak at 9.55 minutes corresponds to 7 µg/l IAA.

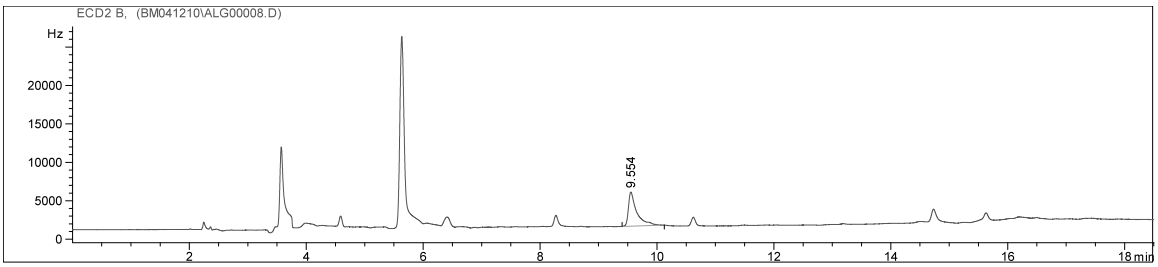

Figure C-51. Batch reactor containing 2 mM HCO_3^-, 5 mg/l C added NOM, 1000 mg/l MnO_2, and 10 mg/l I^- at pH 7 and 48 hours reaction time (Experiment 57M, 04-10-2010). The peak at 9.55 minutes corresponds to 25 µg/l IAA.

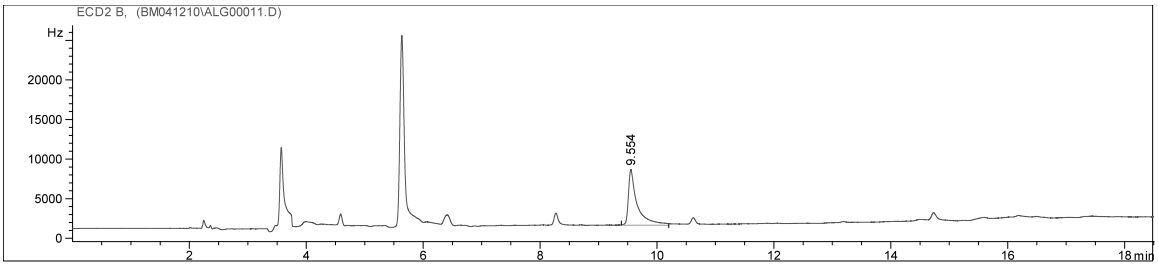

Figure C-52. Batch reactor containing 2 mM HCO_3^-, 10 mg/l C added NOM, 1000 mg/l MnO_2, and 10 mg/l I^- at pH 7 and 48 hours reaction time (Experiment 57M, 04-10-2010). The peak at 9.55 minutes corresponds to 38 µg/l IAA.

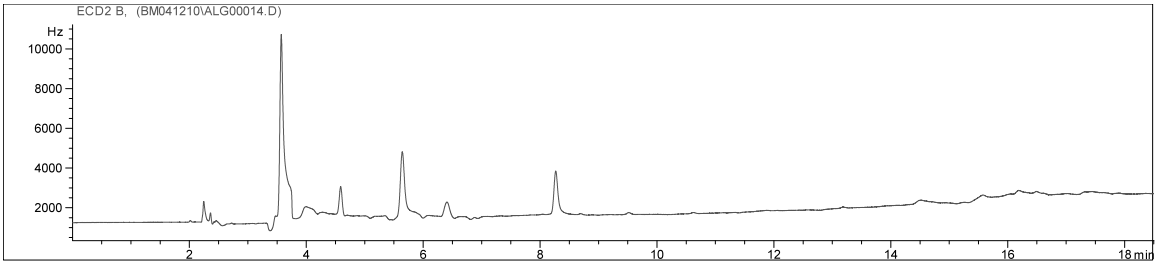

Figure C-53. Batch reactor containing 2 mM HCO_3^-, 5 mg/l C added NOM, no added MnO_2, and 10 mg/l I^- at pH 7 and 48 hours reaction time (Experiment 57M, 04-10-2010). There is no peak at the iodoacetic acid elution time of 9.55 minutes.

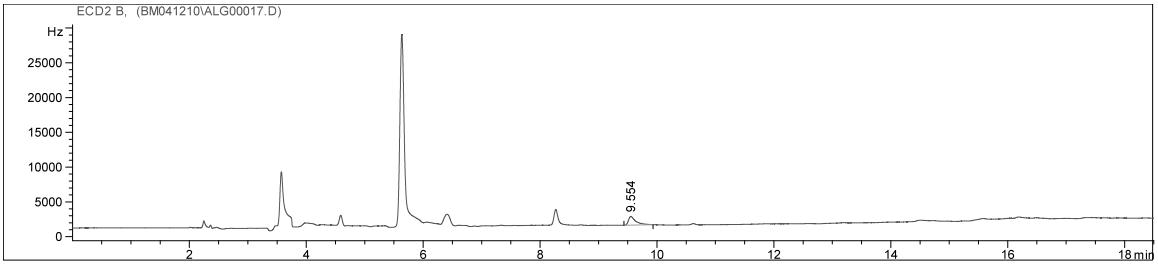

Figure C-54. Batch reactor containing 2 mM HCO_3^-, 5 mg/l C added NOM, 250 mg/l MnO_2, and 10 mg/l I^- at pH 7 and 48 hours reaction time (Experiment 57M, 04-10-2010). The peak at 9.55 minutes corresponds to 7 µg/l IAA.

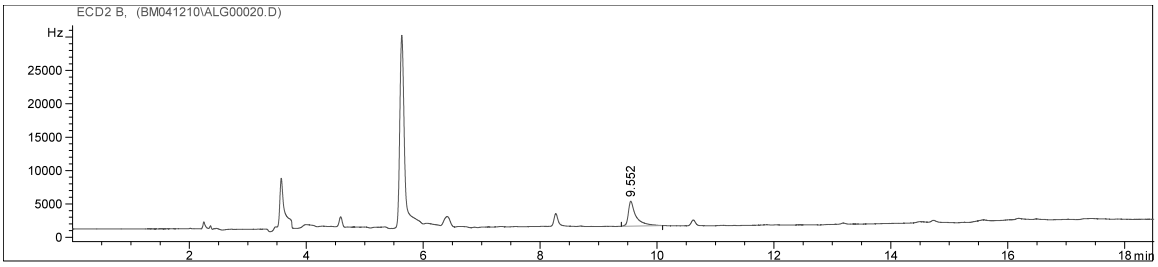

Figure C-55. Batch reactor containing 2 mM HCO_3^-, 5 mg/l C added NOM, 500 mg/l MnO_2, and 10 mg/l I^- at pH 7 and 48 hours reaction time (Experiment 57M, 04-10-2010). The peak at 9.55 minutes corresponds to 18 µg/l IAA.

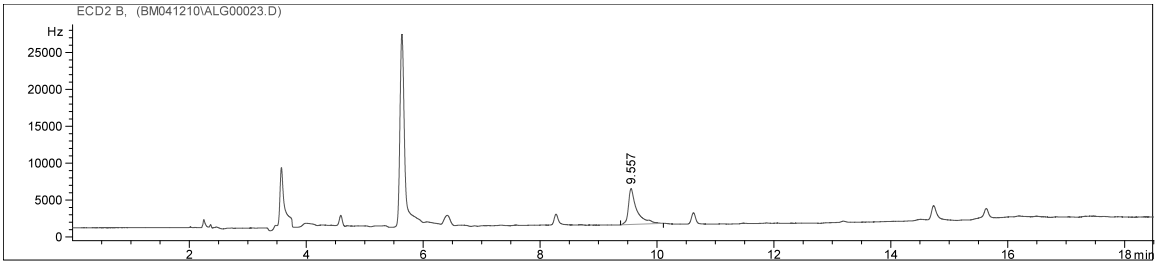

Figure C-56. Batch reactor containing 2 mM HCO_3^-, 5 mg/l C added NOM, 1000 mg/l MnO_2, and 10 mg/l I^- at pH 7 and 48 hours reaction time (Experiment 57M, 04-10-2010). The peak at 9.55 minutes corresponds to 27 µg/l IAA.

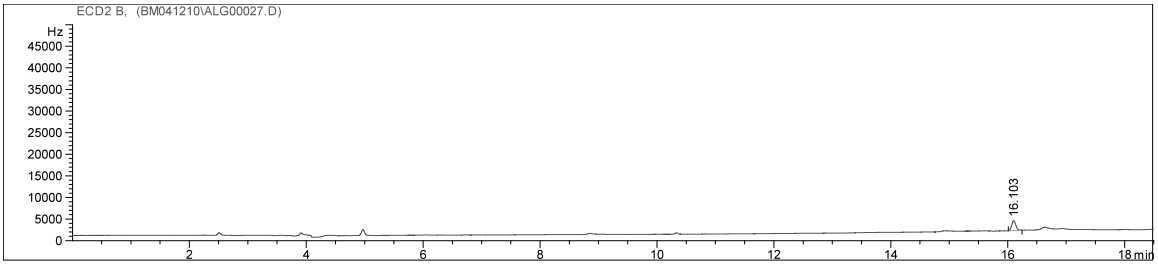

Figure C-57. Batch reactor containing 2 mM HCO_3^-, no added NOM, 1000 mg/l MnO_2, and 10 mg/l I^- at pH 7 and 48 hours reaction time (Experiment 57M, 04-10-2010). The peak at 16.1 minutes corresponds to 5 µg/l CHI_3.

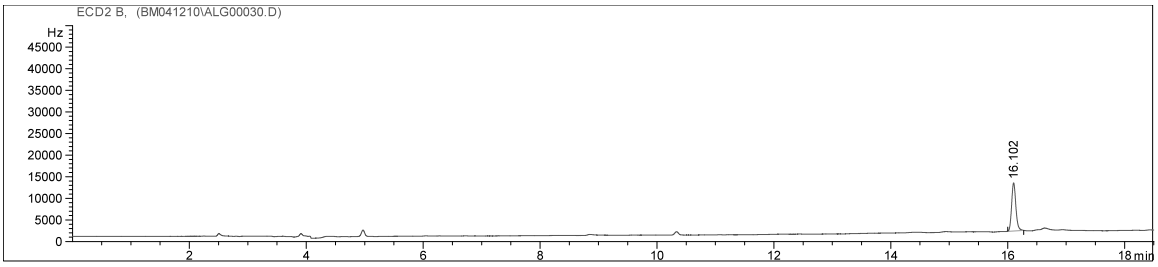

Figure C-58. Batch reactor containing 2 mM HCO_3^-, 1 mg/l C added NOM, 1000 mg/l MnO_2, and 10 mg/l I^- at pH 7 and 48 hours reaction time (Experiment 57M, 04-10-2010). The peak at 16.1 minutes corresponds to 27 µg/l CHI_3.

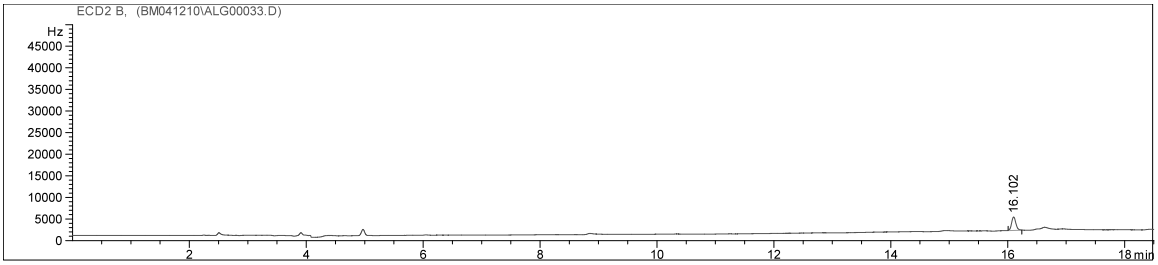

Figure C-59. Batch reactor containing 2 mM HCO_3^-, 5 mg/l C added NOM, 1000 mg/l MnO_2, and 10 mg/l I^- at pH 7 and 48 hours reaction time (Experiment 57M, 04-10-2010). The peak at 16.1 minutes corresponds to 7 µg/l CHI_3.

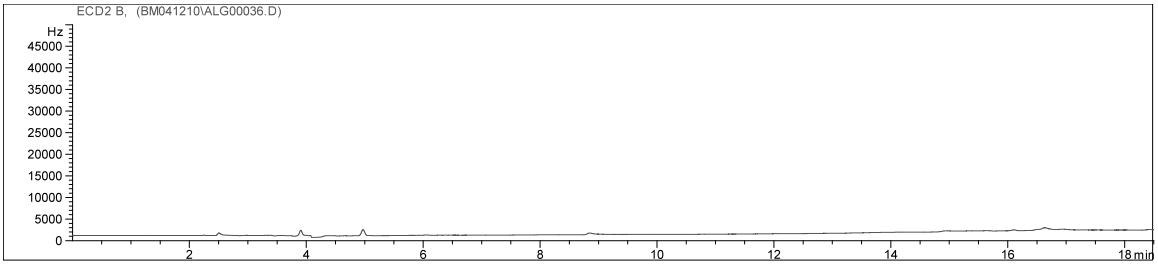

Figure C-60. Batch reactor containing 2 mM HCO_3^-, 10 mg/l C added NOM, 1000 mg/l MnO_2, and 10 mg/l I^- at pH 7 and 48 hours reaction time (Experiment 57M, 04-10-2010). There is no peak at the iodoform elution time of 16.1 minutes.

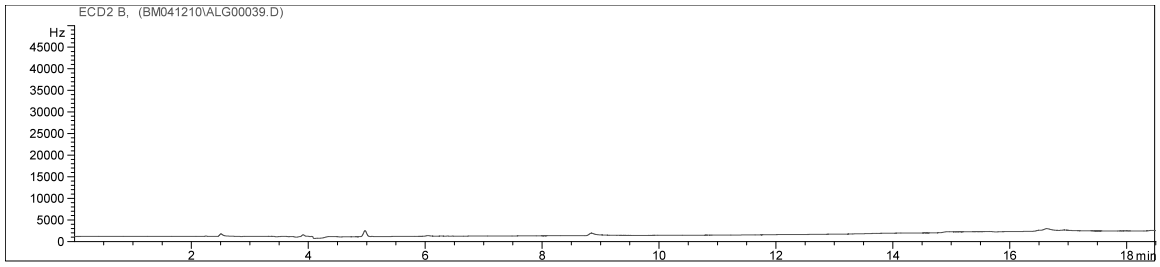

Figure C-61. Batch reactor containing 2 mM HCO_3^-, 5 mg/l C added NOM, no added MnO_2, and 10 mg/l I^- at pH 7 and 48 hours reaction time (Experiment 57M, 04-10-2010). There is no peak at the iodoform elution time of 16.1 minutes.

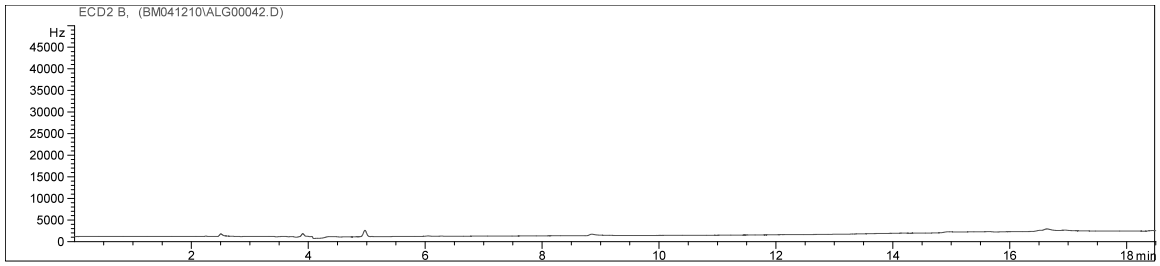

Figure C-62. Batch reactor containing 2 mM HCO_3^-, 5 mg/l C added NOM, 250 mg/l MnO_2, and 10 mg/l I^- at pH 7 and 48 hours reaction time (Experiment 57M, 04-10-2010). There is no peak at the iodoform elution time of 16.1 minutes.

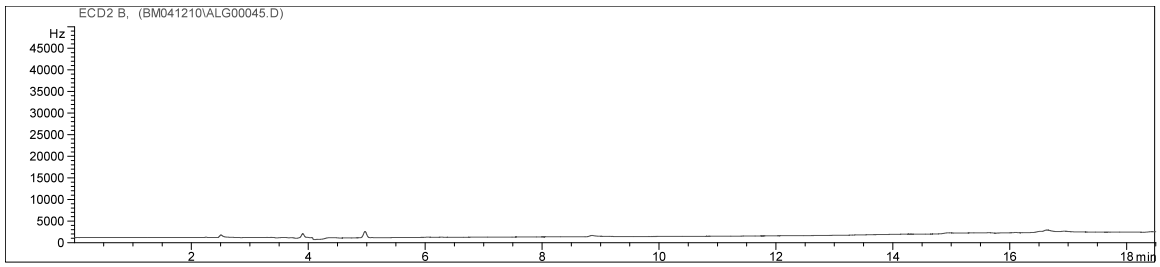

Figure C-63. Batch reactor containing 2 mM HCO_3^-, 5 mg/l C added NOM, 500 mg/l MnO_2, and 10 mg/l I^- at pH 7 and 48 hours reaction time (Experiment 57M, 04-10-2010). There is no peak at the iodoform elution time of 16.1 minutes.

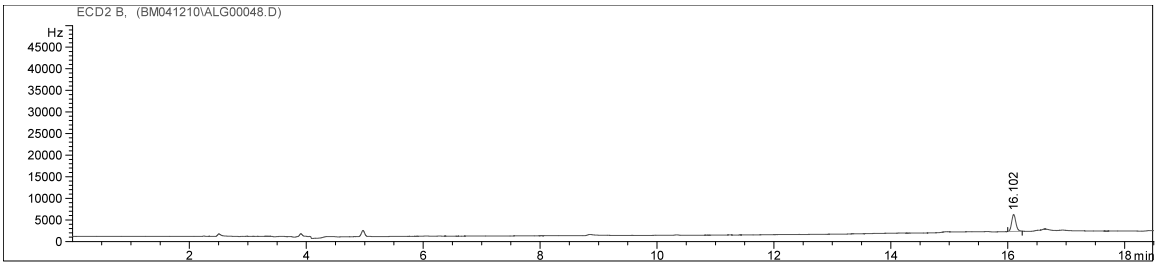

Figure C-64. Batch reactor containing 2 mM HCO_3^-, 5 mg/l C added NOM, 1000 mg/l MnO_2, and 10 mg/l I^- at pH 7 and 48 hours reaction time (Experiment 57M, 04-10-2010). The peak at 16.1 minutes corresponds to 10 µg/l CHI_3.

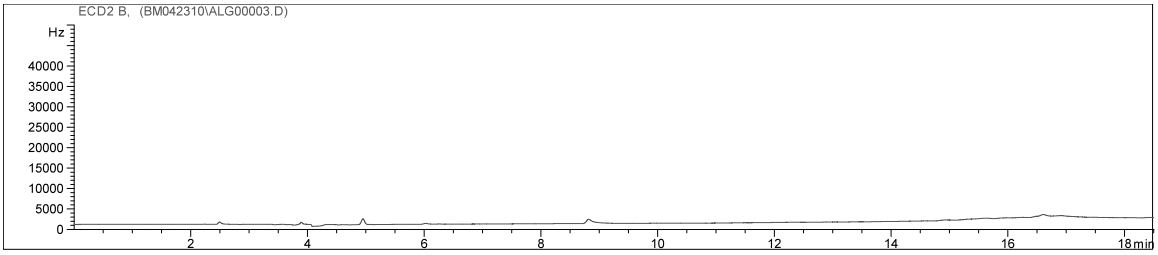

Figure C-65. Batch reactor containing 2 mM HCO_3^-, 5 mg/l NOM as C, no FeO(OH), and 10 mg/l I^- at pH 7 and 48 hours reaction time (Experiment 59M, 04-21-2010), with 100 mg/l sulfite added after 0.1 µm filtration. No iodoform was detected at the iodoform retention time of 16.1 minutes.

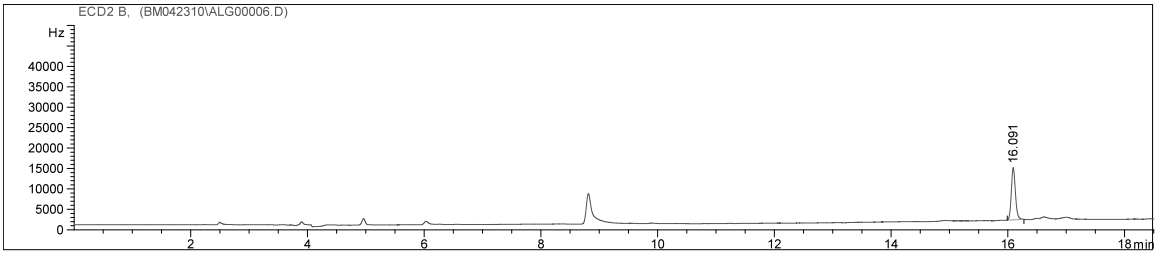

Figure C-66. Batch reactor containing 2 mM HCO_3^-, no added NOM, 1000 mg/l FeO(OH), and 10 mg/l I^- at pH 6 and 48 hours reaction time (Experiment 59M, 04-21-2010), with 100 mg/l sulfite added after 0.1 µm filtration. The peak at 16.1 minutes corresponds to an iodoform formation of 30 µg/l CHI_3.

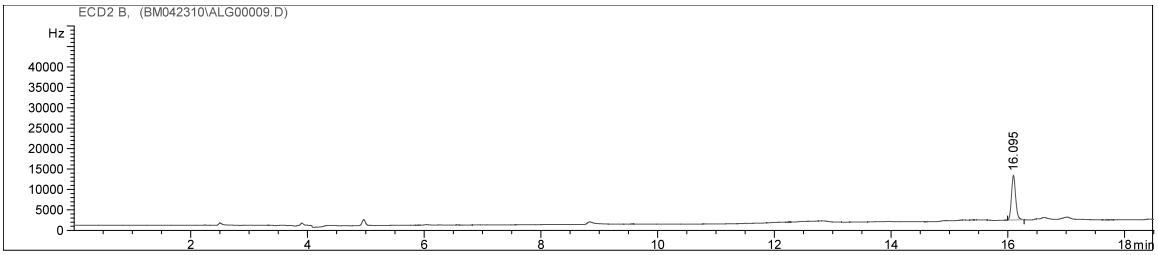

Figure C-67. Batch reactor containing 2 mM HCO_3^-, no added NOM, 1000 mg/l FeO(OH), and 10 mg/l I^- at pH 7 and 48 hours reaction time (Experiment 59M, 04-21-2010), with 100 mg/l sulfite added after 0.1 µm filtration. The peak at 16.1 minutes corresponds to an iodoform formation of 29 µg/l CHI_3.

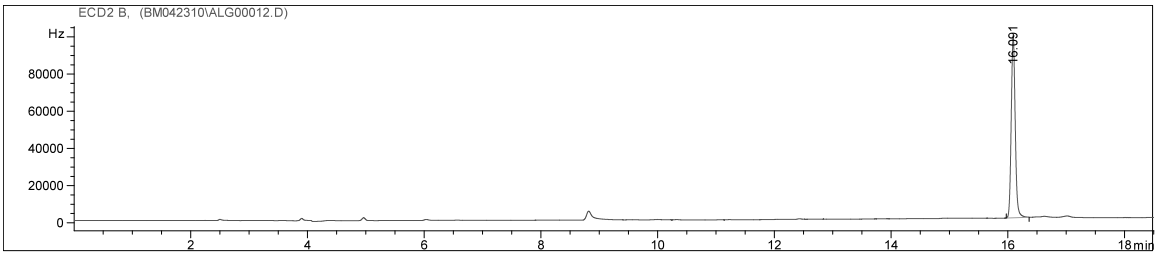

Figure C-68. Batch reactor containing 2 mM HCO_3^-, 5 mg/l NOM as C, 1000 mg/l FeO(OH), and 10 mg/l I^- at pH 6 and 48 hours reaction time (Experiment 59M, 04-21-2010), with 100 mg/l sulfite added after 0.1 µm filtration. The peak at 16.1 minutes corresponds to an iodoform formation of 252 µg/l CHI_3.

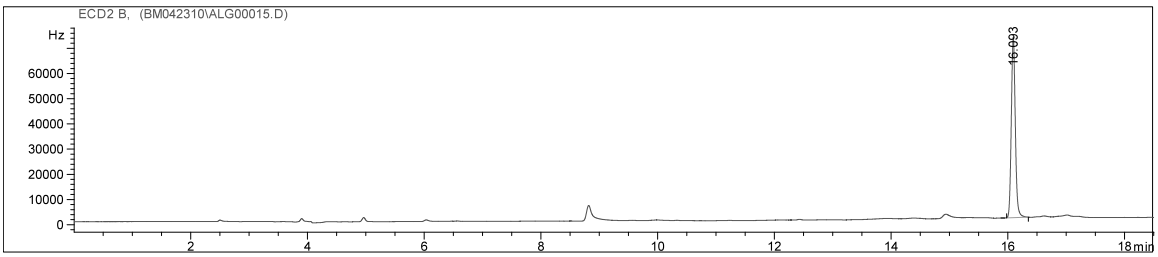

Figure C-69. Batch reactor containing 2 mM HCO_3^-, 5 mg/l NOM as C, 1000 mg/l FeO(OH), and 10 mg/l I^- at pH 6 and 48 hours reaction time (Experiment 59M, 04-21-2010), with 100 mg/l sulfite added after 0.1 µm filtration. The peak at 16.1 minutes corresponds to an iodoform formation of 165 µg/l CHI_3.

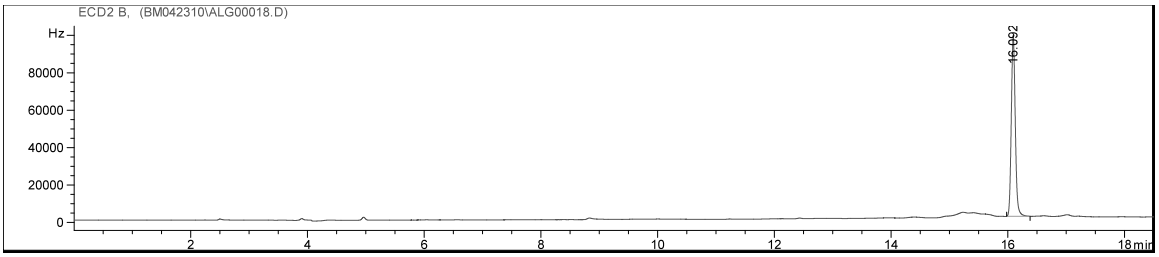

Figure C-70. Batch reactor containing 2 mM HCO_3^-, 5 mg/l NOM as C, 1000 mg/l FeO(OH), and 10 mg/l I^- at pH 7 and 48 hours reaction time (Experiment 59M, 04-21-2010), with 100 mg/l sulfite added after 0.1 µm filtration. The peak at 16.1 minutes corresponds to an iodoform formation of 237 µg/l CHI_3.

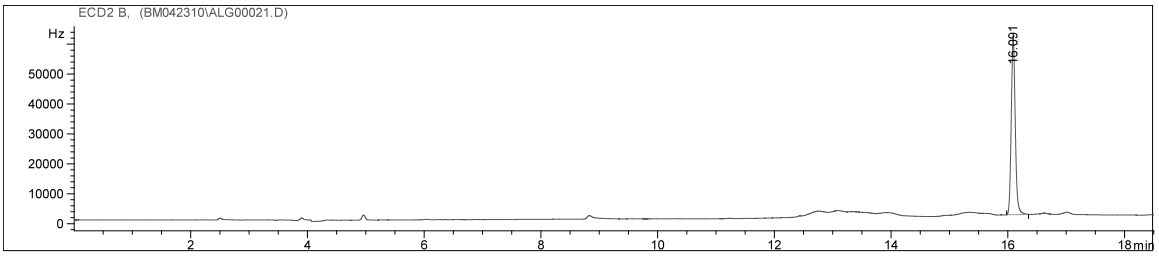

Figure C-71. Batch reactor containing 2 mM HCO_3^-, 5 mg/l NOM as C, 1000 mg/l FeO(OH), and 10 mg/l I^- at pH 7 and 48 hours reaction time (Experiment 59M, 04-21-2010), with 100 mg/l sulfite added after 0.1 µm filtration. The peak at 16.1 minutes corresponds to an iodoform formation of 135 µg/l CHI_3.

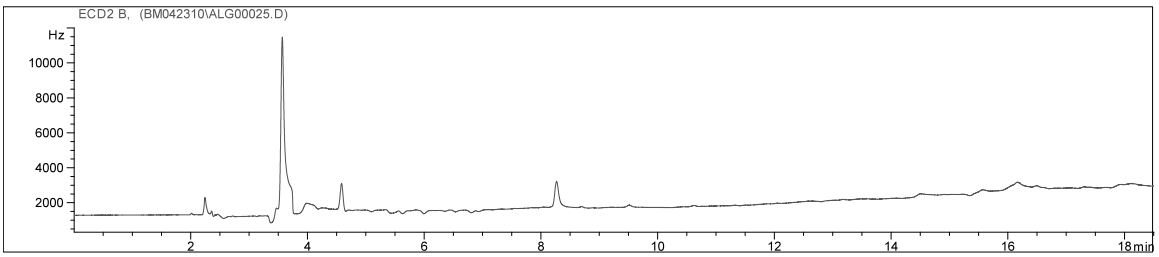

Figure C-72. Batch reactor containing 2 mM HCO_3^-, 5 mg/l NOM as C, no FeO(OH), and 10 mg/l I^- at pH 7 and 48 hours reaction time (Experiment 59M, 04-21-2010), with 100 mg/l sulfite added after 0.1 µm filtration. No iodoacetic acid was detected at the iodoacetic acid retention time of 9.54 minutes.

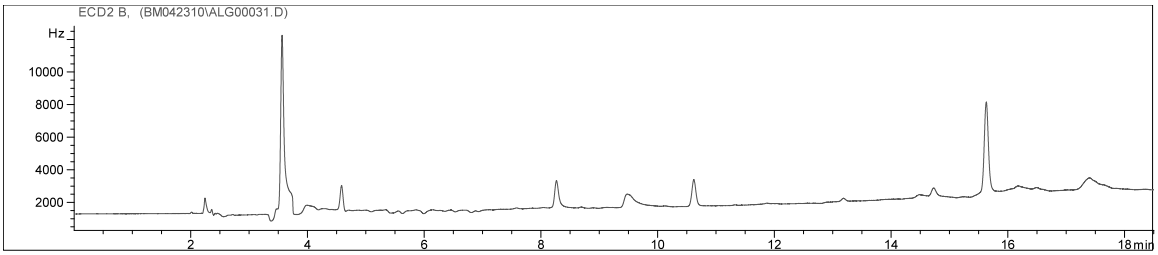

Figure C-73. Batch reactor containing 2 mM HCO_3^-, no added NOM, 1000 mg/l FeO(OH), and 10 mg/l I^- at pH 6 and 48 hours reaction time (Experiment 59M, 04-21-2010), with 100 mg/l sulfite added after 0.1 µm filtration. No iodoacetic acid was detected at the iodoacetic acid retention time of 9.54 minutes. The peak at 9.48 minutes is not a positive detection of iodoacetic acid.

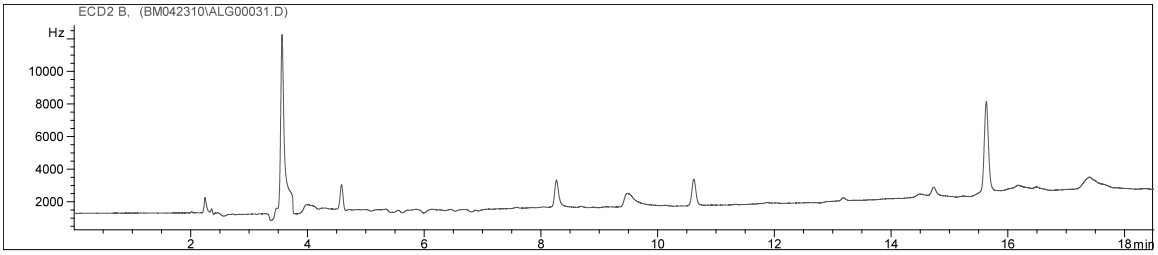

Figure C-74. Batch reactor containing 2 mM HCO_3^-, no added NOM, 1000 mg/l FeO(OH), and 10 mg/l I^- at pH 7 and 48 hours reaction time (Experiment 59M, 04-21-2010), with 100 mg/l sulfite added after 0.1 µm filtration. No iodoacetic acid was detected at the iodoacetic acid retention time of 9.54 minutes. The peak at 9.48 minutes is not a positive detection of iodoacetic acid.

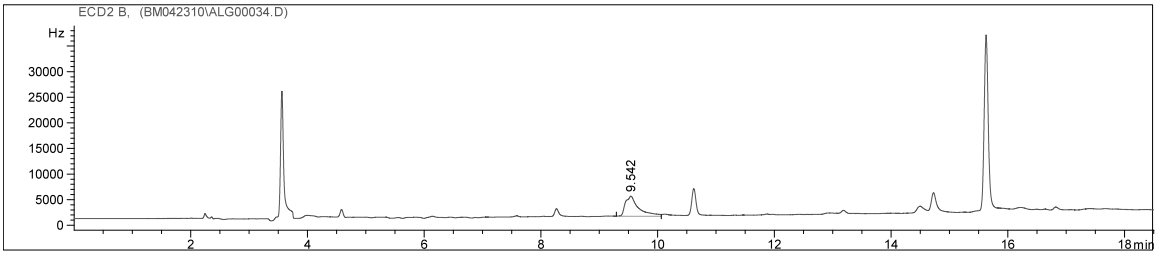

Figure C-75. Batch reactor containing 2 mM HCO_3^-, 5 mg/l NOM as C, 1000 mg/l FeO(OH), and 10 mg/l I^- at pH 6 and 48 hours reaction time (Experiment 59M, 04-21-2010), with 100 mg/l sulfite added after 0.1 µm filtration. The peak at 9.54 minutes corresponds to an iodoacetic acid formation of 33 µg/l IAA.

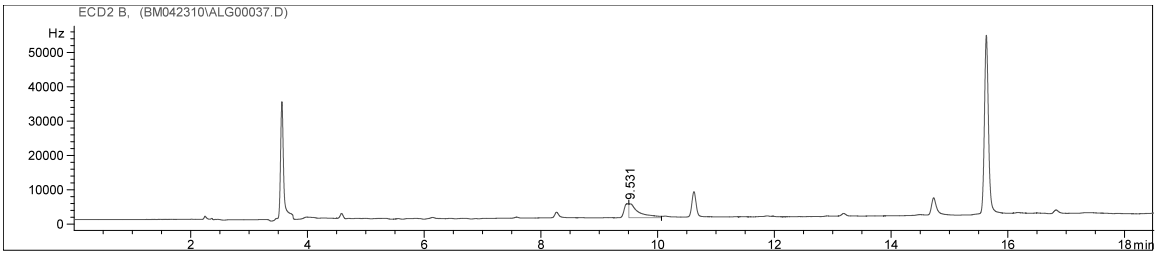

Figure C-76. Batch reactor containing 2 mM HCO_3^-, 5 mg/l NOM as C, 1000 mg/l FeO(OH), and 10 mg/l I^- at pH 6 and 48 hours reaction time (Experiment 59M, 04-21-2010), with 100 mg/l sulfite added after 0.1 µm filtration. The peak at 9.54 minutes corresponds to an iodoacetic acid formation of 26 µg/l IAA.

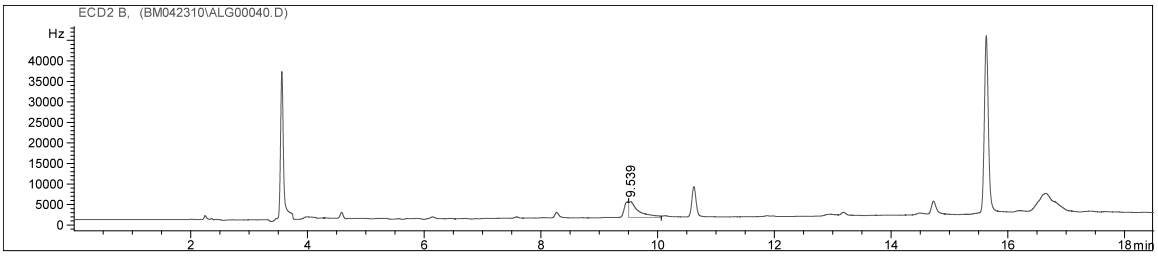

Figure C-77. Batch reactor containing 2 mM HCO_3^-, 5 mg/l NOM as C, 1000 mg/l FeO(OH), and 10 mg/l I^- at pH 7 and 48 hours reaction time (Experiment 59M, 04-21-2010), with 100 mg/l sulfite added after 0.1 µm filtration. The peak at 9.54 minutes corresponds to an iodoacetic acid formation of 26 µg/l IAA.

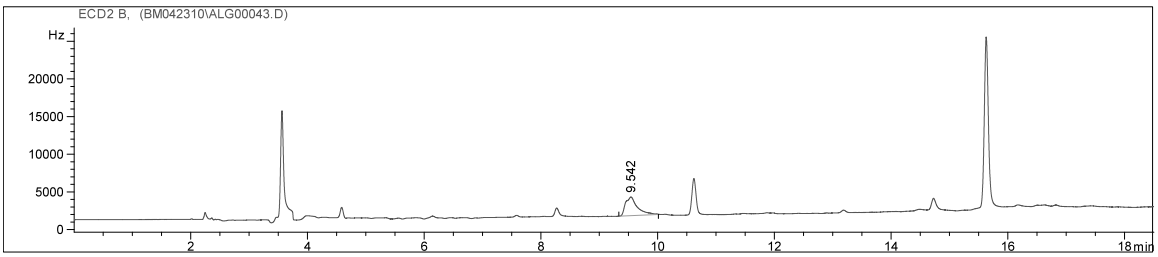

Figure C-78. Batch reactor containing 2 mM HCO_3^-, 5 mg/l NOM as C, 1000 mg/l FeO(OH), and 10 mg/l I^- at pH 7 and 48 hours reaction time (Experiment 59M, 04-21-2010), with 100 mg/l sulfite added after 0.1 µm filtration. The peak at 9.54 minutes corresponds to an iodoacetic acid formation of 22 µg/l IAA.

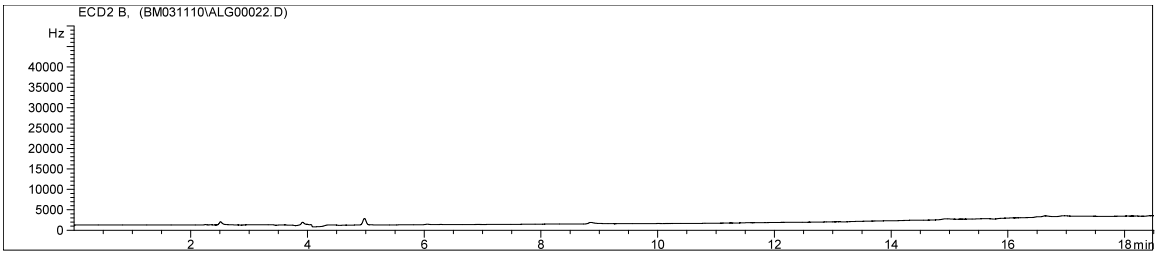

Figure C-79. Batch reactor containing 2 mM HCO_3^-, no NOM, no WDB-A pipe deposit, and 10 mg/l I^- (Experiment 50M, 03-09-2010). Initial conditions: pH 6 and 48 hours reaction time. No iodoform was detected in this chromatogram.

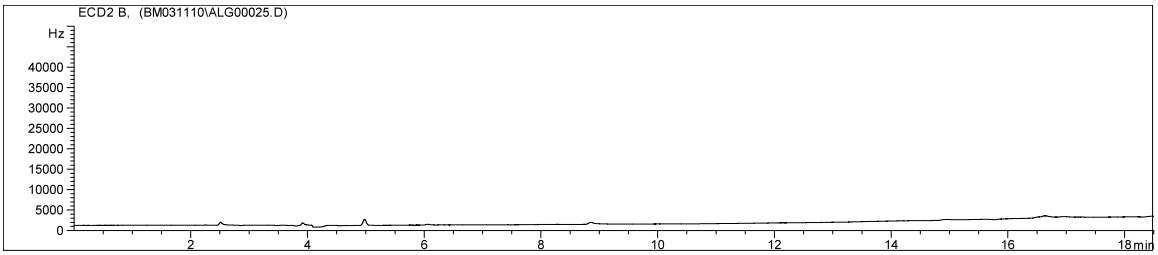

Figure C-80. Batch reactor containing 2 mM HCO_3^-, 5 mg/l NOM, no WDB-A pipe deposit, and 10 mg/l I^- (Experiment 50M, 03-09-2010). Initial conditions: pH 6 and 48 hours reaction time. No iodoform was detected in this chromatogram.

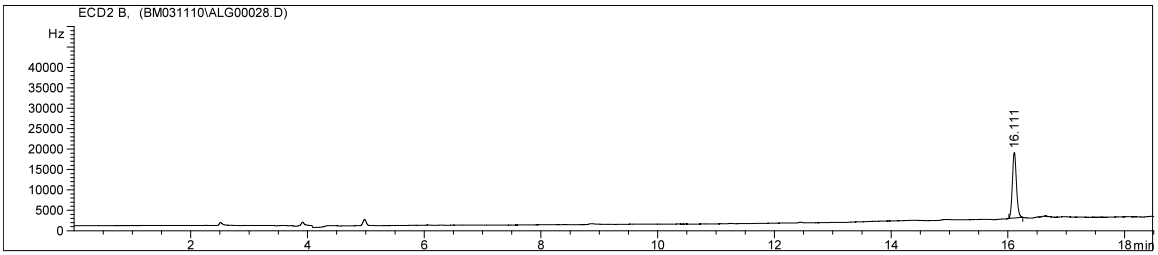

Figure C-81. Batch reactor containing 2 mM HCO_3^-, no NOM, 1000 mg/l WDB-A pipe deposit, and 10 mg/l I^- (Experiment 50M, 03-09-2010). Initial conditions: pH 6 and 48 hours reaction time. The peak at 16.1 minutes corresponds to 42 µg/l CHI_3.

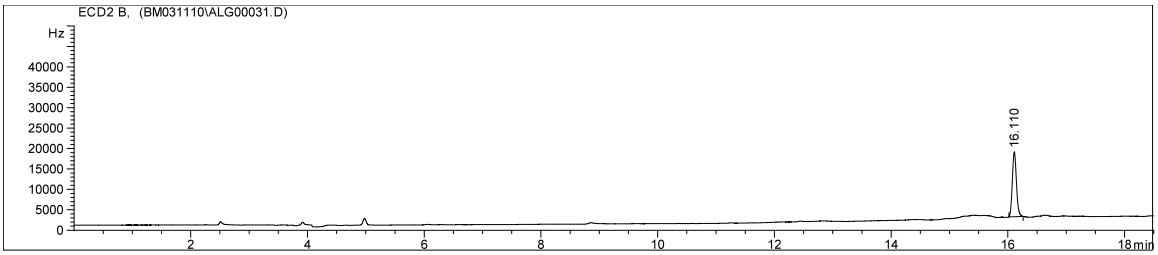

Figure C-82. Batch reactor containing 2 mM HCO_3^-, no NOM, 1000 mg/l WDB-A pipe deposit, and 10 mg/l I^- (Experiment 50M, 03-09-2010). Initial conditions: pH 7 and 48 hours reaction time. The peak at 16.1 minutes corresponds to 38 µg/l CHI_3.

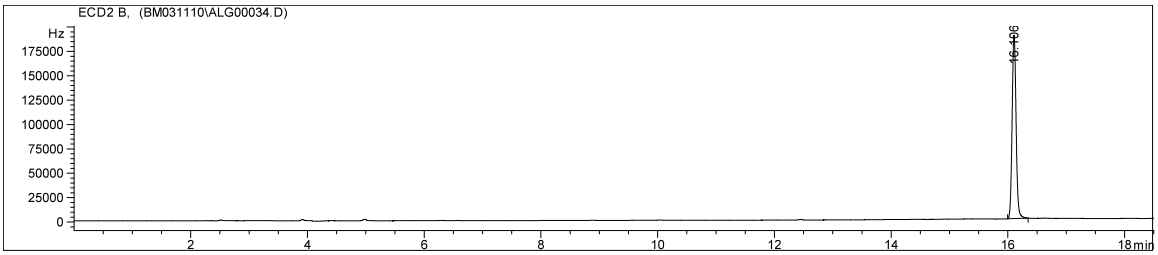

Figure C-83. Batch reactor containing 2 mM HCO_3^-, 5 mg/l NOM, 1000 mg/l WDB-A pipe deposit, and 10 mg/l I^- (Experiment 50M, 03-09-2010). Initial conditions: pH 6 and 48 hours reaction time. The peak at 16.1 minutes corresponds to 469 µg/l CHI_3.

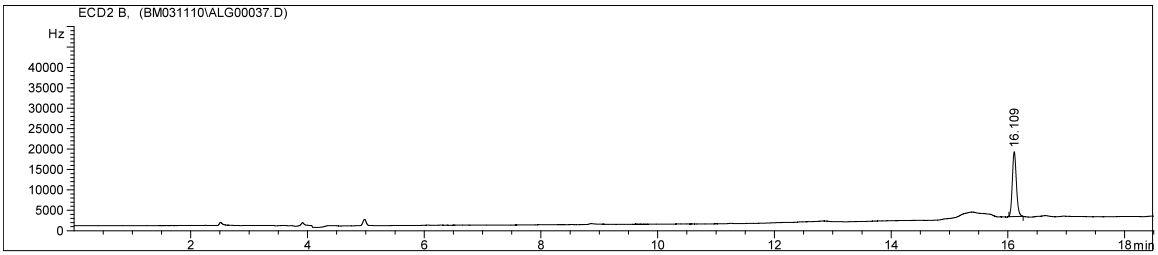

Figure C-84. Batch reactor containing 2 mM HCO_3^-, 5 mg/l NOM, 1000 mg/l WDB-A pipe deposit, and 10 mg/l I^- (Experiment 50M, 03-09-2010). Initial conditions: pH 7 and 48 hours reaction time. The peak at 16.1 minutes corresponds to 40 µg/l CHI_3.

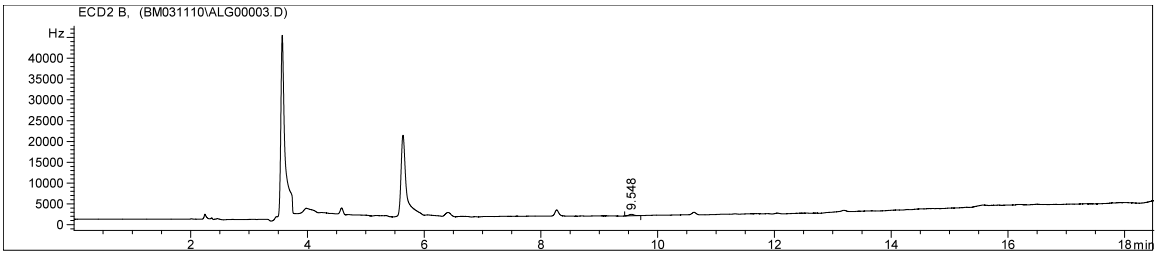

Figure C-85. Batch reactor containing 2 mM HCO_3^-, no NOM, no WDB-A pipe deposit, and 10 mg/l I^- (Experiment 50M, 03-09-2010). Initial conditions: pH 6 and 48 hours reaction time. The peak at 9.5 minutes corresponds to 2 µg/l IAA.

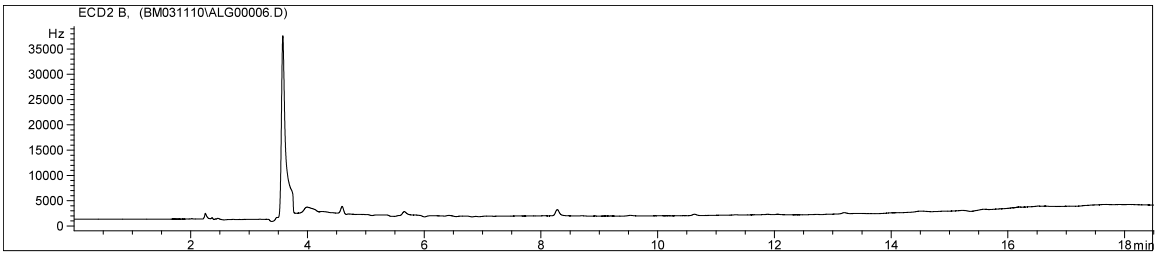

Figure C-86. Batch reactor containing 2 mM HCO_3^-, 5 mg/l NOM, no WDB-A pipe deposit, and 10 mg/l I^- (Experiment 50M, 03-09-2010). Initial conditions: pH 6 and 48 hours reaction time. No iodoacetic acid was detected in this chromatogram.

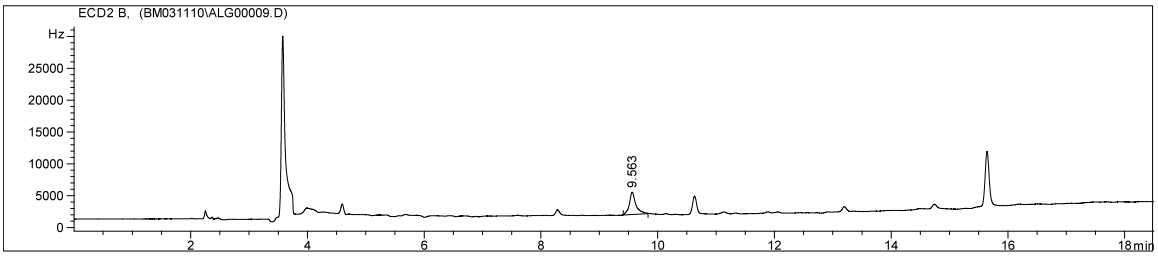

Figure C-87. Batch reactor containing 2 mM HCO_3^-, no NOM, 1000 mg/l WDB-A pipe deposit, and 10 mg/l I^- (Experiment 50M, 03-09-2010). Initial conditions: pH 6 and 48 hours reaction time. The peak at 9.5 minutes corresponds to 15 µg/l IAA.

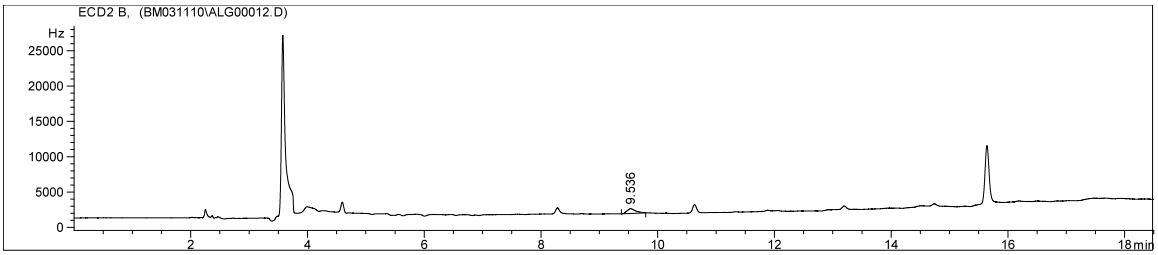

Figure C-88. Batch reactor containing 2 mM HCO_3^-, no NOM, 1000 mg/l WDB-A pipe deposit, and 10 mg/l I^- (Experiment 50M, 03-09-2010). Initial conditions: pH 7 and 48 hours reaction time. The peak at 9.5 minutes corresponds to 5 µg/l IAA.

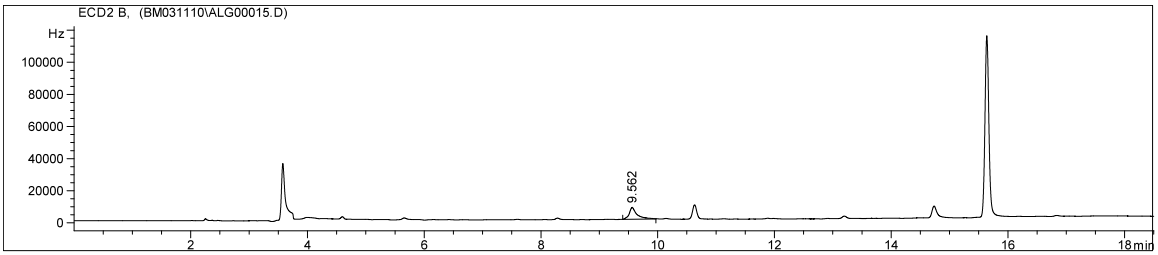

Figure C-89. Batch reactor containing 2 mM HCO_3^-, 5 mg/l NOM, 1000 mg/l WDB-A pipe deposit, and 10 mg/l I^- (Experiment 50M, 03-09-2010). Initial conditions: pH 6 and 48 hours reaction time. The peak at 9.5 minutes corresponds to 36 µg/l IAA.

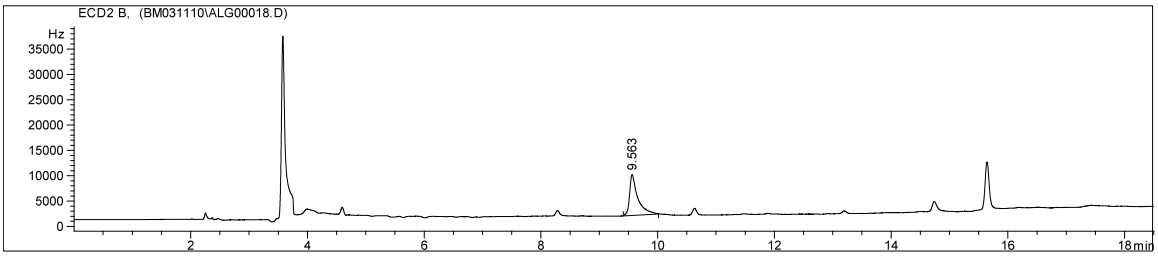

Figure C-90. Batch reactor containing 2 mM HCO_3^-, 5 mg/l NOM, 1000 mg/l WDB-A pipe deposit, and 10 mg/l I^- (Experiment 50M, 03-09-2010). Initial conditions: pH 7 and 48 hours reaction time. The peak at 9.5 minutes corresponds to 41 µg/l IAA.

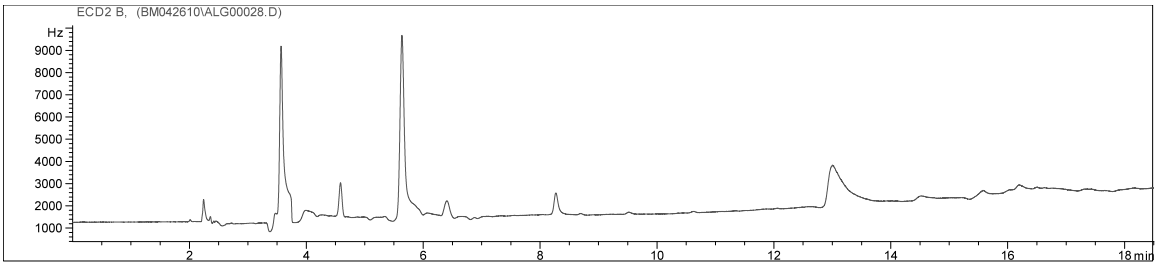

Figure C-91. Batch reactor containing 2 mM HCO_3^-, 5 mg/l NOM as C, no CC-A pipe deposit, and 10 mg/l I^- at pH 7 and 48 hours reaction time (Experiment 62M, 04-23-2010). No iodoacetic acid was detected at the iodoacetic acid retention time of 9.54 minutes.

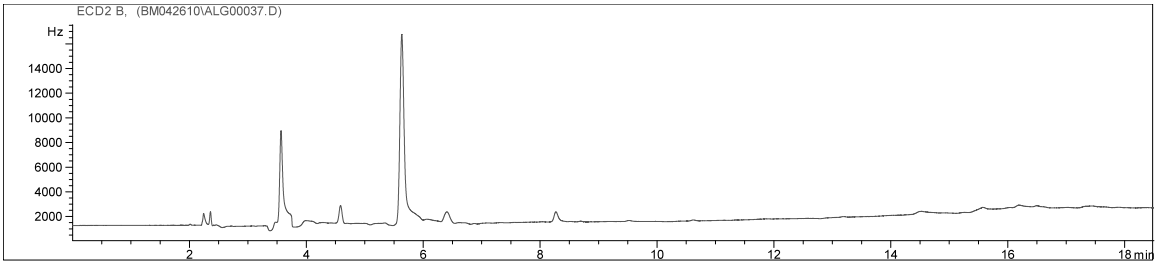

Figure C-92. Batch reactor containing 2 mM HCO_3^-, no added NOM, 1000 mg/l CC-A pipe deposit, and 10 mg/l I^- at pH 7 and 48 hours reaction time (Experiment 62M, 04-23-2010). No iodoacetic acid was detected at the iodoacetic acid retention time of 9.54 minutes.

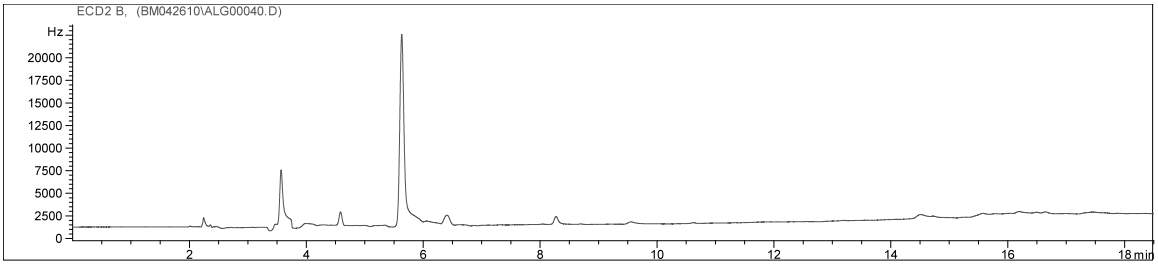

Figure C-93. Batch reactor containing 2 mM HCO_3^-, no added NOM, 1000 mg/l CC-A pipe deposit, and 10 mg/l I^- at pH 7 and 48 hours reaction time (Experiment 62M, 04-23-2010). No iodoacetic acid was detected at the iodoacetic acid retention time of 9.54 minutes.

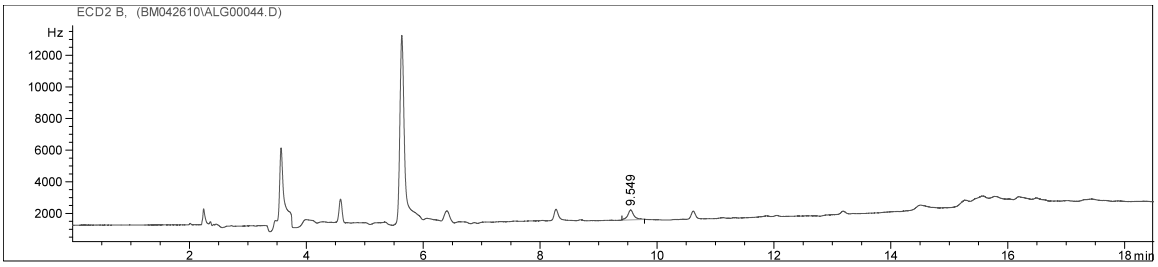

Figure C-94. Batch reactor containing 2 mM HCO_3^-, 5 mg/l NOM as C, 1000 mg/l CC-A pipe deposit, and 10 mg/l I^- at pH 7 and 48 hours reaction time (Experiment 62M, 04-23-2010). The peak at 9.54 minutes corresponds to 4 µg/l IAA.

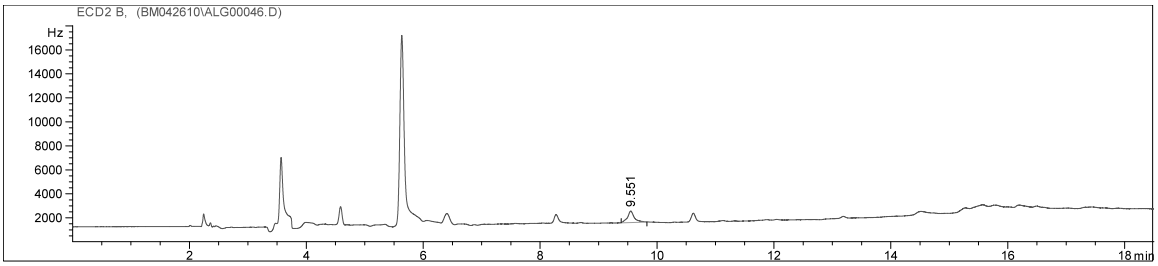

Figure C-95. Batch reactor containing 2 mM HCO_3^-, 5 mg/l NOM as C, 1000 mg/l CC-A pipe deposit, and 10 mg/l I^- at pH 7 and 48 hours reaction time (Experiment 62M, 04-23-2010). The peak at 9.54 minutes corresponds to 5 µg/l IAA.

REFERENCES

Allard, S., von Gunten, U., Sahli, E., Nicolau, R., & Gallard, H. (2009). Oxidation of iodide and iodine on birnessite (delta-MnO2) in the pH range 4-8. [Article]. *Water Research, 43*(14), 3417-3426.

Benjamin, M. M., Sontheimer, H., & Leroy, P. (1996). *Corrosion of Iron and Steel*: AwwaRF.

Bichsel, Y., & von Gunten, U. (1999). Oxidation of iodide and hypoiodous acid in the disinfection of natural waters. [Article]. *Environmental Science & Technology, 33*(22), 4040-4045.

Bichsel, Y., & von Gunten, U. (2000a). Formation of iodo-trihalomethanes during disinfection and oxidation of iodide containing waters. *Environmental Science & Technology, 34*(13), 2784-2791.

Bichsel, Y., & von Gunten, U. (2000b). Hypoiodous acid: Kinetics of the buffer-catalyzed disproportionation. [Article]. *Water Research, 34*(12), 3197-3203.

Cemeli, E., Wagner, E. D., Anderson, D., Richardson, S. D., & Plewa, M. J. (2006). Modulation of the cytotoxicity and genotoxicity of the drinking water disinfection byproduct iodoacetic acid by suppressors of oxidative stress. *Environmental Science & Technology, 40*(6), 1878-1883.

Cwiertny, D. M., Handler, R. M., Schaefer, M. V., Grassian, V. H., & Scherer, M. M. (2008). Interpreting nanoscale size-effects in aggregated Fe-oxide suspensions: reaction of Fe(II) with goethite. *Geochimica Et Cosmochimica Acta, 72*(5), 1365-1380.

Friedman, M. J., Hill, A. S., Reiber, S. H., Valentine, R. L., & Korshin, G. V. (2010). *Assessment of Inorganics Accumulation in Drinking Water System Scales and Sediments*: Water Research Foundation.

Gallard, H., Allard, S., Nicolau, R., von Gunten, U., & Croue, J. P. (2009). Formation of Iodinated Organic Compounds by Oxidation of Iodide-Containing Waters with Manganese Dioxide. [Article]. *Environmental Science & Technology, 43*(18), 7003-7009.

Hua, G. H., Reckhow, D. A., & Kim, J. (2006). Effect of bromide and iodide ions on the formation and speciation of disinfection byproducts during chlorination. *Environmental Science & Technology, 40*(9), 3050-3056.

Lin, Y. P., Washburn, M. P., & Valentine, R. L. (2008). Reduction of lead oxide (PbO2) by iodide and formation of iodoform in the PbO2/I-/NOM system. *Environmental Science & Technology, 42*(8), 2919-2924.

Lytle, D. A., & Schock, M. R. (2005). Formation of Pb(IV) oxides a in chlorinated water. *Journal American Water Works Association, 97*(11), 102-114.

Moran, J. E., Oktay, S. D., & Santschi, P. H. (2002). Sources of iodine and iodine 129 in rivers. *Water Resources Research, 38*(8).

Plewa, M. J., Wagner, E. D., Richardson, S. D., Thruston, A. D., Woo, Y. T., & McKague, A. B. (2004). Chemical and biological characterization of newly discovered lodoacid drinking water disinfection byproducts. *Environmental Science & Technology, 38*, 4713-4722.

Richardson, S. D. (2003a). Disinfection by-products and other emerging contaminants in drinking water. *Trac-Trends in Analytical Chemistry, 22*(10), 666-684.

Richardson, S. D. (2003b). Water analysis: Emerging contaminants and current issues. *Analytical Chemistry, 75*(12), 2831-2857.

Richardson, S. D., Ellington, J. J., Crumley, F. G., Evans, J. J., Plewa, M. J., & Wagner, E. D. (2006). Occurrence of iodo-acid DBPs in US chloraminated drinking waters. *Abstracts of Papers of the American Chemical Society, 231*, 33-ENVR.

Richardson, S. D., Fasano, F., Ellington, J. J., Crumley, F. G., Buettner, K. M., Evans, J. J., et al. (2008). Occurrence and Mammalian Cell Toxicity of Iodinated Disinfection Byproducts in Drinking Water. *Environmental Science & Technology, 42*(22), 8330-8338.

Sarin, P., Snoeyink, V. L., Bebee, J., Kriven, W. M., & Clement, J. A. (2001). Physico-chemical characteristics of corrosion scales in old iron pipes. *Water Research, 35*(12), 2961-2969.

Simon, D. E., Morton, R. W., & Gislason , J. J. (2004). A Close Look at Electrolytic Manganese Dioxide (EMD) and the γ-MnO2 & ε-MnO2 Phases Using Rietveld Modeling. *Advances in X-Ray Analysis, 47*.

Stumm, W. (1992). *Chemistry of the Solid-Water Interface*. New York: John Wiley and Sons, Inc.

U.S. EPA. (1995). Method 551.1: Determination of Chlorination Disinfection Byproducts, Chlorinated Solvents, and Halogenated Pesticides/Herbicides in Drinking Water by Liquid-Liquid Extraction and Gas Chromatography with Electron Capture Detection.

U.S. EPA. (1998). National Primary Drinking Water Regulations: Disinfectants and Disinfection Byproducts (Vol. 63, pp. 69389-69476): Federal Register.

U.S. EPA. (2003). Method 552.3: Determination of Haloacetic Acids and Dalapon in Drinking Water by Liquid-Liquid Extraction, Derivitization, and Gas Chromatography with Electron Capture Detection.

Washburn, M. P. (2008). *Exploratory studies of a novel pathway for the formation of halo-organic disinfection byproducts.* Thesis (M.S.)--University of Iowa, 2008.

Yokota, K., Fukushi, K., Takeda, S., & Wakida, S. I. (2004). Simultaneous determination of iodide and iodate in seawater by transient isotachophoresis-capillary zone electrophoresis with artificial seawater as the background electrolyte. *Journal of Chromatography A, 1035*(1), 145-150.